Global Characterization of Modern Depositional Environments for Reservoir Analogues

Björn Burr Nyberg

Dissertation for the degree philosophiae doctor (PhD)

at the University of Bergen

2015

Dissertation date: May 12th 2015

The price of success is hard work, dedication to the job at hand, and the determination that whether we win or lose, we have applied the best of ourselves to the task at hand.

- Vince Lombardi

Preface to the thesis

This dissertation has been submitted for the degree of philosophiae doctor (PhD) at the Department of Earth Science at the University of Bergen, Norway. The research presented in this dissertation was conducted between October 2011 and January 2015 at the Centre for Integrated Petroleum Research (Uni Research CIPR), including a six month stay at the Australian School of Petroleum at the University of Adelaide, Australia. The research was carried out within a three-year scholarship as part of the Sedimentary Architecture of Field Analogues (SAFARI) phase II project sponsored by the Sed/Strat group within the FORCE consortium of oil companies. The candidate has been supervised by Professor John A. Howell (Uni Research CIPR, now University of Aberdeen) and co-supervised by Dr. Simon J. Buckley (Uni Research CIPR) and Professor Atle Rotevatn (University of Bergen).

This scientific paper-based thesis is separated into three main sections: an introduction to the topic, the papers themselves, and finally a synthesis. This is in accordance with the doctoral dissertation style in Norway. The introduction is used to provide background information, to define the main objectives of the thesis and the current status of previous work within the field. The second part contains four scientific papers that are submitted to international peer-reviewed journals. Part three summarizes the main results of those articles, contributions to the broader scientific community and concluding remarks.

Table of contents

Acknowledgements

During the past three and a half years, I have had the privilege of working and collaborating with a select group of exceptional individuals who have made my PhD studies an extremely rich and memorable experience.

First and foremost, I would like to thank Professor John Howell for his guidance and support throughout these years. He has given insightful discussion, tremendous enthusiasm, mentorship and wisdom to provide an invaluable learning environment, and for that I am grateful.

To my co-supervisors, Dr. Simon Buckley and Professor Atle Rotevatn, I am thankful for your help, encouragement and friendship. Simon's patience, diligence and constructive manuscript reviews deserve additional praise and acknowledgments.

To the other members of the VOG and SAFARI group, past and present; Christian Haug Eide, Oliver Tynes, Nicole Naumann, Tobias Kurz, Andreas Rittersbacher, Aleksandra Sima, Kari Ringdal, Benjamin Dolva and Christian Kehl, I value our friendship and countless discussions. I would also like to express my gratitude to colleagues and other PhD students at the University of Bergen and Uni Research CIPR, especially Luisa Zuluaga, Dongfang Qu, Gijs Henstra, Alina Astrakova and Abduljelil Kedir. In addition, I would like to thank the administrative staff at Uni Research CIPR and the Department of Earth Sciences for their support.

Thanks to Berit Husteli, Aleksandra Smyrak-Sikora and Kim Senger for making my limited stay at UNIS and Svalbard an amazing experience. Gratitude goes to Rachel Nanson, Bruce Ainsworth, Boyan Vakarelov, Tessa Lane and Frank Rarity for welcoming me to the WAVE group during my stay at the University of Adelaide in Australia.

Finally, I wish to thank my family, who, despite being scattered across the globe, have always managed to stay close and be a source of continuous support and reassurance.

Björn Burr Nyberg

January 20, 2015

Abstract

The advent of significant volumes of freely available, global scale, remote sensing and Geographical Information Systems (GIS) data has revolutionized the study of modern depositional systems, especially with reference to their application as analogues for hydrocarbon reservoirs. While it is possible to browse Google Earth (or similar packages) and identify modern analogues, to date there have been no systematic studies which have mapped and categorized depositional systems on a global scale. Furthermore the application of data from modern systems in reservoir studies has commonly been undertaken in a qualitative way. Where measurements of geobodies are made it is often manually and prone to user error and bias. The work presented in this study details a systematic approach to the challenge of utilizing modern data as reservoir analogues from the global mapping of sedimentary basins, through the global classification of shallow marine shorelines to the automated description of sediment body geometries to their implementation in reservoir models. In addition to improved reservoir analogue studies, many aspects of this work, such as the mapping of basins and the quantification of shoreline types, have implications for broader understanding of modern systems and their preservation in the stratigraphic record.

Given that the rock record is wholly comprised of deposits that were laid down in sedimentary basins, it is appropriate to only select analogous for the rock record from modern systems that sit within basins. To this end it was necessary to map the distribution of modern sedimentary basins. This was achieved using GIS algorithms that combine data on surface gradient, geology, climate and tectonics. The key result is the first known map of the World's current terrestrial basins. Analysis of the results suggest that only about 16% of the Earth land surface lies within a basin, the rest is in upland areas that are in long tern net erosion. Within that 16%, 60% is within an arid climate which is significantly more than 27% of the total land proportion. Analysis of tectonic setting suggests that intracratonic and foreland basins are the greatest proportion by area.

Paralic systems are major reservoirs. Clastic coastlines are classified on the relative importance of wave, tide and fluvial processes in transporting and depositing sediments. While this classification has existed for over 40 years, there have been no previous attempts to classify the entire coastline of the World. Using a series of GIS datasets describing factors such as mean wave height, tidal range, fluvial discharge and shoreline shape it has been possible to produce a map within which the coastline is subdivided into 927,577 5 km segments, each of which is categorized on the primary and secondary controlling mechanism. This dataset shows that the World's depositional coastlines are primarily wave dominated (62%) with a significant component being tide dominated (35%) and only 3% being dominated by fluvial deltas. Further analysis suggests that shoreline type is heavily influenced by complex interplay between climate, latitude, shelf width, tectonic setting, ocean basin morphology and plate tectonics. The data have been analyzed by two parameters which are easily definable in the ancient (palaeo-climate and tectonic setting) to produce a probability matrix for a given shoreline type.

The last two articles explore methodologies for the extraction of geometric information from modern depositional environments and outcrop data in a quantitative, objective and automated workflow. This shows a methodology for describing spatial polygons by a centerline and a series of deviations from that centerline. The method described in the third article is applied to two modern systems (the Mitchell Delta in the Gulf of Carpentaria and

the Congo River in the Democratic Republic of the Congo) to show significant improvements in comparison to standard GIS routines. A linear regression line comparing a method based on the minimum bounding box (MBB) of a shape with the method developed here shows that MBB width was exaggerated up to 4.5 times and MBB length underestimated by as much as 0.31 times between the two datasets. As width and length of features are important parameters in object-based reservoir modeling, the potential skewed relationship of width to length ratio could reflect in associated reservoir models.

By expanding on the method proposed in Paper III, the fourth paper shows that mapped 2.5D geobodies from virtual outcrops can automatically describe shape, length, width and centerline deviation. Those attributes are used to define complex shapes for object based modelling. The potential of this approach is illustrated on the non-marine portion of the Cretaceous Blackhawk Formation of the Book Cliffs in eastern Utah where data were extracted and a reservoir model was built.

The results of the study are a step towards the more systematic use of modern systems as reservoir analogues and also shed light on the fundamental controls on the stratigraphic record.

Authorship statement and list of publications

This section is included to summarize the authorship contributions of the four publications in this thesis. All the articles are a result of effort from multiple individuals where the candidate is the principle author. Any omission or misinterpretation presented in any of those articles is the sole responsibility of the candidate. Additional acknowledgements are presented at the end of each respective article.

Paper I – Is the present the key to the past? A global characterization of modern sedimentary basins
Björn Nyberg, John A. Howell
Manuscript submitted to Geology

The candidate was responsible for collecting and processing all available data, designing the workflow, writing the manuscript and creating the figures. John Howell identified the problem, devised the project with regular input into the methodology and reviewed and edited the paper.

Paper II – Global distribution of modern shallow marine shorelines. Implications for exploration and reservoir analogue studies
Björn Nyberg, John A. Howell
Manuscript submitted to Marine and Petroleum Geology

The candidate was responsible for collecting and processing the global datasets, designing the empirical relationship workflows, creating the figures and writing the manuscript. John Howell proposed the original idea, had input to figures, provided insightful discussions and edited the manuscript.

Paper III – Geometric Attribute and Shape Characterization of Modern Depositional Elements: A Quantitative GIS Method for Empirical Analysis
Björn Nyberg, Simon J. Buckley, John A. Howell, Rachel A. Nanson
Manuscript submitted to Computers & Geosciences

The candidate was responsible for the original idea, designing the algorithms and workflows, creating the figures and writing the manuscript. Simon Buckley reviewed and edited the manuscript and discussed various aspects of the methodology. John Howell was instrumental in reviewing the final manuscript. Rachel Nanson provided data and discussion to the Mitchell Delta dataset and reviewed and edited the manuscript.

Paper IV – Automated extraction of architectural element geometries from outcrop interpretations for improved stochastic reservoir modelling
Björn Nyberg, John A. Howell, Simon J. Buckley, Christian Haug Eide
Manuscript submitted to Petroleum Geoscience

The candidate was responsible for the original idea, writing the algorithms, building the reservoir modelling workflows, creating the figures and writing the manuscript. John Howell contributed to the article by adding to the discussion and corrections to the manuscript. Simon Buckley provided valuable discussion, remarks and manuscript revisions. Christian Haug Eide assisted in the LiDAR interpretation and engaged in several discussions.

I

Introduction

1. Introduction

The study of modern depositional environments is a key component for understanding sedimentary systems of the past. It provides knowledge on the geomorphology, temporal and spatial character of sediment distribution that may become preserved, and the processes and controls influencing those systems under deposition. This information is important in reconstructing past sedimentary environments that otherwise are documented by an incomplete stratigraphic record (Miall 2014). Outcrop are examples where the stratigraphy of sediments preserved in vertical cliff sections is used to interpret the palaeo- depositional environment (e.g., Grammer et al. 2004; Eide et al. 2014). However, the information gained from these exposures is limited without a modern perspective to provide insight into planform character and the dynamic processes that are responsible for deposition (Figure 1). That combined knowledge is important in the oil and gas industry as analogues to predict the 3-dimensional geometry, shape, connectivity and lateral distribution of sandbody architecture along dip and strike of a similar subsurface field (e.g., Boyd et al. 1992; Dalrymple et al. 1992; Nichols and Fisher 2007; Ainsworth et al. 2011).

Models of modern depositional environments have been built in the past based on conceptualized and qualitative assessment using limited modern examples to support perceived controls influencing deposition (e.g., Boyd et al. 1992; Dalrymple et al. 1992). A relative few studies have aimed to quantify the global controls on those depositional environments by for instance tectonics and climate, although notable exceptions do exist (e.g., Hartley et al. 2010a; Weissmann et al. 2010; Ainsworth et al. 2011). In the past, this has been hindered by a lack of global high-resolution data that is often required to derive those interpretations and the computational power and geospatial tools needed to analyze the large datasets. In recent years, the dissemination of large volumes of remotely sensed data through applications such as Google Earth, offer new opportunities for sedimentologists to study sedimentological processes and geomorphological features in a unique global and quantitative perspective. However, challenges remain in systematically and objectively extracting quantitative information from these valuable data sources.

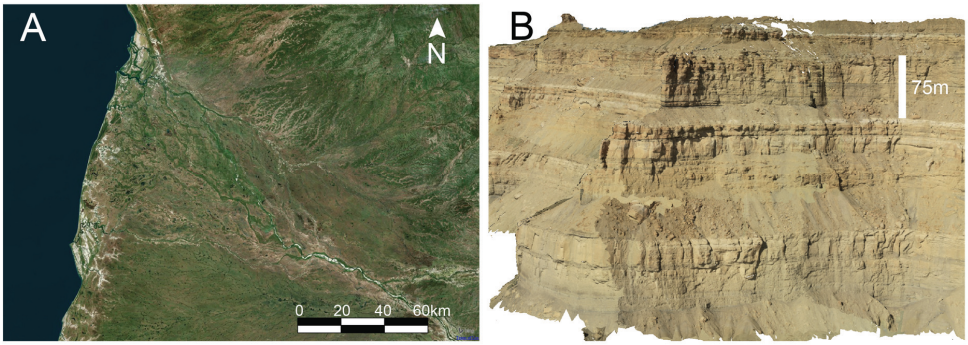

Figure 1 – Typical example of a modern analogue, **A**, and its corresponding analogue in the rock record, **B**. **A** shows a distributive fluvial system (DFS; Nichols and Fisher 2007) from the Mitchell/Nassau rivers in the Gulf of Carpentaria, Australia, characterized by channels radiating outwards from an apex with decreasing channel width towards the shoreline. **B** is a outcrop from the Campanian aged (Late Cretaceous), Blackhawk Formation in the Book Cliffs of eastern Utah, of which parts have been interpreted by previous authors as a DFS system (Rittersbacher et al. 2014). Note the different plane of information gathered from the two sources.

The goal of the current study is to determine the potential for global scale geometric characterization of modern depositional environments utilizing geographical information systems (GIS) and remote sensing techniques. This work has been driven by the recent rise in the access to publicly available data on a global scale, allowing for quantitative analyses, yielding results at scales and levels of detail that previously were not feasible. Global based studies are important in order to derive empirical relationships of the modern to map influences controlling the geomorphology of a depositional environment universally (e.g., climate, tectonics and latitude) rather than conditions that may arise from local or regional settings (Hartley et al. 2010a; Weissmann et al. 2010; Ainsworth et al. 2011; Peakall et al. 2011). An understanding of these fundamental controls can help build and better constrain predictive facies models of the subsurface (Vakarelov and Ainsworth 2013).

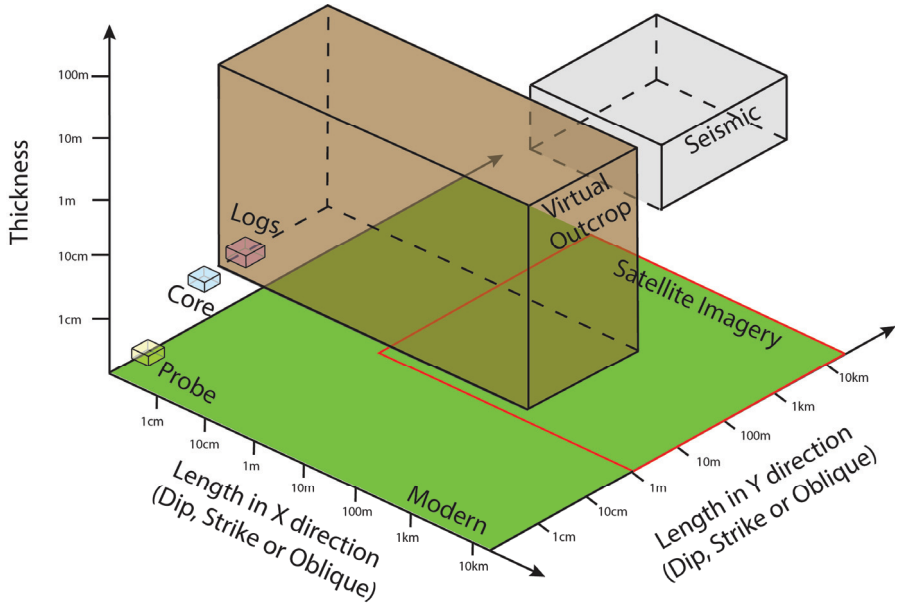

Figure 2 – A 3D illustration of typical thickness and horizontal dimensions of observable sedimentary features from various methods in relation to a general oblique, dip or strike profile. Note the gap in resolution, particularly in the oblique, dip and strike directions, that the modern in green and satellite imagery shown by a red box, may resolve. Modified after Pickup and Hern (2002) and Enge et al. (2007b).

This information cannot be derived from the rock record alone due to the paucity of available evidence. Both in terms of the dynamic relationship of process controls that influence the final sedimentary architecture as well as the limited three-dimensional observations obtained from seismic, outcrop, logs or core (Figure 2). In contrast, modern depositional environments may provide lateral plan-form information on the dip and strike relationships, spatially as well as temporally (i.e. tens of years), in the range of scales that produce sedimentary architecture that are important for heterogeneity and compartmentalization (Ainsworth et al. 2008; Howell et al. 2008). For instance, an outcrop may be considered a 2D or 2.5D cliff analogues along an oblique, strike or dip section of a depositional environment and as such does not provide the entire 3D connectivity of the subsurface (Geehan and Underwood 1993; Enge et al. 2007; Rittersbacher et al. 2014).

Similarly, modern systems represent 2D analogues; however information from the modern provide a unique planar view perspective that can supplement the shortcomings of the other various methodologies and techniques including outcrop (Tye 2004). The challenge is to apply and understand the heterogeneity observed in the present and the dynamic evolution in which it is preserved in the sedimentary record (Hampson and Storms 2003).

1.1. Modern Sedimentary Basins

One unique consideration of the modern is that the architectural, temporal and spatial distribution of elements observed are different in regions of net deposition (sedimentary basins) than those in net erosion (Weissmann et al. 2010). In contrast, the sedimentary history is an incomplete record (Miall 2014) of only net depositional settings that are preserved under conditions of long term subsidence that created accommodation (Jervey 1988; Blum and Törnqvist 2000). As the geometries are often different within sedimentary basins than erosional settings it is important that a suitable analogues for the modern to be defined in a net depositional region (Weissmann et al. 2010). External controls on the sedimentary architecture within a basin are of equal importance to map (e.g. source to sink), for instance the contributing fluvial discharge. It is important therefore to separate erosional versus depositional settings of the modern to quantify the controls on deposition as well as the resulting geometry observed within those basins.

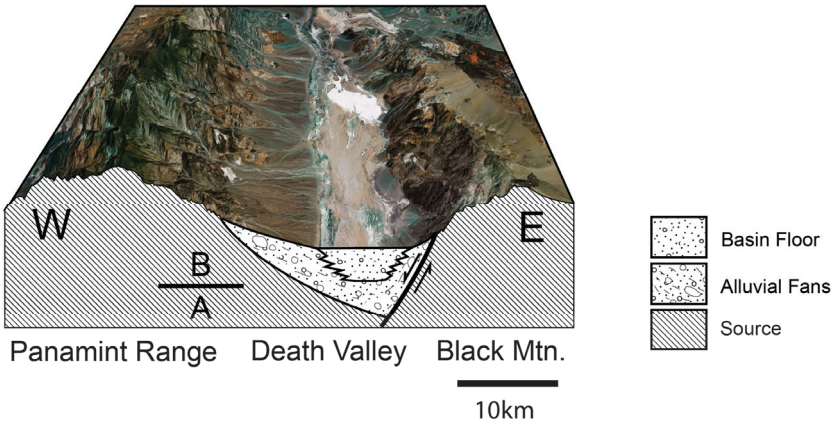

Figure 3 – A typical example of a modern sedimentary basin in the Basin in Range in the western United States, see inset. It illustrates the complicated typology of a modern sedimentary basin that may comprise multiple depositional elements of alluvial fans, fluvial and eloian features to name a few. In addition it shows a dynamic complexity of a transition from a predominately alluvial fan composition in its earliest stage, **A**, to an alluvial fan and basin floor configuration, **B**. In contrast the Black Mountains and the Panamint Range are regions of net erosion that have no preservation potential and are sites of sediment source for the sedimentary basin. Google Imagery ©.

A modern sedimentary basin is defined as an area on the earth's surface that has preservation potential on a long geological timescale (c. > 10^6 ma) due to subsidence that creates accommodation (Jervey 1988; Blum and Törnqvist 2000). The accommodation versus sediment supply (A/S) of a sedimentary basin is an important concept that determines the sedimentary architecture of a depositional environment (Van Wagoner et al. 1990;

Ainsworth et al. 2011). The tectonic regime that may create space can occur in a wide range of settings including convergent regions of foreland, back-arc and fore-arc basins, transform regions of strike-slip basins and divergent settings of extensional, passive margins and intracratonic basins (Figure 4).

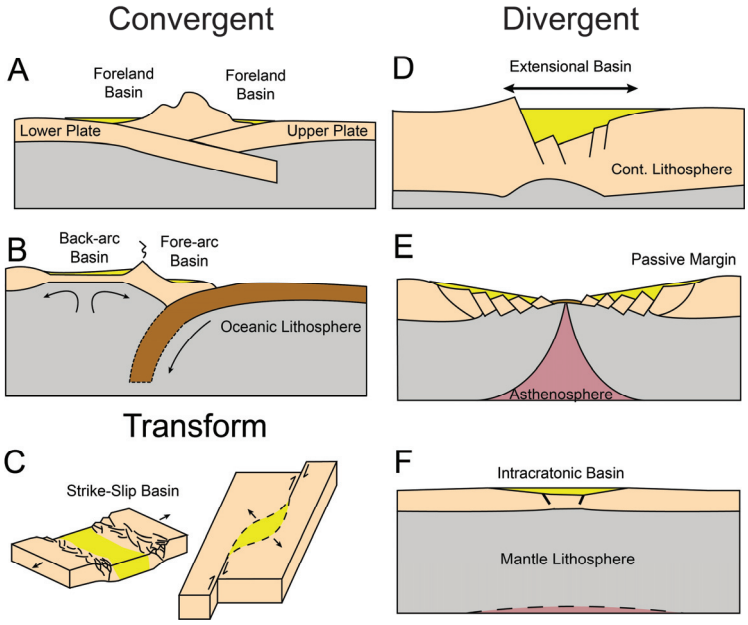

Figure 4 – Typical examples of basin types of **A**, Foreland Basins created from continental lithosphere-continental lithosphere interaction (e.g., Himalayan). **B**, Back-arc and Fore-arc basins created through continental lithosphere - oceanic lithosphere interaction (e.g., Sumatra Shelf, Andes). Strike-Slip basins of transform settings are shown in illustration **C** (e.g., Mongolia). Divergent settings in the intra-continental lithsopehere is demonstrated in **D** of an Extensional basin (e.g., Basin and Range, East African Rift System). **E** shows a rifted passive marigin at the edge of an oceanic spreading ridge (e.g., East coast of the USA). **F** shows an intracratonic basin (e.g., Central Australia). Modified after Allen and Allen (2013).

Within convergent settings, foreland basins are defined as a part of the continental crust that forms an area of accommodation related to a contractional orogenic belt and bordered on one side by a stable craton (Decelles and Giles 1996), Figure 4A. This foreland basin can be partitioned into its wedge-top, fore-deep, fore-bulge and back-bulge components which relate to the dynamic lithospheric flexure associated with a mountain building process. Retro-arc foreland (or retroforeland) basins are related to orogenic arc compressions, while peripheral foreland (proforeland) basins are defined by a continental compression (Dickinson 1974). Back-arc basins are similar to retro-arc foreland basins in that they form at the edge of orogenic arc systems, though back-arc systems are associated with neutral or extensional origins rather than a compressional regime (Marsaglia 1995), Figure 4B. Dickinson (1995) and Dickinson and Seely (1979) described fore-arc basins, as shown in Figure 4B, in relation to its arc-trench interaction as those systems between the magmatic arc to the subduction complex.

Strike-slip basins are characterized by movement parallel to the main fault associated with transform tectonics forming one of the most complex zones of sedimentary basin development (Sylvester 1988), as they are seldom represented by any single end-member. This complexity yields transtensional basins (i.e. pull-apart basins) associated with releasing bends, transpressional basins associated with constraining/restraining bends and potentially transrotational basins represented by a combination of any of those components (Ingersoll 1988; Fossen 2012).

In divergent/intra-plate settings, extensional basins are typically associated with normal faulting to create graben structures (Gawthorpe and Leeder 2000), Figure 4D, controlled by a crustal thinning mechanism, Figure 5A. Passive margins are typically defined by mature crust of the continental lithosphere created at the boundary of rifted margins, Figure 4E, which undergo subsidence due to thermal cooling and sediment loading (Dickinson 1974). Intracratonic (or cratonic sag) basins, as shown in Figure 4F, are large intraplate regions of tectonically inactive zones that experience subsidence as a consequence of cooling and stretching often associated with failed or paleo-rifts (Ingersoll 1988, 2012).

Dickinson (1974), Miall (1984), Ingersoll (2012), Allen and Allen (2013) and references therein are valuable resources that summarize in further detail, the nomenclature and tectonic evolution of sedimentary basins and in particular, an expansion of definitions of basins on the oceanic lithosphere which are outside the scope of this thesis.

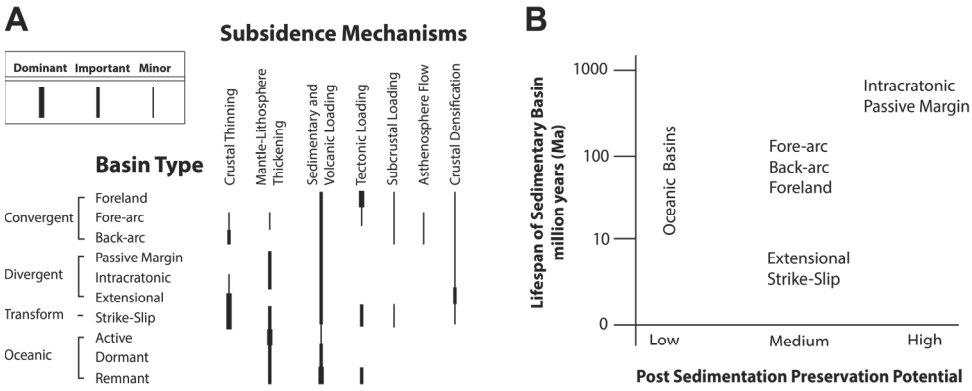

Figure 5 – **A** shows the dominant, important and minor mechanisms for subsidence by a simplified basin type modified after Ingersoll (2012). Note that different basins types are associated with different mechanisms and thereby its influence on subsidence. That rate of subsidence in relation to the longevity of a basin and its post-sedimentation tectonic activity will determine its typical preservation potential, **B**. Oceanic basins have a relatively low preservation potential (although expectations include dormant oceanic basins). Modified from Ingersoll (2012) to show the pertinent basin types used in this thesis (e.g., Figure 3).

The mechanisms that control subsidence on a sedimentary basins can be attributed to a number of factors including crustal thinning, mantle-lithosphere thickening, sedimentary and volcanic loading, tectonic loading, subcrustal loading, asthenosphere flow and crustal densification (Ingersoll 2012). As subsidence rate vary by subsidence mechanism and subsidence mechanisms are related to specific basin types (Xie and Heller 2009), Figure 5A, it is important to differentiate those basin types to understand its potential to create accommodation. The capacity for a sedimentary basin to fill will depend on sediment supply

exceeding the creation of new accommodation. Ultimately, the long term preservation potential of that preserved sediment will depend on the lifespan of a basin and its post-sedimentation preservation, as shown in Figure 5B, which in turn, is a function of tectonic activity after deposition.

1.2. Classification of Depositional Environments

The systems preserved within sedimentary basins are classically defined into three gross depositional environments of continental (terrestrial), marginal marine and deep marine (Reading and Levell 1996). Subsequent hierarchical classification of those systems may subdivide those environments further by studying the controls on those systems that influence the spatial relation and geometry of architectural elements.

For instance, the first stage classification of the marginal marine, define depositional environments by the relationship between transgressive and progradational events (Boyd et al. 1992; Dalrymple et al. 1992). This will depend on A/S which is controlled by base-level rise and/or subsidence associated with basin types (i.e., Figure 4 and 5) and fluvial discharge to the shoreline (Van Wagoner et al. 1990; Boyd et al. 1992; Ainsworth et al. 2008; Howell et al. 2008). A second stage examines the controls from the ternary diagram of Galloway (1975) that relates the relative influence of fluvial, tide and wave acting on a delta. Ainsworth et al. (2011) has shown that this ternary plot can be used to classify beyond deltaic marginal marine systems into the broad spectrum of potential depositional shorelines (Figure 6). The distinction is of importance in a modeling perspective as each depositional environment will be associated with various heterogeneities that may act as baffles or barriers to compartmentalize a reservoir (Hampson and Storms 2003; Howell et al. 2008).

A number of digital databases and nomenclatures are used to classify and relate the growing array of data from outcrop, modern and reservoir models gathered from the spectrum of those depositional environments. These include the shallow marine WAVE database (Vakarelov and Ainsworth 2013), fluvial FAKTS database (Colombera et al. 2012) and the deep marine DWAKB database (Baas et al. 2005). The Sedimentary Architecture of Field Analogues for Reservoir Information (SAFARI) is a database with origins from the early 1990s (Dreyer et al. 1993) with aims to develop a repository of analogues to create better realistic geological reservoirs models. In recent years, the nomenclature of the database has expanded across the range of clastic environments to incorporate both the modern and ancient, and recent studies have developed from that project (Eide et al. 2014; Rittersbacher et al. 2014).

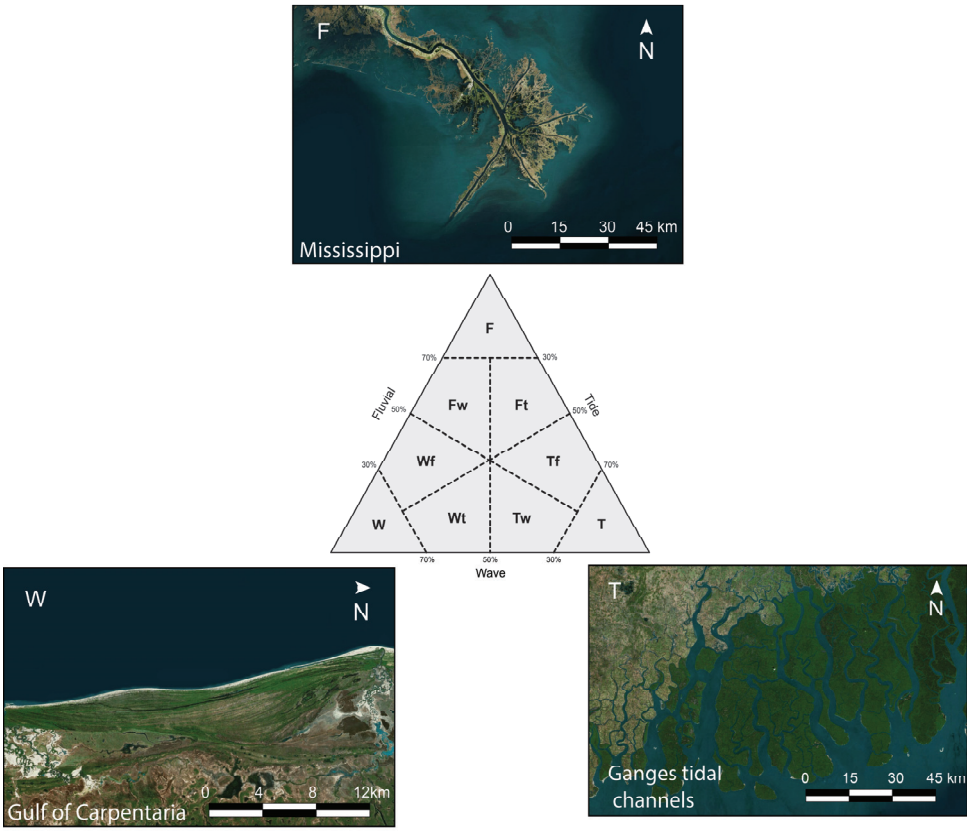

Figure 6 – A simplified 9 category ternary process diagram showing the relative influence of fluvial, tide and wave on the resulting coastline geomorphology. Modified from **Paper II** and based on Ainsworth et al. (2011) and Galloway (1975). These define shorlines as **W** – Wave-Dominated, **Wt** – Wave-Dominated Tide-Influenced, **Wf** – Wave-Dominated Fluvial-Influenced, **F** – Fluvial-Dominated, **Fw** – Fluvial-Dominated Wave-Influenced, **Ft** – Fluvial-Dominated Tide-Influenced, **T** – Tide-Dominated, **Tf** – Tide-Dominated Fluvial-Influenced and **Tw** – Tide-Domainted Wave-Influenced. Images from Bing © show the endmembers of W,T and F.

1.3. GIS & Remote Sensing

The storage, management, analysis and visualization of geospatial data collected from modern depositional environments have been facilitated by advances in GIS software. The use of GIS within the geosciences has significantly aided researchers to expand studies by structuring and relating spatial and numerical data. The integration, management, analysis, merging, defining of complex relationships, querying spatial and non-spatial data and handling large data volumes of geospatial information is achieved through the application of automated algorithms and workflows (see Steiniger and Hunter (2013) for review). The design and programming of those algorithms is the basis of computational geosciences.

Remote sensing is the process of acquiring geospatial information gathered through means of non-physical interaction with the surface of an area. While this may take many forms, on a global perspective and in recent years this has been exemplified by imaging sensors on airborne and satellite platforms. The principle of remote sensing from satellite derived acquisition is a broad and complex topic that has been covered in depth by many authors (e.g., Jensen 2007 and Mather and Koch 2011). A brief summary of the fundamental concepts are included herein as it forms a strong foundation for global scale studies of modern depositional environments. This is important as misinterpretations from satellite data often derive from an inadequate knowledge of remote sensing theory, imperfect data acquisition, sources of errors or limitations in processing and classification algorithms on either the raw or final image product.

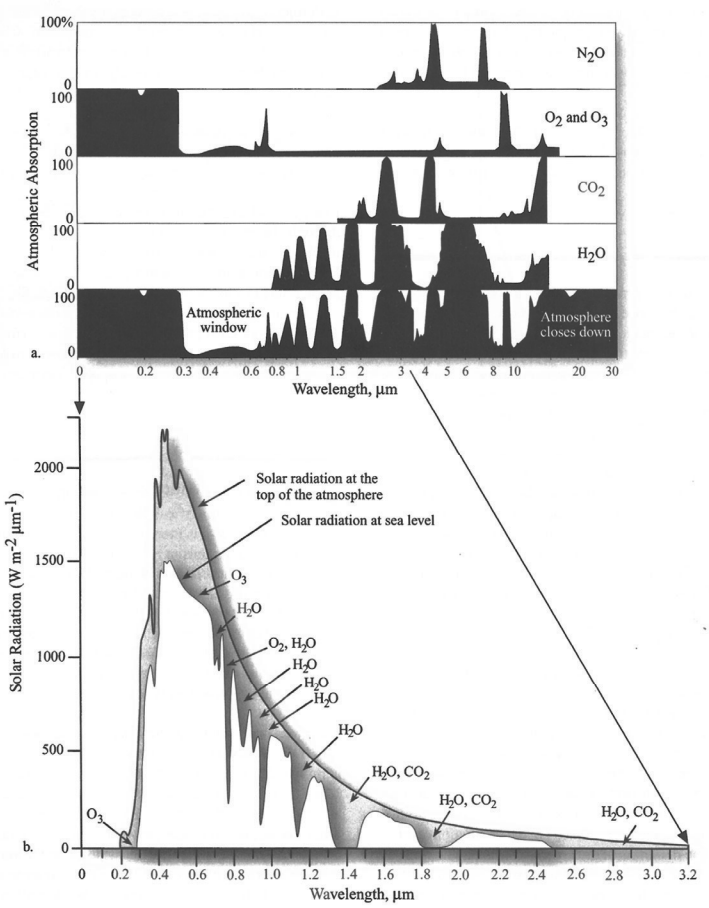

Figure 7 – **A** shows the percentage of electromagnetic radiance absorbed by each individual atmospheric gas between a wavelength of 0 and 30µm including its cumulative effect on the bottom graph. **B** illustrates the decrease in solar radiation energy with increasing wavelength and its strength at the atmosphere as well as at sea level after atmospheric influence shown in **A**. From Jensen (2007). This graph indicates that the useable electromagnetic spectral range from satellite derived acquisition is limited and prone to atmospheric error.

Satellite data acquisition captures differences in radiation from electromagnetic energy at its sensor. The energy of electromagnetic waves is defined as the acceleration of an electrical charge in the form of electric and magnetic wavelengths from a source at the speed of light (Jensen 2007). The sun is the primary source of electromagnetic energy that transmits to the surface of the earth where it is diffused, absorbed and reflected from a surface material to be registered as radiance at the satellite sensor. The variation and intensity in wavelengths associated with that registered radiance differ based on the properties of the surface material and that characteristic can be exploited to map features captured by remotely sensed imagery (Mather and Koch 2011).

It is important to recognize then, that the study of geological features from remotely sensed imagery is often the study of the associated reflectance from covering surface material, in particular vegetation and canopy, or weathering products, rather than the geomorphological feature itself.

The atmosphere plays a pivotal role in the applicable range of the electromagnetic spectrum for remotely sensed data acquisition from satellites. Figure 7A shows the individual and cumulative absorption rates of the electromagnetic wavelengths by individual gases as solar radiance transmits through earth's atmosphere. The atmospheric windows, illustrated in white, show the restricted range of the electromagnetic wavelengths for image acquisition from a satellite platform. As shorter wavelengths have a higher energy, the solar irradiance transmitted to sea level (and hence reflected to the satellite sensor) in relation to the absorption rate of the atmosphere, are higher in those wavelengths (Figure 7B). Table 1 shows a limited selection of satellite sensors that primarily operate within those restricted windows. The impact of radiance diffusion, refraction and absorption as it transmits and reflects from the surface of the earth are sources of noise and error (Jensen 2007).

The resolution of satellite imagery depends on four main criteria of spectral, spatial, radiometric and temporal resolution of radiance registered at the satellite sensor (Jensen 2007; Mather and Koch 2011). The spectral resolution is the resolution of a sensor to record the intensity of radiance within a given wavelength range. Spatial resolution can be defined as the area on the ground captured by an instantaneous field of view (IFOV) from a satellite at any given time. This may or may not be related to the pixel resolution as the pixels of an image are a resample of the radiance within the IFOV (Jensen 2007). Radiometric resolution is the sensitivity of a sensor to collect and record the intensity of radiance, an expression defined in binary bits. Temporal resolution is the frequency by which an image can be acquired for any given spatial location. The selection of an appropriate satellite sensor (e.g., Table 1) should be carefully chosen based on the desired application and resolution requirements. For instance, MODIS may be more suitable for global based studies that require a large spectral resolution to differentiate features beyond the visible electromagnetic spectrum. IKONOS or QuickBird may be more appropriate for smaller scale research that requires higher spatial and temporal resolution.

Table 1 - Selected satellite sensors and their resolution

Satellite Sensor	Spectral (μm)	Spatial (m)	Radiometric (bits)	Temporal (days)	Bands	Operational
Landsat TM	0.45 -1.75*, 10.4 - 12.5, 2.08 - 2.35	30 - 120	8	16	7	1982 - 2012
Landsat ETM+	0.45 -1.75*, 10.4 - 12.5, 2.08 - 2.36, 0.5 - 0.9ŧ	15 - 60	8	16	8	1999 -
IKONOS	0.45 - 0.9 0.45 - 0.9ŧ	0.8 - 4	11	3	5	1999 -
QuickBird	0.45 - 0.9 0.45 - 0.9ŧ	0.61 - 2.44	11	1 - 3.5	5	2001 -
MODIS	0.405 - 14.385	250 - 1000	12	1 - 2	36	1999 -
ASTER	0.52 - 0.86, 1.6 - 2.43, 8.12 - 11.65	15 - 90	8 - 12	16	14	2000 -
WorldView-1	0.4 - 0.9ŧ	0.46	11	1.7 - 5.7	1	2007 -
WorldView-2	0.4 - 1.04*, 0.45 - 0.8ŧ	0.46	11	1.1 - 3.7	9	2009 -

Table 1 – Modified after Jensen (2007) and Mather and Koch (2011) to show a selective range of satellite sensors that are commonly used in the interpretation of modern depositional environments from software. Their relative spectral, spatial, radiometric and temporal resolutions are shown as well as the number of spectral bands and operational period for the satellite sensor. *Note – the spectral range for individual bands have not been separated. ŧ - panchromatic band

1.4. Integration of Modern Analogues in Reservoir Modelling

The integration of modern analogue data from remotely sensed satellite acquisition into subsurface modeling may manifest in one of several forms including pixel based geostatistical models, object based models, deterministic models or as general input to the knowledge of facies models (Grammer et al. 2004). The aim of any methodology is to describe the heterogeneity, spatial connectivity, geometry and shape that otherwise are important for subsurface plays (Larue and Legarre 2004; Tye 2004; Howell et al. 2008; Larue and Hovadik 2008; Massey et al. 2013).

Geostatistics gathered from remotely sensed data can help to quantify the spatial correlation between sandbodies within a modern depositional environment. Colombera et al. (2012) has shown that a structured database that subdivides modern and ancient analogues into genetic units can be used to populate reservoir models by pixel-based methods that employ sequential indicator simulations (SIS), indicator cross-variograms and transitional probability matrices. In many standard reservoir modeling suites, however, a limitation of pixel-based approaches is that the variogram used to describe relationships between facies is restricted to a two-point analysis whereas many depositional environments are more complicated than two facies (Caers 2001).

Multipoint geostatistics (MPS) is an extension of a pixel based approach to address subsurface fields with multiple facies characteristics (Caers 2001; Caers and Zhang 2004) by applying algorithms that rely on training images to capture and reproduce stochastic patterns. Training images may derive from multiple sources including modern depositional environments (e.g., Figure 8; Caers and Zhang 2004; Hashemi et al. 2014). Issues related to the stationary of a training image and applying 3 dimensionality to otherwise 2D modern training images are improving (Hu and Chugunova 2008; Comunian et al. 2012), thereby increasing the practicality of those techniques to capture realistic geological models and trends.

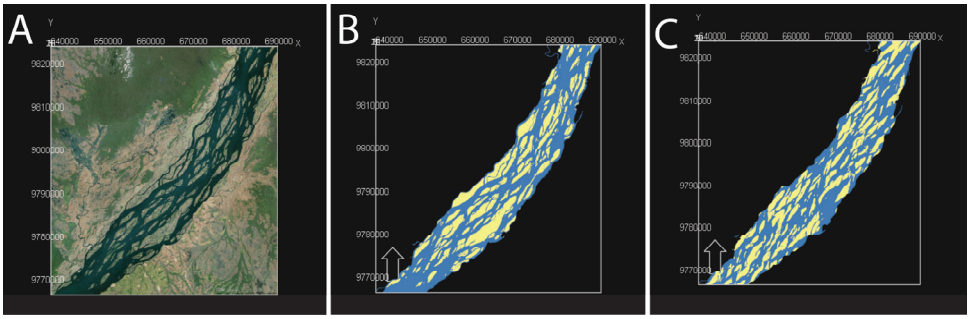

Figure 8 – **A** shows a typical 2D training image gathered from a modern depositional environment of the Congo River in the Democratic Republic of the Congo based on Bing Imagery ©. **B** shows the automated 2 categorical supervised classification (and deterministic model) of mid channel bars implemented directly within Roxar RMS. Given the stationary of the classification in **B**, the resulting MPS model in **C** is well reproduced with a sand content of 35%.

Numerical dimensions and shape gathered from architectural elements within a modern depositional environments can be applied to constrain the dimensions of sandbodies for object based modelling (Nanson et al. 2012) and conditioning to well and core data can supplement a 3D aspect (Tye 2004). Additional fieldwork information such as auguring, coring and shallow seismic may be used to build the planform sandbody geometry into a 3D deterministic model (Best et al. 2003; Massey et al. 2013). Finally the value of geostatistical and numerical data of the modern and gathered thru remotely sensed data acquisition, should not be discounted in developing an improved understanding on the controls of modern depositional environments (e.g, Ainsworth et al. 2011; Hartley et al. 2010a;). That information may be integrated in a reservoir modelling context as a predictive tool on the likely depositional environment and character that should be modelled using existing reservoir software tools and techniques.

1.5. State of the Art

The use of remotely sensed information for sedimentological and geomorphological studies of the modern has been applied in a wide range of gross depositional environments for several decades.

In recent years, improved bathymetric, seismic and side-scan sonar acquisition have abetted the study of modern submarine features on a regional scale to analyze canyon channel, lobe and fan geomorphology, to name a few (Popescu et al. 2004; Lastras et al. 2009; Peakall et

al. 2011). Of the terrestrial land surface and since the inception of aerial photography and satellite imagery acquisition, regional scale continental systems have been analyzed in detail to document geomorphology (Wilson 1972; Kocurek and Ewing 2005; Ashworth and Lewin 2012). The broad spectrum of marginal marine depositional environments on the range of fluvial, wave, tide and mixed processed paralic shorelines have been studied in detail as well based on remotely sensed data (Heap et al. 2004; Short 2006; Goodbred and Saito 2012; Choi et al. 2013; Nanson et al. 2013).

Yet global based studies of modern depositional environments have been limited in the past, although recent work on continental and marginal marine system have in particular, taken the full advantage of recent global seamless high-resolution satellite imagery (Hartley et al. 2010a; Weissmann et al. 2010; Ainsworth et al. 2011; Holzweber et al. 2014; Hudock et al. 2014). The epitome of this new advance is through the dissemination of valuable quantitative information from sources such as OneGeology, Reverb, NASA World Wind, USGS and Google Earth to the public domain. In modest terms, we know more of the modern today simply because we have more data to analyze at a quantitative and global perspective. However, global based studies are hampered both in terms of where to study relevant modern environments that are analogous to the rock record and the ability to extract quantitative geometric information gathered from those mapped depositional environments of interest. These challenges need to be addressed if the distributions of global modern depositional environments are to be quantified.

One challenge for global based studies of modern depositional environments is restricted by an inadequate knowledge on the extent of modern sedimentary basins. Unpublished maps of sedimentary basins (Fugro Robertson 2008) typically characterize ancient sediment accumulations (i.e. thick packages of sediment) based on nomenclature standards of the successive development and evolution of basins (Kingston et al. 1983). The physical extent of modern sedimentary basins have not previously been mapped; examples (Ingersoll 2012) and coordinates (Weissmann et al. 2010) remain the limit of this research. Consequently it is difficult to classify, analyze and extract useful information from modern depositional environments globally, both in terms of automated remote sensing and GIS techniques as well as by manual interpretation. The only alternative is a systematic and manual analysis of the world's surface area for depositional environments of interest (Hartley et al. 2010a; Weissmann et al. 2010; Holzweber et al. 2014; Hudock et al. 2014), though as a subjective and time consuming option, this is not ideal for quantitative analysis. Furthermore it is difficult to provide a justification for the inclusion or exclusion of particular regions of the world to study and to quantify the significance of their aerial extent in comparison to environments globally.

This is particularly true for marginal marine systems where a limited number of global modern depositional studies currently exist. Ainsworth et al. (2011) has recently provided data on selective samples worldwide on the influence of shelf width as a predictor for their new marginal marine ternary plot classification scheme (Vakarelov and Ainsworth 2013) based on original work by Galloway (1975). However the bulk of research on the controls of marginal marine models within sedimentology is often conceptualized with limited quantitative support (e.g., Boyd et al. 1992; Dalrymple et al. 1992; Ainsworth et al. 2011). The heterogeneity otherwise associated within those modern environments of different ternary process have played an important role in reservoir plays and behavior (Hampson and Storms 2003; Howell et al. 2008). New research into the global distribution of marginal marine systems that take advantage of the newly advent of high-resolution freely accessible

remotely sensed data would bring about a considerable wealth of unique information in quantifying the controls on those existing models.

As global datasets do increase, an inherit problem with increased volume of data is to extract useful information from those areas of interest. The type of geometric data from the modern that may be of importance to gather are its architectural elements aerial extent, its relative connectivity, length, width and shape (Tye 2004; Nanson et al. 2012) all of which have important implications for heterogeneity of a subsurface reservoir. While algorithms and functionality in GIS suites provide the opportunity to automate and address some of these issues in a more advanced manner than basic Google Earth viewing (Lisle 2006), limited resources are available for automated attribute and shape characterization within a sedimentological or geomorphological context (Gardoll et al. 2000). Likewise for the ancient, while there has been a desire to capture large quantitative information from outcrop by new methodologies such as LiDAR (Enge et al. 2007; Buckley et al. 2008; Eide et al. 2014; Howell et al. 2014; Rittersbacher et al. 2014), the ability to derive geometric information from those valuable resources are often limited to the same subjective and manual interpretations of the geologist.

A gap in the current state of research therefore exists in describing a complete workflow to define modern depositional environments on a global scale, classifying those environments and to extract quantitative geometric information of the modern and ancient to apply within reservoir modelling.

1.6. Objectives

The unprecedented volume of current geospatial information offers novel opportunities to study modern depositional environments that may highlight new insights on a quantitative and global perspective on the controls of sedimentary architecture. The aim of the present study is to address some of the challenges faced in global based studies of modern depositional environments from finding appropriate modern environments to research to the integration of knowledge within those systems for reservoir modelling. The thesis explores the concept that the study of modern depositional environments should be restricted to regions that have preservation potential and are thereby analogous to the rock record. The benefit of GIS and programming in analyzing the vast array of information needed for the classification of global based studies. Finally, the automated extraction of geometric attributes from modern depositional environments for the interpretation of those global based studies.

These hypotheses can used for an improvement to global based studies of modern depositional environments by demonstrating the necessary workflow and tools needed to quantify the distribution of modern systems and to describe their geometric attributes for interpretation. This forms part of the broader SAFARI project to build methodology that may be used to describe and quantify modern environments that are analogous to outcrop and reservoirs in order to build better and more realistic representations of the subsurface geology.

This is achieved through three main objectives;

1) To map the global distribution of modern sedimentary basins that defines the analogous modern to the rock record.

2) To demonstrate the benefit of an automated and objective approach to classify depositional environments globally by showing its application to the complex marginal marine systems.

3) To develop new methods to quantitatively extract useful geometric data from depositional environments of interest in a sedimentological and geomorphological context for improved reservoir modeling.

1.7. Publication Summary

The main objectives behind each article as it pertains to the thesis are described below by highlighting the existing gap in previous research that article aims to address and a brief summary of those findings.

Chapter 2 – Is the present the key to the past? A global characterization of modern sedimentary basins

Björn Nyberg, John Howell
Manuscript submitted to Geology

Our understanding of past geological history is highly dictated by that which we can study in the sedimentary record. Yet the sedimentary record is an incomplete record of geological time as only those regions that undergo active subsidence to create accommodation will have any preservation potential. As a main focus of this thesis has been to characterize modern depositional environments that may be analogous for the ancient, only those systems within sedimentary basins should be considered. It quickly became apparent though that previous literature and research into the topic on the extent of modern sedimentary basins was lacking and therefore the objective of **Paper I** was to delineate modern sedimentary basins.

By considering the geomorphology of modern sedimentary basin as low lying depression containing unconsolidated sediments with elements of high relief (i.e., alluvial fans and aeolian deposits), a combination of low-gradient, Quaternary sediment distributions and manual editing was performed. This is achieved by examining high resolution global digital elevation models (DEM) to highlight low gradient regions that spatially coincide with Quaternary geology distributions. Additional processing of the DEM dataset incorporated higher relief alluvial fan contributions based on the basin ridge drainage delineation that connect to those basins within intermontane regions.

The results highlight that a mere 4.5% of the earth's surface (or 16% of the terrestrial land) are within sedimentary basins. Of the marine realm, the continental lithosphere represents approximately 13% of the earth to suggest that globally approximately 17% of the continental lithosphere is potentially in net deposition. Climate analysis of the terrestrial portion shows that over half of all sedimentary basins (~60%) are within arid dry conditions displaying a large discrepancy to the distribution of arid climates globally that only represent one quarter of the area (~27%). While equatorial and warm-temperate sedimentary basins are distributed similar to their global proportions, the largest difference shown in this study is that snow and polar climates that are significant globally but aerially non-extensive within sedimentary basins. Tectonically, intracratronic (~49%) and foreland (~29%) settings are the most prominent whereas passive margins (~10%), extensional (~7%), strike-slip (~4%) and

fore-arc (~1%) basins are the least representative. Expanding the tectonic classification to include the marine realm of the continental lithosphere shows that passive margins increased significantly by 31% to ~41%, back-arc basins represent ~17%, fore-arc basins at ~10% whereas intracratonic represent a mere ~12%. Extensional (~3%) and Strike-Slip (~2%) settings remain the least prominent.

Chapter 3 – Global distribution of modern shallow marine shorelines. Implications for exploration and reservoir analogue studies

Björn Nyberg, John Howell
Manuscript submitted to Marine and Petroleum Geology

Marginal marine deposits compose important reservoirs for hydrocarbon storage. The ternary plot which relates the relative influence of fluvial, tide and wave power on shoreline geomorphology is typically used in sedimentology to classify those systems. Varying intensities of fluvial, tide and wave power influence the heterogeneity and potential compartmentalization of a similar analogous reservoir that otherwise influence reservoir production and behavior. To date, no ternary process of the World's shorelines exists although regional demonstrations have shown that the perceived influences of fluvial, wave and tide on shoreline geomorphology do indeed correlate numerically. The aim here is to resolve the challenges to find a relative relationship between the ternary processes based on global remotely sensed datasets.

Global geospatial proxies for the relative ternary relationship have been complied by using watershed analysis for fluvial power, mean significant wave height for wave power and tidal range for tidal power. In addition, coastline geomorphology has been considered by segmenting the shoreline into 5km sections to map the roughness and funnel shape shoreline character to either increase the probability of wave or tidal dominance. A semi-quantitative ternary plot classification scheme that maps the proportions of those relative powers has been used to classify the marginal marine into a two-tier classification scheme of 9 categories (F, Ft, Fw, T, Tw, Tf, W, Wf, Wt). The first tier defines the dominant ternary process classification (e.g., fluvial-dominated) and a second tier classification defines an influenced parameter (e.g., fluvial-dominated wave-influenced). Relating those ternary processes to known and potential controls on shoreline geomorphology can then be quantified.

The results show that an automated and objective classification of shorelines by ternary process can be achieved globally. It indicates that on a global scale as a whole, the marginal marine is a wave-dominated environment (83%) that is largely depended on the current geographical distribution of continents today. That configuration of continents is associated with varying climates, shelf widths, tectonics and distribution of net depositional regions. The influence on those factors on ternary process dominance at the shoreface has been quantified. The 28% of the shoreline that is net deposition are more tidally modified by nearly 19% resulting in a significant drop of wave-dominated shorelines by 31%. The distributions of those more mixed-influenced depositional regions are centered around the equator and steadily decrease toward the poles. Climate influences shoreline process by controlling fluvial discharge and wave strength. Wide continental shelves are nearly 3 times as tide-modified in comparison to narrow shelves and within depositional settings more than half of wide-shelves are tide-modified. Tectonically, foreland, extensional and strike-slip

basins are the most tide-modified whereas fore-arc basins are typically characterized by narrow shelves and a wave-dominated character.

The complex relationship of controls on ternary process suggests difficulty in applying direct relationships of the modern to predict marginal marine conditions of ancient systems. The tectonic plate distribution is a primary component controlling shelf width, tectonic regime, climate and distribution of sedimentary basins and therefore the ternary process. Interpretations from ancient systems reliability only quantify climate and tectonic regime, thereby limiting the ability in predicting ternary process and the geomorphology of the marginal marine system. The relationship between climate and tectonic regime as quantified in the modern of the current study is important as it provides one of the only key perspectives into predicting the depositional character of paleo-marginal marine systems.

The study has shown an initial global quantification on the controls of ternary process on shoreline geomorphology. In addition, the results may serve a reservoir modeling perspective by providing a global and systematic way of finding appropriate modern analogues of the marginal marine based on the controls on ternary processes that best describes a reservoir play.

Chapter 4 – Geometric Attribute and Shape Characterization of Modern Depositional Elements: A Quantitative GIS Method for Empirical Analysis

Björn Nyberg, Simon Buckley, John Howell, Rachel Nanson
Manuscript submitted to Computers and Geosciences

The continual rise in the availability of remotely sensed datasets can be of significant benefit to sedimentologists and geomorphologists to capture global trends rather than local variability within depositional environments. With increased data come added difficulties to analyze the vast array of information; to find trends and statistical correlations, to separate the relevant versus irrelevant. The first step of which is the ability to extract quantitative yet accurate geometric attributes from mapped modern architectural elements in a context that is important to analyze and constrain the geometry of a similar analogous reservoir model. Previously this has not been needed, in part due to a lack of geospatial data to be analyzed in a quantitative manner. The aim of **Paper III** is to demonstrate the benefit of objectively describing geometric attributes and shapes from mapped depositional features to gather information to analyze the heterogeneity and geometry of modern systems.

The paper expands on traditional geographical information system (GIS) algorithms to show the benefit of automated workflows that describe a multitude of parameters including width and centerline deviation of mapped depositional elements. This is achieved by calculating the centerline of a digitized polygon element and relating that to a suite of values measured at an equal spacing. A centerline deviation is the distance between the shortestpath of an object to its centerline. Width is taken as the perpendicular angle to multiple segmentations along the centerline. The combined information obtained from centerline deviation and width along the distance of an object may be used to define shape of a feature in an automated and objective manner as ellipsoidal, cresentic or sinuous with a symmetrical, asymmetrical or linear profile. In addition, connectivity analyses of modern depositional environments have been addressed in two aspects by examining the number of connected geobodies and the perimeter length connecting those geobodies.

The methods have been applied to two datasets of the mixed-influenced Mitchell Delta in the Gulf of Carpentaria and the Congo River in the Democratic Republic of the Congo. Compared to a standard GIS operation of a minimum bounding box that measures a features minimum length (longest axis) and maximum width (shortest axis), a significant improvement is shown in the proposed automated method. The MBB results defined the regression slopes of sandbodies in the Mitchell Delta as 1.25-4.47 times wider and 0.31-0.97 times shorter resulting in higher width:length ratios. The connectivity of those elements was analyzed as well to show that channels connect the most number of sandbodies within the potential reservoir analogue. However, the total perimeter of those channels connecting other reservoir elements is proportionally very low, particularly channel to beach ridges (2.6%) and channel to chenier ridges (0.7%). Clusters of beach and chenier ridges show intra-connected connectivity with a significant proportion of heterogeneity arising from swales and tidal floodplains. When applied to 2221 mid-channel bar elements in the Congo River, a linear regression slope shows a MBB as 1.06 times wider and 0.97 times shorter, thereby providing reasonable width:length ratios. A width to length ratio analysis of mid-channel bars downstream of the river changes from 0.26 to 0.21 upstream. Channel width changes from a mean of 925 m to 530 m and asymmetry of mid-channel bars increases upstream as well. The results would raise caution in the application of standard GIS tools for populating geometric attributes of modern depositional elements for reservoir modelling as it may not provide an accurate representation.

By transiting from a manual approach to an automated perspective, a repeatable and auditable approach is developed that does not suffer from the same subjective bias. Not only then has this methodology shown its automated and objective capabilities to analyze geometric attributes and shapes of mapped depositional environments. The approach allow for new methods to describe and compare geometric attributes from modern depositional environments that are useful in a reservoir modelling concern.

Chapter 5 – Automated extraction of architectural element geometries from outcrop interpretations for improved stochastic reservoir modelling

Björn Nyberg, John Howell, Simon Buckley, Christian Haug Eide
Manuscript submitted to Petroleum Geoscience

Recent advances in the use of LiDAR and photogrammetry to create virtual outcrops have promoted a quantitative analysis of architectural elements to capture large scale sedimentary architecture that is important for reservoir behavior and production. Yet the extraction of geometric data from mapped elements on virtual outcrops remains manual. As a result, this subjective and manual approach is prone to human error and inefficiencies. The aim of **Paper IV** is to provide a new objective methodology that can automatically extract geometric attribute and shape information from mapped architectural elements derived from outcrop interpretations.

By expanding on the methodology of previous research in **Paper III**, it has been shown that mapped 2.5D geobodies from virtual outcrops can be described by its shape, length, width and centerline deviation. This is accomplished by translating the 2.5D mapped architectural element into a 2D object to be applied within a GIS suite. The centerline is then defined which is used to relate multiple equally spaced measurements rather than a single minimum or maximum value of previously available GIS techniques. In turn, that additional information can be used to define complex user-defined shapes for object based modeling.

Shapes are defined by normalizing the width around the centerline deviation combined with a normalized definition of an objects length. Normalizing the geometry of an object has the benefit of grouping similar geobody shapes regardless of geometric size. A user-defined object is then created based on the along, across and planform dimensions of similar grouped geobodies. The shape of those grouped objects, along with its geometric attributes and variability, can then be reproduced within reservoir modelling suites by standard object-based modelling tools that employ user-defined objects.

A virtual outcrop model of the Cretaceous Blackhawk Formation of the Book Cliffs in eastern Utah is used as an example for the methodology. This has been interpreted as a distributary fluvial system (DFS) similar to that of the Mitchell or Gilbert Deltas in the Gulf of Carpentaria, Australia. 69 channel bodies (61 strike, 8 dip) were measured as 2.5D polyline objects on the virtual outcrop model. Those were then automatically analyzed utilizing the proposed methodology to show the geometric attributes. Along strike the averaged width was 221 m (+/- 170m) with a mean maximum thickness of 5.6m (+/- 2.8m) and a majority of those were described by an asymmetrical ellipsoidal shape (38%). Along dip the averaged width was 169 m (+/- 166 m) with a mean maximum thickness of 5.4m (+/- 2.5m) and a majority of those were described by an asymmetrical ellipsoidal shape (50%). The combinations of those shapes with the modern analogue of the Mitchell Delta were used as a showcase for building a user-defined object. A reservoir model measuring 1700 x 500 x 50m with 5 x 5 x 0.5m regular grid increments and 3.4 million cells was built to demonstrate the application of that user-defined object to display its reproduction of complex shapes by an object-based algorithm.

The results and methods presented in the current study have shown a unique workflow to automatically and objectively describing geometries from outcrops. This could provide a new approach to storing geometric attributes within sedimentological databases for improved reservoir modelling by not only providing one single value defining the maximum length and width of an object (or width and thickness) but relating those values to a geobody's shape.

PAPER II

III

Global Distribution of Modern Shallow Marine Shorelines. Implications for Exploration and Reservoir Analogue Studies

Global distribution of modern shallow marine shorelines. Implications for exploration and reservoir analogue studies

Björn Nyberg[1,2*], John A. Howell[3]

Uni Research CIPR, P.O. Box 7810, 5020 Bergen Norway.[1]

Department of Earth Sciences, University of Bergen, P.O. Box 7803, 5020 Bergen, Norway.[2]

Department of Geology and Petroleum Geology, University of Aberdeen, Meston Building, Old Aberdeen, AB24 3UE UK[3]

Abstract

Deposits of marginal marine depositional systems make up significant hydrocarbon reservoirs in the rock record. These systems are deposited by a complex interaction between competing depositional processes which can result in heterogeneous and compartmentalised reservoirs. Shallow marine systems are described using a ternary classification which describes the relative importance of wave, tide and fluvial processes at the coastline. With the advent of freely available remote sensing data, modern systems are being increasingly used as analogues for the ancient, however to date, there has been no systematic quantification of the distribution or global proportions of modern paralic systems. The aim of the present study has been to map and classify all of the World's shorelines by dominant and secondary process and to consider the distribution of the different shoreline types with respect to climate, latitude, shelf width and tectonic setting.

The semi-automated classification of marginal marine clastic shorelines has been achieved by combining data from a series of proxies for the key processes (tidal range, mean significant wave height, fluvial discharge). These proxies, combined with data on shoreline morphology have been used to produce an algorithm which predicts shoreline classification with a >85% success rate when compared to manual interpretation. Using this algorithm, the global shoreline has been subdivided into 927,577, 5 km segments and the distribution and proportions of these analysed.

The first order classification is to subdivide the coasts into depositional vs erosional (rocky) coastlines. Depositional systems make up 28% of the total. Within the depositional coastlines 62% are wave-dominated, 35% tide dominated and 3% fluvial dominated. Analysis of the distribution of these suggests a complex network of inter-related controlling factors. Of these palaeo-climate and tectonic setting are reasonably well constrained in the ancient and can be used to predict the probability of a specific shoreline type. In addition to shedding insight into the controls on the distribution of different classes of paralic system, the results of this study can also be used to quickly identify suitable modern analogues for ancient systems, which in turn can be used to extract data for better reservoir characterisation.

1. Introduction

Within sedimentology, paralic and shallow marine depositional systems are traditionally described using a ternary classification based upon the relative importance of fluvial, tidal and wave processes on sculpting the shoreline geomorphology (Galloway, 1975). The different processes will drastically impact the morphology and distribution of sandbodies within a depositional environment and introduce heterogeneity into shallow marine reservoirs (Hampson and Storms, 2003; Ainsworth et al., 2008; Howell et al., 2008; Ainsworth et al., 2011). The advent of freely available, moderate to high quality, remote sensing data has seen a significant increase in the use of modern systems as analogues for the rock record and for hydrocarbon reservoirs in particular. Understanding the distribution of modern shoreline systems and the controls on these distributions at a global scale is therefore highly desirable.

Paralic and shallow marine systems may be classified in a number of different ways. In addition to the ternary plot of Galloway (1975) it is also useful to consider whether the shoreline is in net deposition or net erosion over several distinct timescales. Boyd et al. (1992) subdivided shorelines on whether they were progradational or transgressive noting that there are significant differences in sediment body geometry and distribution between the two. Progradational shorelines occur where sediment supply exceeds accommodation and the shoreline moves basinward through time. They are typically deltas or strandplains. Transgressive shorelines, in which accommodation is greater than sediment supply and the shoreline moves landward through time are dominated by barrier islands and estuaries. In addition to the systems described by Boyd et al. (1992), there are also "rocky shorelines" or "high relief transgressive" shorelines (sensu Howell, 2005) which are parts of the coast that are in long term, net erosion over timescales of millions of years. These were not included in the classifications of Galloway (1975) or Boyd et al. (1992) because they do not become a part of the geological record except as unconformity surfaces (e.g. Sheppard 2006), their recognition is however important in the modern since they account for a significant proportion of modern coastlines.

Prior to the work of Galloway (1975), Wright and Coleman (1973) classified systems based upon the relative importance of fluvial vs "basinal" processes, this work was superseded by Galloway (1975) classification. Orton and Reading (1993) extended the ternary plot into a 3rd dimension with grainsize as the additional parameter. Most significantly Ainsworth et al. (2011) further subdivided the ternary diagram and added a systematic method for the description and classification of shorelines which is described below.

Here we present a global classification of shoreline type based upon previously available data on the distribution of wave and tidal processes and, newly generated data on the relative importance of fluvial processes at and away from specific fluvial input points. These parameters have been quantitatively combined to generate a global classification of shoreline type, based upon the first two levels (dominated and influenced) of Ainsworth et al.'s (2011) modification of Galloway's (1975) classification scheme. The results of this global classification can be used to define the importance of parameters such as shelf width, climate, structure, latitude and basinal energy in controlling shoreline type. The resultant maps can also be filtered by parameters such as climate and basin type in order to locate suitable modern analogues for ancient systems.

2. Previous work on global classification of shorelines

The coastal environment is a dynamic zone which lies between the sub-aerial and sub-aqueous realms. From social, economic, climatic, ecological, biochemical and sea-level

perspectives; it has been the subject of significant research interest (Costanza et al., 1998; Crossland et al., 2003; Talaue-McManus et al., 2003; Jorgenson and Brown, 2005; Buddemeier et al., 2008; Vafeidis et al., 2008; Bird et al., 2013). The nomenclature used to subdivide and classify shorelines typically reflects the needs of the specific field or study. Previous efforts to produce global shoreline typologies include the LOICZ project for biochemical coastal zonation (Crossland et al., 2003; Buddemeier et al., 2008); vulnerability to sea-level rise (Vafeidis et al., 2008) and littoral marine habitat (Bird et al., 2013) databases. To date there has been very few attempts at global classification of shoreline type in a framework that is appropriate to sedimentology and geomorphological.

The first global classification of shoreline by geomorphology and tectonics was by Inman and Nordstrom (1971). This study classified shorelines as mountainous, narrow-shelf, wide-shelf, deltaic, reef or glaciated coasts, within the newly emergent field of plate tectonics, placing them in collisional, trailing edge and marginal sea settings. Second order classifications subdivide these geomorphological categories into wave erosion, wave deposition, river deposition, wind deposition, glaciated and biogenous at scales of approximately ~100km. Dürr et al. (2011) has expanded and digitized the geomorphological classification of coastlines to categorize regionally, locations of small deltas, large rivers, estuaries, lagoons, tidal systems, arheic settings and fjords. Focusing on the application of global fluvial discharge to estuaries, the study is defined at 0.5 degrees (approximately 50km) using the boundaries of river basins as it shoreline delineation (Vörösmarty et al., 2000b, a). In addition, the shoreline classification does not aim to characterize any regional scale variability in its analysis of shoreline geomorphology. Hence while shorelines are segmented at scales of 50km, its dominant classification are typically at scales similar to the delineated by Inman and Nordstrom (1971). For our purpose, these datasets do not provide the level of detail or appropriate nomenclature to efficiently identify suitable modern analogues of the marginal marine.

Regionally, Harris et al. (2002) demonstrated that a distinct statistical variation between wave height, tidal range and fluvial discharge can differentiate recognized classifications of shoreline geomorphology of the Australian coastline. Work by Short (2006) is the result of an impressive 17 year analysis of Australian shorelines (1987-2004) to classify 15 shoreline geomorphologies and their association to four main processes of wave-dominated, tide-dominated, tide-modified and beaches on rocky/coral flats based on tidal range, breaking wave height and manual interpretation of regional maps and aerial photography. Also in Australia, Nanson et al. (2013) made a detailed, manual classification of the marginal marine depositional elements in the Mitchell Delta, Gulf of Carpentaria, using the hierarchical and ternary process classification scheme of Ainsworth et al. (2011) and Vakarelov and Ainsworth (2013). To apply a similar manual interpretation at a global scale is impractical. To our knowledge, no previous global classification of shorelines by ternary process currently exists.

The challenge that remains is to apply the ternary process classification (Galloway, 1975; Ainsworth et al., 2011) to the coastlines of the entire world. The goal here is to apply the ternary plot classification using an automated approach that limits subjective bias and allows for a quantitative study of controlling parameters.

3. Ternary classification of shallow marine systems

The ternary diagram of Galloway (1975) relates the relative influence of fluvial, tide and wave processes on the classification of deltaic environments. Subsequent ternary plot classifications have expanded that concept to describe the range of marginal marine

depositional environments (Boyd et al., 1992; Ainsworth et al., 2011). Recent work by Ainsworth et al. (2011) and Vakarelov and Ainsworth (2013) have incorporated a semi-quantitative method to categorize ancient and modern marginal marine systems by the proportion of elements associated with each process. In this schema they also added two additional degrees of granularity describing dominant, influencing and affecting for the main, second order and third order processes on a given shoreline. This schema then states a depositional environment is classified first by the dominant ternary process (W, T or F) (e.g., Fluvial-Dominated), then by the secondary process (e,g., Fluvial-Dominated, Tide-Influenced) and finally by the tertiary process (e.g., Fluvial-Dominated, Tide-Influenced and Wave Affected; **F**t*w*). This schema gives 15 possible classes. For the purpose of the current worldwide study, we have used the first two-tiers of this classification (Dominated and influenced; Figure 1.).

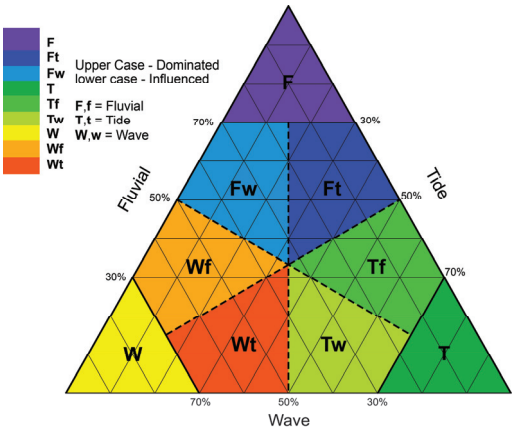

Figure 1. A two tier ternary plot modified after Ainsworth et al. (2011) to classify shoreline type as dominated and influenced based on the relative importance of wave, fluvial and tidal processes at the shoreline. These include; F - Fluvial-dominated, Ft - Fluvial-dominated Tide-influenced, Fw - Fluvial-dominated Wave-influenced, T - Tide-dominated, Tf - Tide-dominated Fluvial-influenced, Tw - Tide-dominated Wave-influenced, W - Wave-dominated, Wf - Wave-dominated Fluvial-influenced and Wt - Wave-dominated Tide-influenced.

This two-tier classification of ternary process modified from (Ainsworth et al., 2011) will describe 9 different shoreline types (**F**, **Ft**, **Fw**, **T**, **Tf**, **Tw**, **W**, **Wf** and **Wt**; Figure 1). The heterogeneity and compartmentalization associated with each shoreline type is important to understanding their potential subsurface reservoir behavior (Hampson and Storms, 2003; Howell et al., 2008).

Fluvial-dominated (**F**) shorelines, Figure 2a, are generally characterized by progradational deltas dominated by a fluvial processes with only very minor wave or tidal reworking. They range in size from small to very large systems dependent on the size of the river discharge. These reservoir systems are composed mainly of mouth-bar sandstones cut by distributary channel deposits. The presence of dipping clinoforms in the mouthbars will impact reservoir performance (Howell et al., 2008). A typical modern example is the Mississippi Delta or the Wax Lake Delta (Wellner et al., 2005) in the Gulf of Mexico. Ferron Sansdtone in Ivie Creek, Utah is an excellent outcrop example (Enge and Howell, 2010; Deveugle et al., 2014).

Fluvial-dominated *Tide-influenced* (**Ft**) shorelines (Figure 2b) are otherwise similar to the geomorphology to the **F** shorelines but they illustrate a strong tidal influence which manifests in the geometry of the distributary channels which are strongly funnel shaped. There are also a series of tidal channels, flats and floodplains on the delta plain. Mouthbars may include a degree of tidal reworking and modification. Modern examples include the Irrawaddy Delta, Myanmar and Ganges-Brahmaputra, India/Bangladesh (Goodbred and Saito, 2012). Reservoir modeling considerations are similar to those of Fluvial-Dominated deltas although channels and mouth-bars may be more heterolithic with more mud draped bedforms.

Fluvial-dominated *Wave-influenced* (**Fw**) shorelines, Figure 2c, are characterized by a deltaic protrusion on the coastline that is heavily modified by wave action. Sediment introduced by the fluvial system is reworked along strike by wave activity. There are a limited number of distributary channels and the mouthbar(s) are heavily modified by wave action. Away from the fluvial entry point the shoreline is dominated by linear sand dominated shorefaces. Beach ridges are common. In systems with a strong component of longshoire drift there may be a difference between the shoreline systems on the updrift and down drift sides of the input point (Bhattacharya and Giosan 2003), The reservoir quality associated with **Fw** systems produces excellent quality reservoirs similar to wave-dominated shorelines although locally their maybe an increase in intra-shoreface shales near the river mouth Eide et al. (2014). Modern examples may include the Paraiba do Sul Delta in Brazil and the Usumacinta - Grijalva delta in Mexico (Bhattacharya and Giosan, 2003).

Tide-dominated (**T**) shorelines, Figure 2d, are characterized by funneled branching tidal channels, tidal bars, tidal mudflats and salt marshes unassociated with any fluvial influence. In the sub-tidal region, migrating sub-tidal dunes lie withinsub-aqueous channels bordered by large sand flats. Landward, the inter-tidal zone is typified by an increasingly mud-dominated and sandy heteroliths. Modern examples include the western portions of the Ganges delta in Bangladesh and India. Due to the heterolithic nature of tide-dominated deposits, these systems make challenging reservoirs though sub-tidal portions may make good reservoirs that are otherwise flanked by a heterogenous inter-tidal zone (McIlroy et al., 2005; Martinius et al 2014).

Tide-dominated *Fluvial-influenced* (**Tf**) shorelines, Figure 2e, are similar to tide-dominated shorelines exhibiting branching and funneled channels, sub-aqueous and sub-aerial tidal bars, tidal flats and floodplains and salt marshes. The main difference is presence of a fluvial component to the system which introduces sediment to the near-shore environment which is then reworked into tidal bars, channels and flats. The distinction between **Tf** and **Ft** is that in the **Tf** the fluvial input is not significant enough to prograde a prominent mouthbar. The shoreline associated with the foreland basin of southern Papa New Guinea is a good modern example of a tide-dominated system that is locally influenced by fluvial input. Reservoirs face similar challenges to those in tide-dominated systems whereby the best quality reservoirs are potentially of the sub-tidal sand bedforms bounded laterally by the inter-tidal heterolithic zone. Fluvial sediment input may locally improve the reservoir quality of those heterolithic zones.

Tide-dominated *Wave-influenced* (**Tw**) shorelines, Figure 2f, are characterized by funneled channels associated with tidal bars, flats, floodplains and salt marshes that are wave-modified to include beach ridges and wave-generated shoreface deposits. In the sub-tidal region, tidal dunes and tidal channels are reworked by wave-generated storm processes. In the inter-tidal zone, tidal flats, floodplains and channels will be modified by wave action to create isolated fore-shore, beach and chenier ridge deposits that are often parallel to an open-body of water. Good quality reservoirs may be associated with these wave-modified shoreface sediments although heterolithc tidal deposits may impede reservoir production. Modern shoreline examples may include portions from the southern Gulf of Carpentaria in Australia or Western regions of Madagascar.

Wave-dominated (**W**) shorelines, Figure 2g, are characterized by linear shorefaces with land attached strandplains often with well-developed beach ridges. Sediment input is from longshore drift and erosion from a nearby erosional shoreline or fluvial output. As reservoirs these systems form excellent laterally extensive (strike) sandbodies that may form thick

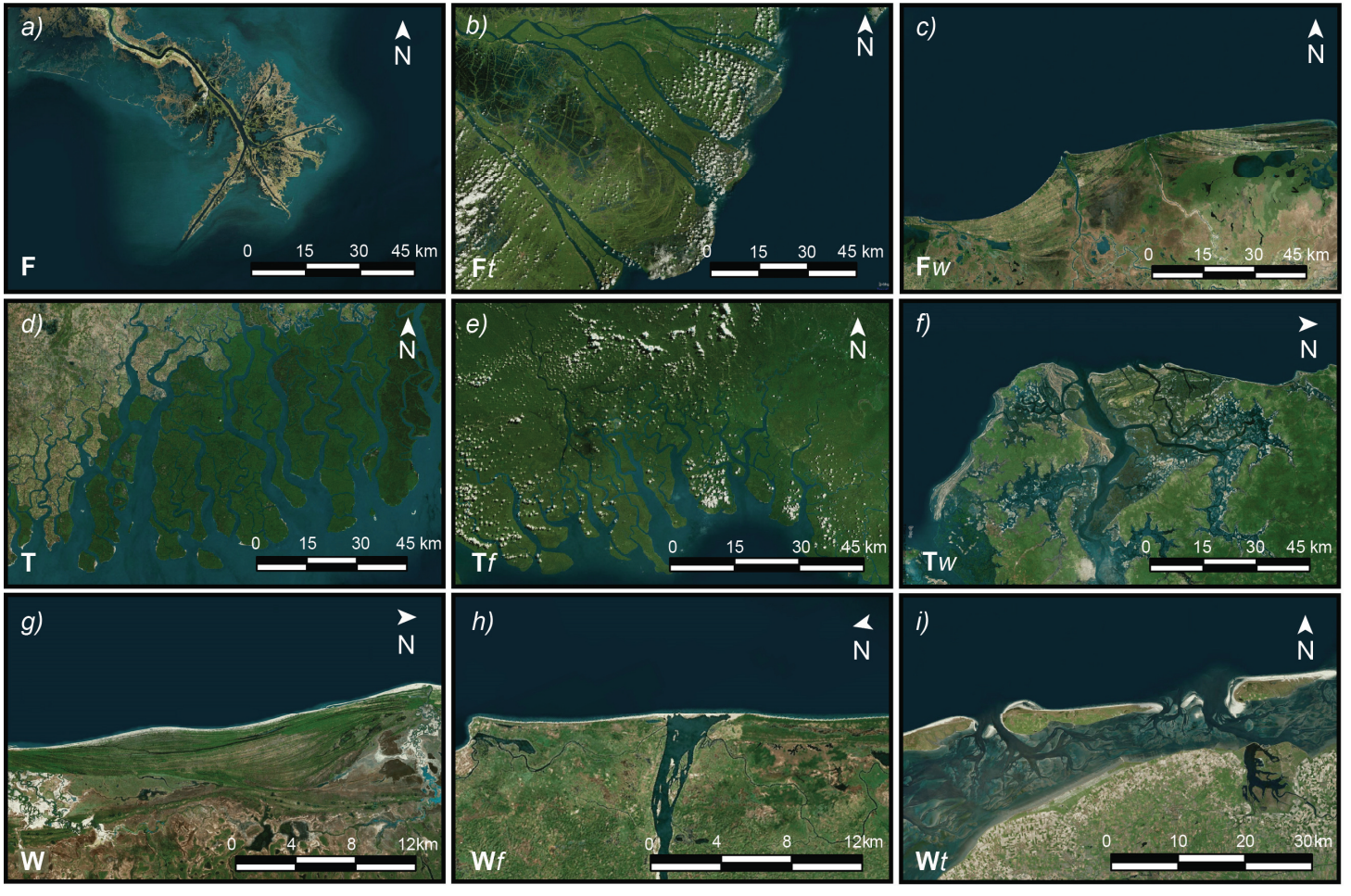
a)
N
F
0 15 30 45 km
b)
N
Ft
0 15 30 45 km
c)
N
Fw
0 15 30 45 km
d)
N
T
0 15 30 45 km
e)
N
Tf
0 15 30 45 km
f)
N
Tw
0 15 30 45 km
g)
N
W
0 4 8 12km
h)
N
Wf
0 4 8 12km
i)
N
Wt
0 10 20 30km

Figure 2. Examples of modern shorelines within the classification of Ainsworth et al. (2011) as used in this study. **a) – c)** display systems dominated by a fluvial component which are characterized by a protruding delta lobe. **a)** shows a fluvial-dominated system (**F**) of the Mississippi Delta in the Gulf of Mexico, USA. **b)** an example of fluvial-dominated, tide-influenced tidal delta on the Mekong Delta, Vietnam. **c)** the Usumacinta - Grijalva delta in southern Mexico, a typical example of a fluvial-dominated wave-influenced (**Fw**) system. **d) – f)** are examples dominated by a tidal component characterized by a shoreline with an overall funnel shaped character. **d)** example of a tide-dominated (**T**) shoreline from a fluvially inactive portion of the Ganges–Brahmaputra Delta in eastern India/ southern Bangladesh. **e)** an example of a tide-dominated fluvial-influenced system (**Tf**) is shown in eastern Papua New Guinea by numerous tidal channels fed by an active fluvial component. **f)** shows an example of a tide-dominated wave-influenced (**Tw**) system in Senegal, Western Africa which is characterized by a funnel shape with prominent beach ridge developments. **g) – i)** show modern systems dominated by wave activity characterized by a linear shoreface profile. **g)** shows a series of linear beach ridge complexes of a wave-dominated (**W**) system of the northeastern Gulf of Carpentaria, Australia. **h)** a wave-dominated fluvial-influenced (**Wf**) shoreline from eastern Madagascar characterized by a linear shoreface profile with a fluvial input source. **i)** an example of a wave-dominated tide-influenced (**Wt**) system where a straight shoreface profile of wave-dominated barrier complex is in-cut by tidal channels. Imagery from Microsoft Bing©.

successive sequences partitioned by flooding surfaces. In transgressive settings, wave-dominated shorelines are barrier islands with similar shoreface profile on the seaward side and lagoons on the landward side. Modern examples may include the Nayarit, Brazilian and much of coastline of the Gulf of Mexico.

Wave-dominated *Fluvial-influenced* (**Wf**) shorelines, Figure 2h, are similar to wave-Dominated shorelines with straight and parallel shoreface deposits with beach ridges. The minor fluvial influence does not generate a protruding delta/mouthbar and is often heavily modified by the wave action. Modern day examples include many systems off the western coast of South America and eastern Madagascar. The subsurface behavior of these depositional environments is similar to the wave dominated systems, with fluvial input points producing minor heterogeneity.

Wave-dominated *Tide-influenced* (**Wt**) shorelines, Figure 2i, are characterized by shoreface systems with a greatly expanded foreshore and beach section, which is exposed at low tide (Vakarelov et al., 2012). The shoreface is also cut by sub-tidal channels. In embayed areas there may be minor tidal flats with tidal channels. Modern examples include many shorfaces of northern Australia and shorelines of West Africa. Many **Wt** reservoirs make excellent reservoirs that are very extensive in a strike direction, although they have greater heterogeneity than their wave dominated counterparts.

4. Methodology

The geometry of paralic and shallow marine sediment bodies is strongly controlled by the dynamic relationship of fluvial, tide and wave processes at the shoreline. The goal of this paper is to produce an automated global classification of modern shoreline type based upon available datasets which describe the distribution of these parameters.

When working at a global scale it is necessary to use numerous data sources, many of which will be proxies for the parameter that is ultimately required. Previous studies have used wave height and/or tidal range to predict geomorphology and/or ternary process at a shoreline (Davis Jr and Hayes, 1984; Harris et al., 2002; Short, 2006; Dürr et al., 2011). The current study combines improved data resolution with a mapped shoreline geometry to produce a much finer resolution and level of detail than has not been achieved by previous global studies

(Dürr et al., 2011). This is achieved by segmenting the shoreline every 5 km's (Wessel and Smith, 1996) for landmasses greater than 250km^2 and mapping the relative global ternary power influencing every stretch of shoreline (Figure 3). It is also important to note that the mapping reflects shorelines processes at the decadal timescale excluding episodic and seasonal variations, while also focusing on the process dominance at the shoreline now rather than mapping the long term evolution of a system. Greenland and Antarctica have been excluded from our analyses because of a lack of digital elevation models (DEM) which are required to calculate fluvial impact.

4.1. Sources of data

Data applied in the empirical classification only considers global quantitative information representing an averaged value in an annual timeframe or greater. The description and further processing of those datasets is described below.

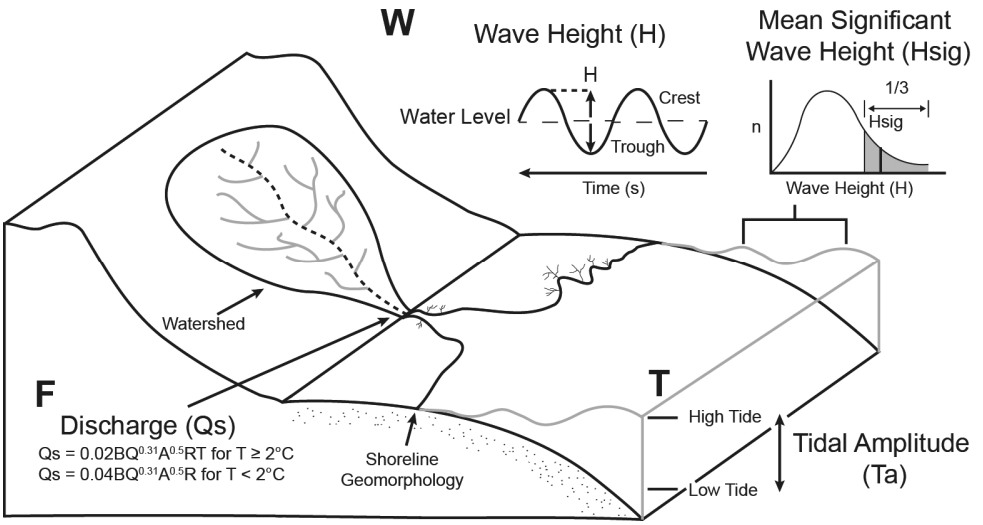

Figure 3. Parameters and datasets used as proxies for the automated ternary process classification (**F, T** and **W**) of a given shoreline section. Fluvial proxy (**F**) is determined from discharge (Qs) based on the area of the watershed, relief, lithology and temperature (see text; Milliman and Syvitski, 2007). Tidal proxy (**T**) is defined by the amplitude for each tidal constitute that combined compose the tidal range. Wave proxy (**W**) is based on mean significant wave height (Hsig) defined as the mean of the third highest wave heights where a wave height (H) is determined as the height between the trough and crest of a wave.

4.1.1. Mean Significant Wave Height

Mean significant wave height (Hsig) is a measurement of the mean of the third highest wave heights. A wave height is defined as the distance between trough and crest between any given wavelength cycle (Figure 3; Tolman, 2002).

A global dataset of Hsig has been amalgamated from two sources to provide seamless coverage. The first source of data is provided by the National Oceanic and Atmospheric Administration (NOAA)'s WAVEWATCH III program (Tolman, 2002). The mean of over 20,000 hindcast datasets calculated every 3 hours between 2006 and 2013 were combined and provide global coverage including significant regions of the arctic at 0.5 degree resolution

(approx. 50km). Though, the Mediterranean, Black Sea, Red Sea and the Persian Gulf are not included in this model. To supplement those regions, the WorldWaves Global Offshore Database developed by Fugro OCEANOR was used, an analysis of Hsig between 1997 and 2006 (Mørk et al., 2010). The global dataset is gridded at a 0.5 degree resolution (approx. 50km) based on the European Centre for Medium-range Weather Forecasts (ECMWF) models relying on Topex satellite altimeter data that are subsequently calibrated to global buoys. Hsig used in this study ranges from 0 to 4.4 m.

4.1.2. Tide

Global tidal models have been derived through the Global Tide FES2012 (Carrère et al., 2012) project available through Aviso (Aviso, 2012). This model is based on altimetry datasets in conjunction with improved bathymetry and tidal barotropic equations to provide global coverage at a 1/16 degree resolution to model 32 individual tidal constitutes. Here we use the main diurnal (K_1, O_1) and semi-dirunal (M_2 and S_2, N_2) tidal constitutes to map global tidal range as $2(K_1 + O_1 + M_2 + S_2 + N_2)$. The global tidal range used in this study varies from 0 to 13.8 m.

4.1.3. Fluvial

There is no global dataset that provides direct information on mean fluvial discharge for all of the World's rivers. These proxies are derived from hydrological models that study the contributing drainage area (watershed) to a sink (pour point) by analyzing digital elevation models (DEM) that reflect its fluvial network. Many studies have proposed basin delineation and global discharge models that reflect that watershed (Milliman and Syvitski, 1992; Vörösmarty et al., 2000b, a; Fekete et al., 2002; Global Runoff Data Centre, 2007; Milliman and Syvitski, 2007). The current study requires a global exoheric analysis of relative fluvial discharge at its fluvial mouth at a resolution that captures the variability of small fluvial rivers that may influence shoreline geomorphology. This is important as it is recognized that small mountainous rivers have significance to the fluvial discharge budget (Milliman and Syvitski, 1992) and thereby by extension modern coastline geomorphology. For this purpose, we feel that existing digitally available basin discharge models (Vörösmarty et al., 2000b, a; Fekete et al., 2002; Global Runoff Data Centre, 2007) are insufficient in capturing those small rivers.

To provide the highest possible fluvial discharge model we use two amalgamated sources to delineate basin watersheds worldwide. A 15-arc second watershed derived from the HydroSHEDS project (Lehner et al., 2008) based on a hydrologically conditioned SRTM digital elevation model (DEM) at a 90 m resolution data between 60 degrees north and south. To supplement this dataset in the northern parts, a 15 arc-second breakline emphasis (a resampled DEM that highlights ridges) of the GMTED2010 DEM dataset (Danielson and Gesch, 2011) was used to calculate watersheds utilizing standard hydrological tools available in ArcGIS (ESRI, 2014). A relative discharge associated with this watershed model followed the proposed methodology of Milliman and Syvitski (2007) with the assumption that this finer watershed model upscales accordingly. This is based on equation 1;

$$Qs = 0.02BQ^{0.31}A^{0.5}RT \; for \; T \geq 2\,^{\circ}C \qquad \text{eq. 1a}$$

$$Qs = 0.04BQ^{0.31}A^{0.5}RT \; for \; T < 2\,^{\circ}C \qquad \text{eq. 1b}$$

$$Q = 0.075A^{0.8} \qquad \text{eq. 2}$$

where Qs is discharge in kg/s, B captures information regarding lithology, glacial erosion and

anthropogenic conditions, Q is watershed discharge in m^3/s (eq. 2) , A is watershed area in km^2, R is maximum relief in km and T is mean basin temperature in Celsius. Lithology is based on a systematic analysis of global maps produced by Syvitski and Milliman (2007) showing the distribution of the major 425 basins. Smaller basins were based on the proportion of lithologies (Dürr et al., 2005) within each watershed as defined in Table 1, reflecting the description of lithologies and coefficient used by Syvitski and Milliman (2007). We ignore anthropogenic conditions and ice erosion in our calculation that may attribute an additional 17% to the observed discharge (Milliman and Syvitski, 2007).

Table 1. Lithologies and thresholds used to determine the lithology factor (B) of watersheds. Dominant threshold defines the threshold percentage that the lists of lithology codes compose the lithology of the watershed. Otherwise a default value of 1 is taken. Hard rock = Pr, Pb, Pa, Mt, Cl; volcanics = Va and Vb; sedimentary = Ss, Sm Su; carbonates = Cl; Ad = Alluvial

Category	Dürr *et al* (2005) Lithology Code	Dominant Threshold	Lithology Factor
Hard rock acid plutonic or metamorphic rocks	Pr, Pb, Pa, Mt, Cl	> 80% hard rock	0.5
Hard rock but mixed lithology	Pr, Pb, Pa, Mt, Cl	>80% hard rock & > 50% Cl or > 20% hard rock & >10% Vb or Va	0.75
Volcanic, carbonate outcrop or mixed hard/soft lithologies	Va, Vb, Sc, Ad	> 20% volcanics/carbonates & < 35% Ad & < 20% Sm	1
Soft lithologies with significant hard rock lithologies	Ss, Sm, Su, Sc, Ad	50 - 65%	1.5
Predominatley soft lithologies	Ss, Sm, Su, Sc, Ad	> 65%	2

Maximum relief, R, is taken as the highest elevation within its given watershed based on GMTED2010 data at a 15-arc second resolution (Danielson and Gesch, 2011). Mean temperature, T, is taken from MODIS, the annual day-time land surface temperature of 2013 (NASA LP DAAC, 2001). A visual inspection of the resulting distribution of watersheds with high resolution satellite imagery deemed that a discharge (Qs) greater than 5 captured most small fluvial outputs that influenced the morphology of the shoreline relative to the 5km segmentation. For dry hot desert localities defined by a Bwh or Bwk of the Köppen-Geiger classification scheme (Kottek, 2006), a higher threshold of 15 Qs was more appropriate, in particular to exclude such areas as the Skeleton coast of Namibia. The resulting discharge thereby ranges from 5 to ~57,000 kg/s (Amazon Delta).

A fluvial mouth is defined here as a stretch of shoreline that intersects with a watershed or a watersheds closest proximity to a shoreline. As a watershed is a tributary function draining to a single point according to its upstream DEM accumulation profile, the distributary character of multiple channels fan from an apex, especially in fluvial dominated systems is not captured. To address this issue, the discharge associated with a single watershed of the world's major river deltas (e.g., Makaham, Nile) were manually assigned to adjacent fluvial mouths characterized by an individual river and protruding delta lobe. 6991 fluvial mouths were identified globally.

4.2. Combining the parameters to classify the shoreline segments

Mean significant wave height (Hsig) is used as the base value. The relative tidal power is corrected by a coefficient, *K*, in equation 3 to correct for its higher amplitude, as noted by Harris et al. (2002). The relationship best suited to represent the relative fluvial influence of a

coastline is determined by equation 4 where Qs is the discharge in kg/s and D is the distance from fluvial mouth. This states that the relative fluvial influence decreases at half the cubed rate with distance from its fluvial mouth whereby the minimum distance is ≥ 10km. The initial fluvial mouth outlet is given a distance of 5km as we hypothesis that this initial contact will have a stronger fluvial impact. As multiple fluvial outputs may be insignificant compared to a nearby larger fluvial system, this algorithm will determine the largest relative influence at a particular location according to equation 4 rather than to its closest fluvial output mouth.

$Tide = TaK$ eq. 3

$Fluvial = \frac{1}{2}(Qs/D^3)\ where\ D\ is \geq 10km$ eq. 4

These function and thresholds were determined after iterative examination of their relative sensitivity above and below those deemed most suitable. This relationship provided a reasonable shoreline type description of ternary process based on visual inspection using high-resolution satellite imagery (see procedures outlined in section 5.2.). However, regional variability associated with depositional versus erosional coastlines and shoreline geomorphology is not considered. This challenge has been addressed below.

4.2.1. Depositional versus erosional

Inman and Nordstrom (1971) used a shoreline nomenclature that separated mountainous and erosional shorelines from depositional shorelines associated with wave and fluvial deposits. Defining this in the current study is important for two reasons i) the ternary process classification and, ii) when looking for modern analogues for ancient systems.

To separate depositional environments from erosional (rocky) shorelines, a high resolution global lithological map (Hartmann and Moosdorf, 2012) was assigned to the most proximal stretch of coastline whereby waterbodies (wa) or unconsolidated sediments (su) were defined as potentially depositional. This does not however differentiate thin veneers of sediment that may be associated with mountainous rocky shorelines and as such digital elevation models of the world, SRTM (Reuter et al., 2007) and GMTED2010 (Danielson and Gesch, 2011), were used to highlight low lying gradients (<0.8) regions that are above 250km^2 in area. An examination of the difference between the two datasets highlighted on a regional scale, areas that are in net erosion, in particular, the shorelines of eastern Chile off the Andes and many Pacific islands were excluded to produce the final product shown in Figure 4.

The relative tidal influence of equation 4 in relation to those erosional coastlines was found to be significantly less than depositional settings and as such a coefficient of tide * 0.25 is applied. A subcategory of erosional settings, Fjords, as defined by Dürr et al. (2005), were deemed even less tidally influenced, an important distinction to define the particularly wave-Dominated shorelines of the Labrador Sea, offshore Northwestern Canada and Eastern Greenland with a coefficient of tide * 0.15.

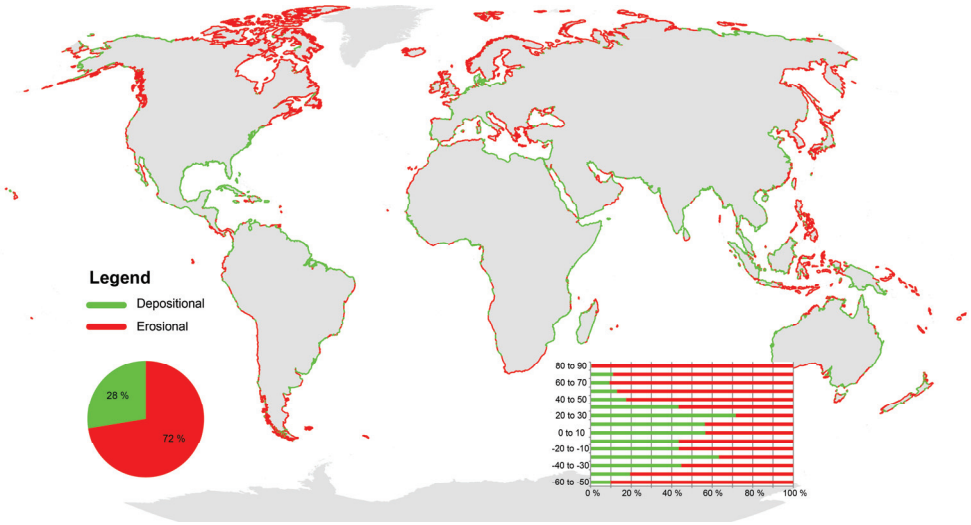

Figure 4. Global classification of shorelines as erosional (rocky) or depositional. Pie chart and a 10 degree binned latitude graph show the proportion and latitude related distribution of erosional versus depositional shorelines.

4.2.2. Geomorphology

In a global study such as the present one, the resolution of data that describes the relative basinal energy components (i.e. tide and wave power), may not be able to capture the smaller scale subtleties associated with coastline geomorphology which may locally, significantly modify the relative dominant depositional process. To capture these subtleties in the absence of more detailed global data series, modifications were assigned to the various parameters based on the shoreline geometry. Observations of modern systems indicate that shorelines are more likely to be wave dominated if they are straight and smooth (Davis Jr and Hayes, 1984) and more likely to be tide modified when characterized by highly embayed, rough shorelines with funnel shaped features (Ainsworth et al., 2011). Therefore a measure of the plan view "shoreline roughness" can be used to improve the predicted classification from the purely process based approach.

To measure coastline geomorphology a function of roughness index, RI, (shoreline length / shortest distance) was used to distinguish relatively smooth shoreline stretches from rough shorelines, Figure 5. Within depositional settings, a very rough shoreline (RI >2) such as many portions of western Florida in the Gulf of Mexico, have a slightly higher tidal influence and therefore the tidal strength is increased by a factor of *1.5. In contrast extremely straight shorelines (RI <1.15) will have a higher probability of being wave-dominated and the tidal strength is reduced (* 0.6).

In erosional settings that have rough shorelines are not necessarily associated with a higher tidal influence but rather a rocky coastline with erosional inlets (e.g. Mediterranean) that otherwise do not have the ability to rework unconsolidated sediment. Straight shorelines of erosional settings (rocky coastlines) are particularly wave-dominated, even in macro-tidal settings (e.g., Bahia Grande, Argentina or Sea of Okhotsk, Russia), as are shorelines associated with desert climates (defined here by a dry hot desert climate classification, Bwh or Bwk, of Kottek (2006)), and those regions were assigned a lower tidally influence by a function of tide * 0.25.

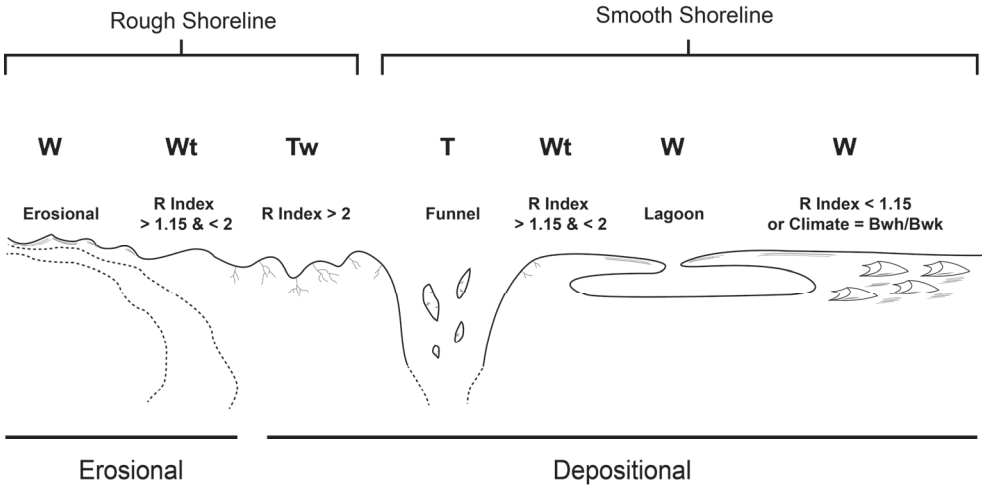

Figure 5. Shows a schematic illustration of the variation of shoreline geomorphology of erosional and depositional settings. Smooth shoreline stretches measured by an RI index less than 1.15 may comprise aeolian, beach ridge and lagoon environments and have a higher probability of wave-dominance (e.g., **Wt** or **W**). In contrast rough shoreline stretches (RI > 2) have a higher probability for tidal modification (e.g., **T** or **Tw**), expect for erosional headland settings. However funnel shaped shoreline geomorphologies may have a smooth shoreline that otherwise are tide-dominated (**T**).

Funnel shaped shorelines are not captured well by the RI index, for instance the tide-dominated channels of the Niger Delta, Nigeria, Figure 6A, have a relatively smooth shoreline when examining the 5 km coastline segments used in this study, Figure 6B. This piece of shoreline is clearly funneled and tide dominated therefore an alternative modification is required. While it may be possible to define these funnels using an adaptive RI method that would determine the appropriate shoreline length to measure over its shortest path, this was not considered due to the complexity its implementation on a global scale.

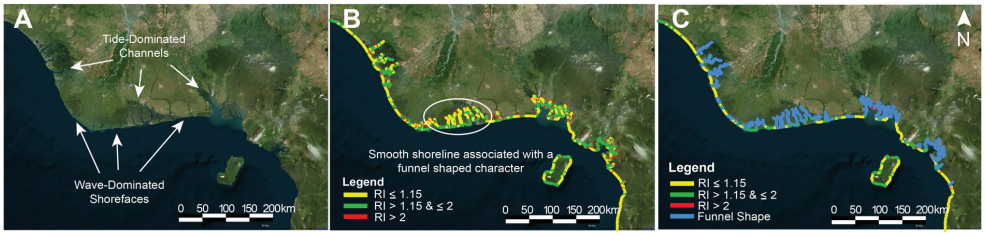

Figure 6. Illustrates the problem arising from the characterization of shoreline geomorphology solely based on the calculation of a shoreline roughness index (RI in Fig. 5). **A** shows satellite imagery of the Niger Delta in Nigeria (see Figure 7) which is characterized by a mix of tide-dominated channels and wave-dominated shorefaces. **B** shows the calculation of a RI index based on 5 km shoreline segments to identify a significant portion of smooth shorelines within a tide-dominated funnel shape. One solution is presented in **C** that will define funnel shapes as those sections of shoreline that intrude landwards to create a funnel shape with a perpendicular landmass within 35 km. Imagery from Microsoft Bing©.

Instead, a funnel shaped stretch of shoreline was determined by an additional algorithm. The first step of this algorithm calculated the seaward direction along a stretch of shoreline as the direction that is not adjacent to a terrestrial landmass (Wessel and Smith, 1996). Once the

seaward direction was determined, a second stage measured a 35k m perpendicular line to each 5km segment of shoreline and calculated whether that intersected with the same landmass body. If it did, it was assigned as funnel shaped, Figure 6C. It will also register a funnel if the orthogonal landmass to a shoreline is depositional whether that be a strait (e.g. Strait of Malacca) or tidal bars within a larger funnel shape (e.g. Amazon). To ensure that funnels were not registered in enclosed lagoons or fjords, the global definition of Dürr et al. (2011) has been used to eliminate those from consideration. Manual modification to the definition of lagoons was made to correct for its lower dataset resolution (e.g. to separate estuaries of North Eastern USA from their lagoons). Restricted bays that are embayed but otherwise wave-dominated may partly be classified as funnel shaped however their relative openness will tend for their automated funnel length calculation to be rather small, an important step in determining tidal impact of a funnel in the next step although this is also a source of potential error. Therefore minimal manual editing was performed to address a few of those concerns to produce the map in Figure 7.

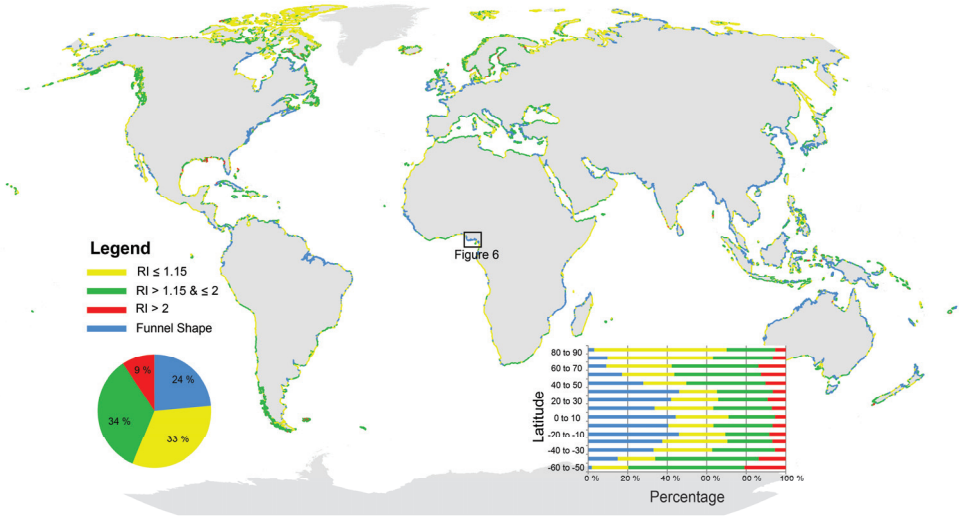

Figure 7. Global shoreline geomorphology displayed with a pie chart and a 10 degree binned latitude graph to show the proportion of RI indices and funnel shaped shorelines. The black box shows the locality of the Niger Delta, Nigeria, used in the example for Figure 6.

The relative impact of a funnel shape on the shoreline process dominance was determined by a combination of funnel length and relation to the tidal range. The length of a funnel was determined as the cumulative length that a stretch of shoreline is determined to be within the confines of a funnel shape, while tidal range is split into microtidal (<2m), meso-tidal (2-4m) and macro-tidal (>4m; Davies, 1964). Here we use these as a proxy to relate a relative funnel by its tidal range although we recognize that the geomorphological shape, bathymetry, volume and its relation to tidal prism are not considered. The tidal power is amplified in equation 5 by a funnel geomorphology coefficient (Fg), which is determined by the tidal range and funnel length (Fl) in km. Unlike an RI index, a funnel shape greater than 10km (limit of the shoreline segmentation resolution) can be determined regardless of size.

$Fg = \frac{Fl}{25} if\ Fl \geq 25\ km$ for micro-tidal conditions ($\leq 2m$) equation 5a

$Fg = \frac{Fl}{15} if\ Fl \geq 15\ km$ for meso-tidal conditions ($> 2 \leq 4m$) equation 5b

$Fg = \frac{Fl}{10} if\ Fl \geq 10\ km$ for macro-tidal conditions ($> 4m$) equation 5c

One further consideration is that micro-tidal lagoons (lagoons with a tidal range less than 2 m) were considered to be influenced by minimal tides and thereby a function to the tidal power of tide * = 0.01 was applied (e.g., Gulf of Mexico). By combining the influence of depositional versus erosional shorelines and coastline geomorphology, a set of coefficients have been determined to describe the dominant basinal energy components. The relative influence of those tide and wave components were renormalized to its original basinal energy to ensure that it remained relative to the fluvial component in equation 4.

4.3 Shoreline Classification

Once values of fluvial, tide and wave power have been derived for each 5 km stretch of shoreline their values were combined and the segments classified according to the two-tier ternary scheme described above (Fig 1).

The final modification is reserved for small fluvial mouths that were deemed significant in section 4.1.3., though had a discharge too small to be proportionally significant in the proposed classification algorithm, particularly in high energy environments. Thereby, any small fluvial output connected to a shoreline that was not assigned a fluvial classification was assigned as having a fluvial-influenced parameter. These regions are of particular importance in mountainous regions where there are numerous small fluvial input points such as the Andes in South America and eastern portions of Madagascar (e.g., Figure 2h).

5. Results

5.1. Global Distribution

A total of 246,777 segments were classified representing 927,577 km of coastline (Fig 8). These results show that the majority (84%) of the World's coastlines are wave dominated, of which 74% are **W**, 8% **Wt** and 2% **Wf**. Waves are especially important in erosional coastlines and the percentage figures are somewhat skewed because of the irregular geometry of such shorelines exaggerates their global significance. In particular, Fjords, which comprise nearly 41% of the global shoreline length . Tidal systems make up 16% of the global shorelines; **T**, **Tw** and **Tf** have a relative distribution of 10, 5 and 1 % respectively. Fluvial dominated systems make up <1% of the global shoreline. The global distribution show that most shorelines are wave dominated, including most of South America, southern portions of Australia and Africa, New Zealand, Japan, Eastern Madagascar, Northeastern China and a majority of the Arctic. Tide dominated portions are constrained primarily to the mid latitudes in areas such as northern Australia, Southeast Asia, Indonesia, Malaysia, Papa New Guinea, Brazil, India and West Africa.. The major fluvial deltas are associated with major drainage basins on passive continental margins include the Amazon, Irrawaddi, Mississippi, Danube, Ebro, Martaban, Nayarit, Po and the Sao Francisco deltas. Numerous smaller fluvial outputs are distributed throughout the world with notable **Wf** settings on the western coast of South America, Figure 9A and Eastern coast of Madagascar and **Tf** are particularly common around southeast Asia.

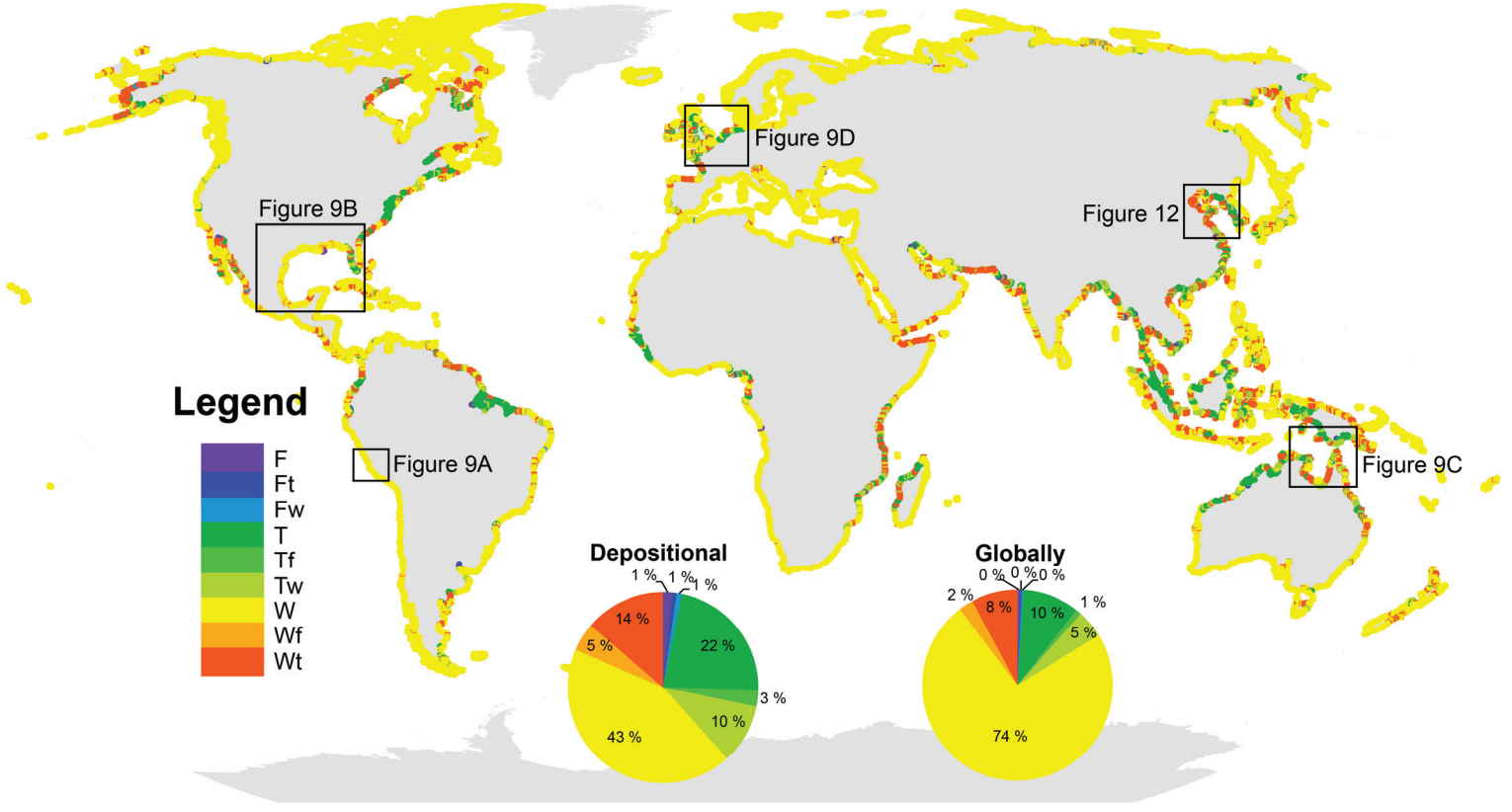

Figure 8. Global two-tier ternary process classification (Fig 1) of modern shorelines. The two pie charts show to the proportion of the ternary process within depositional settings and globally (see Figure 4). Black boxes show the extent of insets used in Figure 9 and Figure 11 to show higher resolution examples of the classification.

Depositional shorelines show a similar distribution to the global shorelines with a majority of wave dominated processes. However the predominance of wave dominated processes (W, Wt and Wf) is less, representing only 62% of the total, while tidal processes increase to 35% and fluvial processes are represent by 3%, Figure 8. The most significant change is the decrease of **W** shorelines by nearly half from 74% to 43% in depositional settings. This decrease in wave processes is related to an increase in **T** shorelines from 10% to 22% and **Tw** shorelines from 5% to 10%. Fluvial conditions are more pronounced with fluvial-dominated systems (**F**, **Ft**, **Fw**) all increasing above 1% and both **Wf** and **Tf** systems increase to 5% from 2% and 3% from 1%, respectively. Figure 9 shows four selected regional examples around the world that represent a variety of different shoreline types.

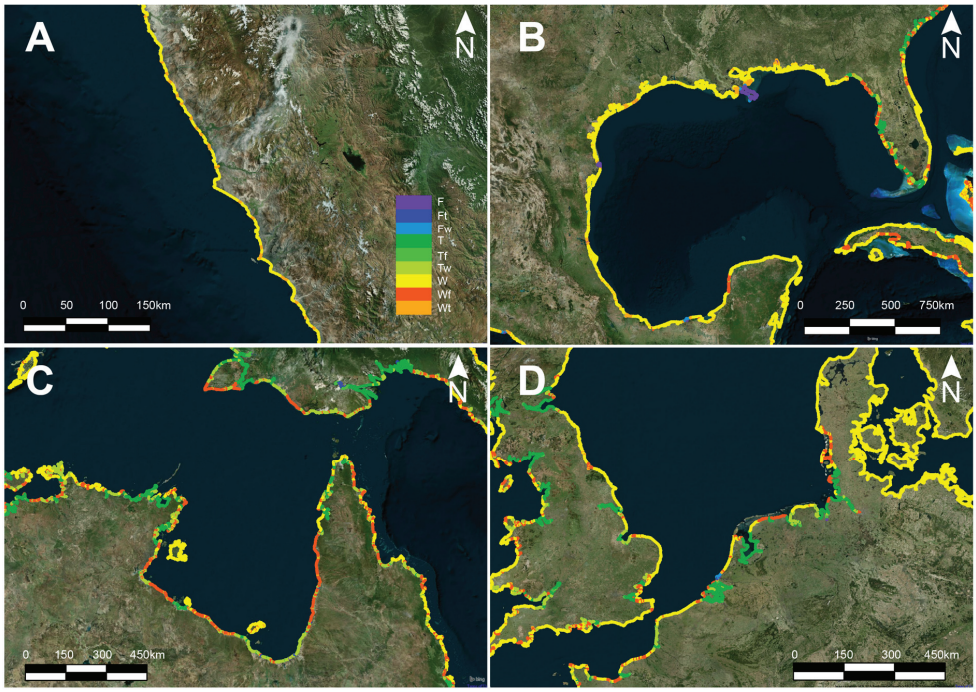

Figure 9. Selective examples of ternary process classification from the insets shown in Figure 8. **A** shows a **W** shoreline with regular fluvial inputs to yield a **Wf** shoreline on the Peruvian coastline in South America. **B** shows a predominately depositional and wave-dominated coastline in the Gulf of Mexico with numerous fluvial inputs to create **F** shorelines in the low basinal energy environment such as the Mississippi and Usumacinta - Grijalva Delta. **C** shows a mixed-influenced regional scale overview of the Gulf of Carpentaria in northern Australia and eastern Papua New Guinea. The Gulf of Carpentaria is characterized by a transition from a **W** process on its north-eastern margin transiting to a more-mixed influenced and **T** process southwards that develops into a predominately **Wt** environment with embayments of **T** and **Tw** towards the west. **D** shows an example from Europe to show wave dominated shorelines interweaved by tide-dominated shorelines and deltas such as the Rhine-Meuse Delta. Imagery from Microsoft Bing©.

5.2. Validation & Quality Control

To validate the accuracy of the proposed classification, 100 points within depositional settings (Figure 10) were chosen at random and manually classified from high resolution satellite imagery based on the geomorphology (e.g., Figure 2) following the classification

scheme of Ainsworth et al. (2011). The results are summarized in Table 2 to show a correct matrix for the proposed automated classification versus its manual interpretation. 85% of those localities were classified correctly by the automated algorithm and an additional 8% identified the dominant process correctly. 7% were identified as partially correct and no classifications were completely wrong within the sampled quality control region.

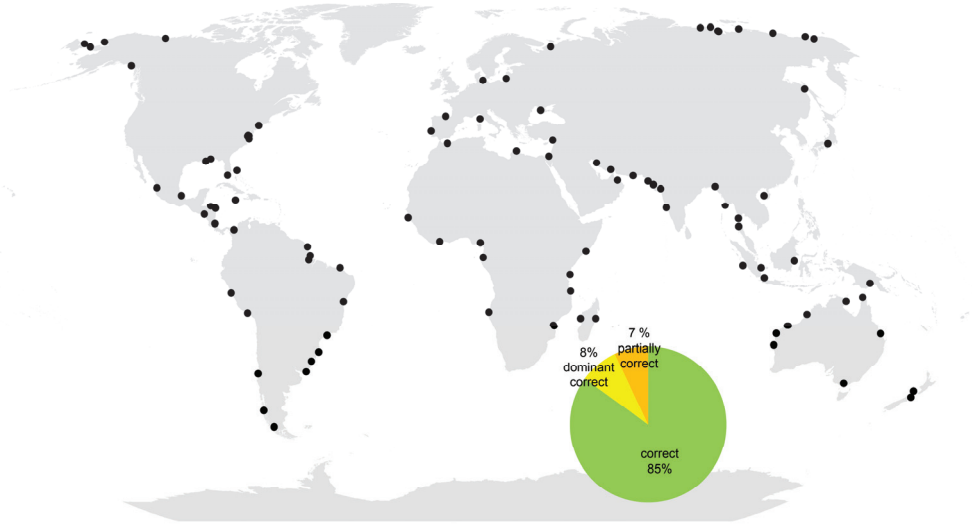

Figure 10. Random selection of 100 samples points used to quality control the automated classification versus a manually assessment (Table 2). A pie chart shows the proportion of those samples where the automated classification is correct, dominant process is correct or partially correct.

Table 2. Shows the number of correct values the automated classification identifies in comparison to a manual interpretation from high-resolution satellite imagery of 100 randomly selected points (Figure 10) on the global shoreline shorelines. Green boxes indicate that the classification is correct, yellow boxes show that the dominant process is correct, orange boxes show that the classification is partially correct and red boxes indicate that the classification is completely wrong.

		Automated Classification								
		F	Ft	Fw	T	Tf	Tw	W	Wf	Wt
Manual Interpretation	F	1								
	Ft	1	1		1					
	Fw			3				1		
	T				20		3			3
	Tf					2				
	Tw				2		5			
	W							42		
	Wf							1	5	1
	Wt				1		1			6

5.2.1. Comparison to previous studies

A comparison of the result gathered in the current study to the manual quantitative

analysis by Short (2006) of Australian coastlines is summarized in Figure 11 to show comparable findings both visually (see Figure 13 in Short, 2006) and quantitatively. The southern coastlines of Australia are highly wave-dominated related to the open-body of water and narrow shelves to create wave-dominated estuaries, deltas, lagoons and strand-plains. The northeastern coastline shows an increasingly tide-dominated characteristic although isolated packages of strand-plains and wave-dominated deltas are found along the rocky shoreline of the Great Escarpment. Towards the northwest, a wide continental shelf may promote a higher tidal influence although a few wave-dominated strand-plains are consistent with this area. Finally the restrictive Gulf of Carpentaria is a highly mixed process environment but shows a general trend from a wave-dominated northeastern shoreline towards a tide-dominated southern shoreline followed by a mixed process of tide and wave before a tide dominated northwestern shoreline, Figure 9C. Interweaved within this complexity are multiple fluvial inputs to yield significant delta developments.

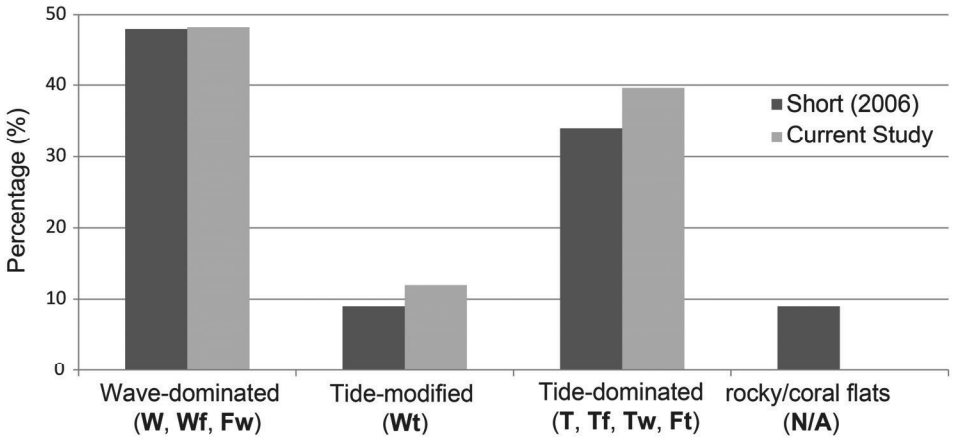

Figure 11. A comparison of the manual shoreline classification defined of Short (2006) for the Australian coastline and its corresponding automated classification used in this study denoted by bold letters within brackets. Note that the beaches associated with rocky/coral flats category of Short (2006) do not have a corresponding classification in the current study. **F** shorelines that represent less than 1% of Australian coastlines have been excluded.

Expanding the resolution and detail captured around Australia to the global scale and comparing that to the previous global shoreline typology study of Dürr et al. (2011) show some distinct differences. Most notable is that tidal systems of the current study have decreased on a global scale from 22% to 16%.

This can be accounted for in the present study by improved datasets that have been used to capture an improved shoreline delineation which has been used to capture regional variability. For instance, the Yellow and Bohai Sea, is represented by a high tidal range however a significant portion of the eastern shoreline is represented by a wave-Dominated coastline that in part is captured by the model here (Figure 12). In general, this region shows that erosional settings are predominately wave-dominated while tidal influence is restricted within protected embayments and funnels. Mapping the individual fluvial outputs rather than stretches of coastline that contain fluvial output show that fluvial may be significantly less at 3% than previously thought (32%; Dürr et al. 2011).

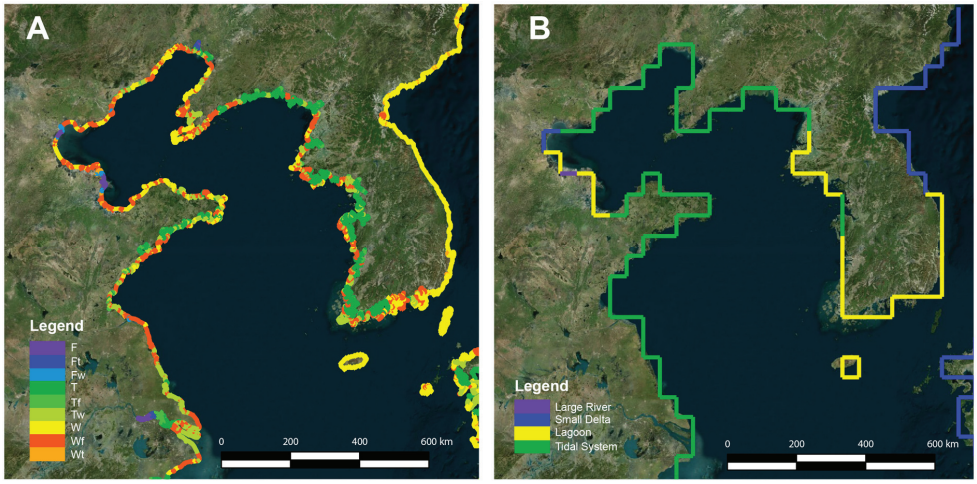

Figure 12. Comparison with previous work in the Yellow/Bohai sea in eastern China/North and South Korea (see Figure 8). **A** shows the ternary process classification used in the current study. **B** shows the classification scheme of Dürr et al. (2011) for the same region. Note the discrepancy in resolution and the added variability captured by the current model. This increased resolution highlights a more wave-dominated environment, particularly on the eastern shorelines of the Yellow Sea and the Bohai Sea. Imagery provided by Bing©.

5.2.2 Sources for Potential Error

While the overall match between the automated manual classifications is reasonable (Table 2; Figure 11, 12), it is useful to consider the sources of the errors that are observed. These errors are considered to have arisen for a variety of reasons. Firstly, the resolution of the data that were used to construct the classifications is significantly lower than the subsequent classification. The wave power (mean significant wave height) has a gridded resolution of approximately a 50 km (0.5 degrees) and the tidal data is gridded at every 6 km (1/16 degrees). Both datasets typically model offshore oceanic conditions well but are less accurate in shallow conditions. These were then used to classify the coastline into 5 km intervals. It is therefore possible that detail is lost here. Data for watersheds and fluvial output is generated from a delineation of drain basin area from a global digital elevation models (DEM) and uses empirically derived relationships to determine output and delta mouths, this is also a potential source of error. A further source of error in the fluvial portion of the input is that the output from a fluvial system at the river mouth is assigned to a single node which in larger deltas, with distributary patterns on the delta plain may reduce the wider spread of fluvial influence along the coastline. Finally the results of the algorithm are also heavily influenced by shoreline morphology and there is potential error in the shoreline delineation defined by Wessel and Smith (1996) which may propagate into the classification present herein.

The majority of errors occur in low energy environments where the systems are very sensitivity to the relationship between tide and wave heights as those values converge around zero (Davis Jr and Hayes, 1984) making a basinal process classification increasingly susceptible to change. While the classification is not perfect and there is considerable potential for error we feel that the accuracy presented here appropriately defines ternary process on a global scale with an element of regional variability to a level that is useful and

can shed light on the global controls on shoreline type.

6. Correlation and causation; controls on shoreline geometry

Figure 8 shows the global distribution of depositional process, highlighting the relative proportions on all shorelines on shorelines that are depositional. In the following section we attempt to investigate this distribution by correlating it against a series of parameters that are traditionally thought to exert some control on shoreline systems. These include latitude, shelf width, tectonic basin type and climate. Whilst correlation does not always imply causation, the results shed interesting light on the relative importance of these factors.

6.1. Latitude

The relative proportions of the 9 process classes were analyzed in 10 degree latitude bins (Figure 13). Results show that the equatorial and mid latitude regions show a more mixed process environment (**T**, **Tf**, **Tw**, **F** and **Ft**) which passes to greater wave dominance at higher latitudes. A similar bell-shaped profile is shown for **Wf** and **Wt** which are more common around the equatorial and mid-latitudes in comparison to higher latitude regions. This is a reflection of the distribution of depositional shorelines at present (see Figure 4), which are concentrated around the equatorial and mid-latitudes.

Plotting the basinal energy (combined tide and wave) by latitude shows a general decrease towards the northern hemisphere, with the exception of a significant peak around 50 and 60 degrees latitude (Figure 14A; B). This overall northward decrease in basinal energy mirrors the proportion of land versus ocean by latitude which shows the opposite trend (Figure 14C) suggesting that basinal energy is greater where there are large open bodies of water. This trend drastically changes at approximately 60 degrees North as basinal energy peaks in correspondence to the highest proportion of land (over 70% between 60 and 70 degrees North). This would suggest that the configuration of continents today acts as a funnel constricting the strongest tides and waves around the Labrador Sea offshore Greenland and Bering Sea/Gulf of Alaska. This may restrict a significant proportion of tidal resonance from the arctic which makes it difficult for large tides to propagate while recent sea-ice loss may be increasing wave-action in those settings (Overeem et al., 2011). The energy environment is largely controlled by the tectonic plate distribution of the present day.

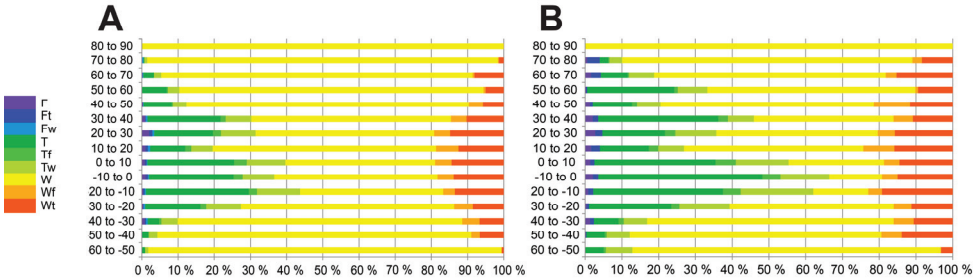

Figure 13. **A** shows the global distribution of ternary process in 10 degree latitude bins. **B** shows the distribution of ternary process in 10 degree latitude bins for depositional shorelines. Both graphs show that the distributions of mixed-process environments (fluvial, tide and wave) are centered on mid- and equatorial-latitudes whereas wave-dominated shorelines increase towards the poles. Depositional settings are more mixed-influenced but otherwise show a similar profile to the global distribution.

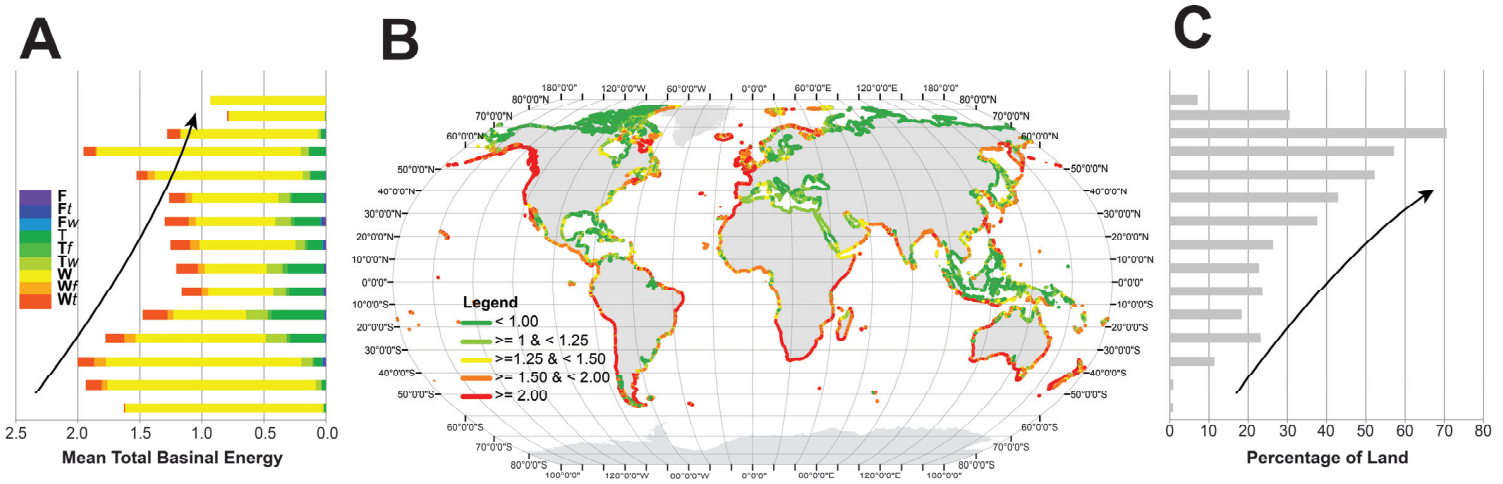

Figure 13 – The relationship between basinal energy and landmass by latitude. **A** the mean total basinal energy (tide and wave) by latitude overlain by the ternary process in Figure 13A. **B** the global shorelines classified by mean basinal energy. **C** the percentage of land by latitude corresponding to the map in **B**. The plots suggests a general decrease in basinal energy while a contrasting increase in the proportion of land versus water towards the northern hemisphere.

6.2. Fluvial Distribution

An analysis on the distribution of fluvial outputs shows the majority occurring around the equatorial and mid-latitudes (Fig 15). Given that fluvial discharge is largely controlled by the amount of precipitation (Milliman and Syvitski, 2007), it is not surprising that the most fluvial influence at the shorelines occurs in the tropical latitudes where rainfall is greatest (Fig. 15A). Over 60% of the fluvial outputs in this study were found to be along coastlines that are in net deposition. The proportion of fluvial outputs on depositional versus erosional coastlines by latitude (Fig 15B) does not suggest any particular relationship. This would indicate that any large fluvial output regardless of latitude will be within a depositional setting. The marked decrease between 50 and 60N observed in the proportion of fluvial mouths within depositional settings is attributed to the mainly erosional shoreline of the Sea of Okhotsk that has a significant number of small fluvial outlets (Figure 15B).

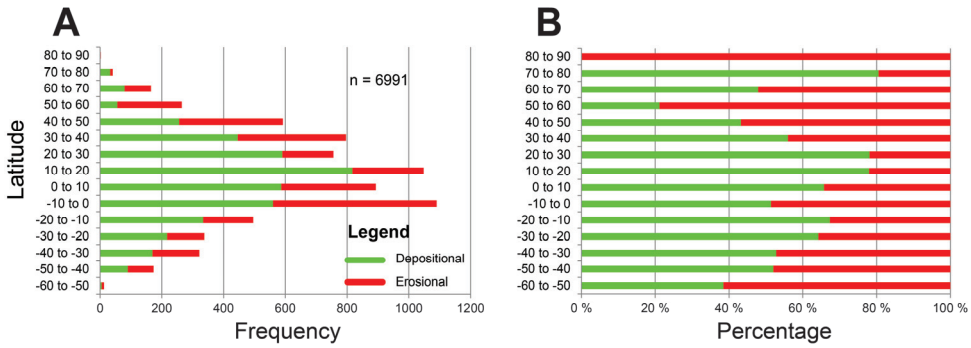

Figure 15. **A**, the frequency of fluvial outputs by 10 degree latitude bins and overlain by the proportion of depositional versus erosional settings. **B** highlights the percentage of fluvial outputs within depositional versus erosional settings binned by 10 degree latitude bins.

The distribution of different types of fluvial dominated and influenced shorelines (**F, Fw, Ft, Wf** and **Tf**) is summarized in Figure 16. Tide-modified fluvial outputs (Figure 16A) are more common in comparison to the proportions of tides globally (Figure 8). This may be reflect that most fluvial outputs occur around the mid latitudes (Figure 16A) and that depositional, more mixed influenced systems also occur in those localities (Figure 4). Wave-dominated fluvial mouths remain the most predominate fluvial-modified shorelines however an examination of the basinal energy associated with each fluvial output (tide and/or wave) binned by a log function from 1 to >10000, Figure 16B, shows that the majority of the largest rivers are tide-dominated. In contrast smaller fluvial outputs are more frequent and are often wave-dominated (e.g., Red Sea, Andes). A decrease in tide modified fluvial conditions between 1000 and 10000kg/s is a reflection of a few of the high-energy discharge fluvial outputs off the Andes coastline that are wave-dominated. Within depositional settings (Figure 16C) tidal systems increase with **Tf** processes by 7% and **Ft** by 2% whereas **Wf** environments decrease by 11% and **Fw** systems remain constant at 4%. This increased tidal-modification is observed in the lower discharge bins (< 1000), as higher discharge fluvial settings are predominately within depositional settings nonetheless (Figure 16B, D).

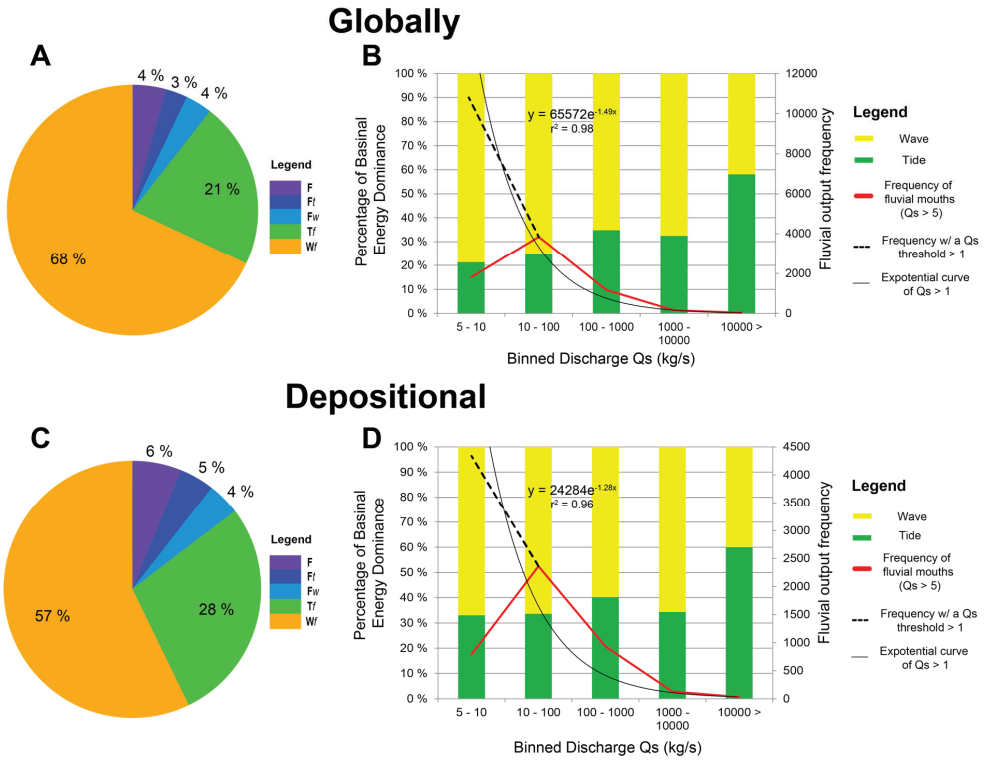

Figure 16. **A** and **C** show the proportion of fluvial processes (**F**, **Ft**, **Fw**, **Tf** and **Wf**) on global and depositional shorelines, respectively. **B** and **D** portray the proportion of dominant basinal energy (tide or wave) of those fluvial processes binned by a log scale of fluvial discharge, globally and depositional, respectively. Overlain on those plots is the frequency of fluvial outputs highlighted by a red line with a Qs threshold greater than 5 as used in Section 4.1.3. Extending the fluvial frequency with a cutoff at Qs > 1 to be consistent with the log scale bins is shown by a dotted black line along with its associated exponential curve fit by a solid black line.

Plots 16B and D, show the frequency of fluvial outputs within each bin showing that most fluvial sources in lower discharge environments are wave-dominated. As the threshold deemed significant for a fluvial output to a 5 km stretch of shoreline was set at Qs > 5 in section 4.1.3, a decrease in the frequency is shown for the lowest bin. If one expands that to include the full range from Qs > 1 it becomes evident that the frequency of fluvial outputs from small mountainous rivers is greater in erosional settings (Figure 16B) than depositional regions (Figure 16D). This would suggest that fluvial outputs on depositional settings are more likely to be tidally modified due to their higher discharge in comparison to the numerous smaller fluvial outputs on erosional shoreline counterparts.

A measurement of fluvial length versus its watershed area (above 500 km^2) in Figure 17, shows a strong power law relationship, supporting the findings of Vörösmarty et al. (2000b) who suggest that the potential discharge associated with those fluvial outputs is correlated to the maximum distance to the source. As a watershed area is a strong component in fluvial discharge in equation 1 (Milliman and Syvitski, 1992; Milliman and Syvitski, 2007), that information may be a useful indicator in palaeo-reconstructions to predict fluvial size by combing it with other assumptions on lithology, maximum relief and climate.

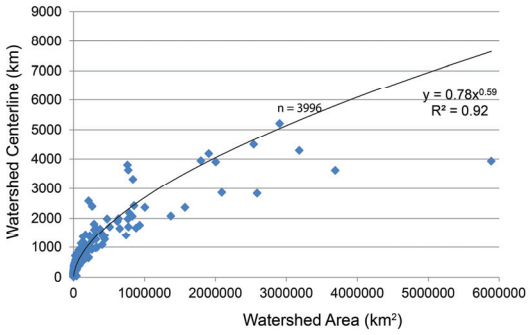

Figure 17 (left). The centerline length of a watershed versus its area in km^2 for watersheds with an area greater than 500 km^2. The centerline length of a watershed is a measurement of the longest upstream river network length from its fluvial mouth.

6.3. Shelf Width

The influence of continental shelf width on tidal amplification has been documented for several decades (Cram, 1979; Clarke and Battisti, 1981; Longhitano et al., 2012). Most recently (Ainsworth et al., 2011) linked the occurrence of wide shelves with increased tidal influence at the shoreline and conversely suggested that narrow shelves favored the development of more wave dominated systems. To test and quantify this relationship a calculation of shelf width was made, based on a shorelines proximity to the continental slope as defined by its 140 m bathymetry mark by Menot et al. (2010).

The threshold for a wide continental shelf was defined by Inman and Nordstrom (1971) as 50 km while Ainsworth et al. (2011) classified this boundary at 75 km. The definition of Ainsworth et al. (2011) was followed in this publication but further subdivided into narrow (≤25km), medium (>25km and ≤ 75km) and wide shelves (>75km) including a separate class for epicontinental seaways (Figure 18) which were manual added as those stretches of shoreline are not parallel to a continental slope boundary.

Within depositional settings wider shelves are more prominent at 42% and narrow shelves least common at 19% compared to a global distribution where wide shelves are 28% and narrow shelves 26%.

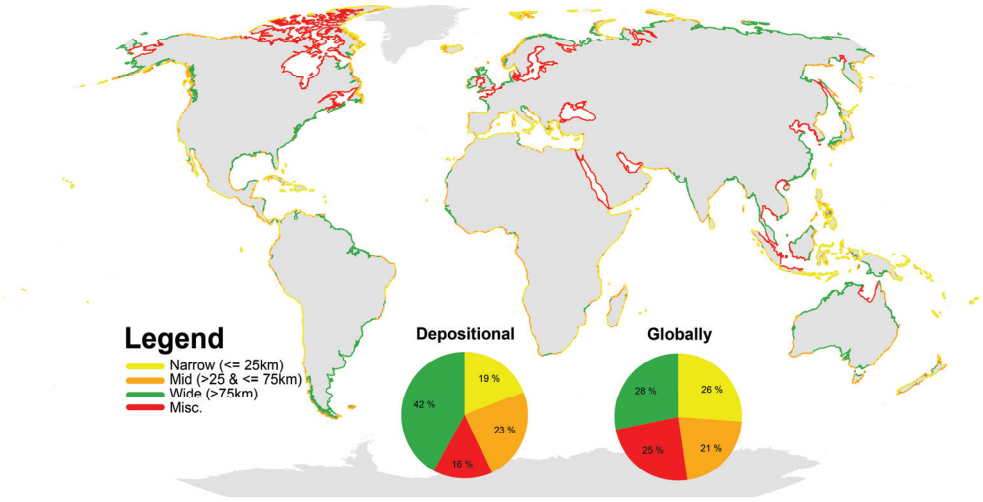

Figure 18. The global distribution of shorelines by binned categories of shelf width. Two pie charts are shown to relate shelf width within depositional settings and globally (see Figure 4).

Results illustrate that an increase in shelf width is associated with an increase in tidal influence at the shoreline, (Figure 19). Tidal processes are related to wider shelves on all shorelines (erosive and depositional) however this relationship is much greater in depositional shorelines (Figure 19B). On a global scale, narrow shelves are strongly wave modified at over 90% and tides less than 5% whereas a wide shelf increased tides to over 30%. Within depositional settings, tide dominated shorelines increase from less than 20% of narrow shelves to >50% on wide shelves. Wider shelves are also more prone to tidal modification of fluvial systems (**Tf** and **Ft)** whereas narrow shelves show a higher proportion of wave modified fluvial systems **(Wf)**. In general mid and wider shelves are more fluvial influenced.

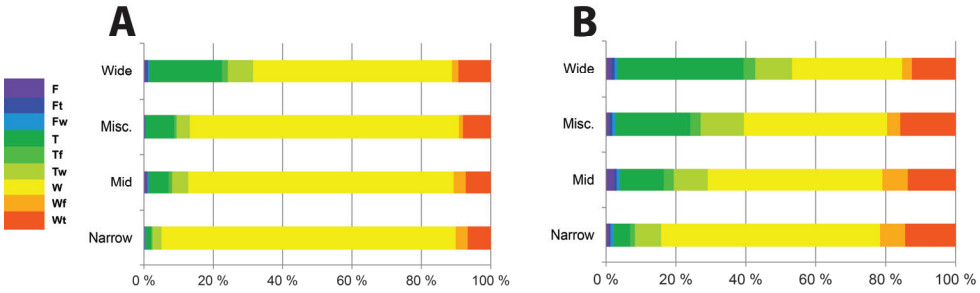

Figure 19. Plots showing the relationship between binned shelf widths in Figure 16 with ternary process in Figure 8. **A** the ternary process distribution by shelf width globally. **B** the ternary process distribution.

6.4. Tectonic Distribution

A combination of tectonic plate distribution (Bird, 2003), stress maps (Zoback, 1992; Sperner et al., 2003) and documented modern distributions (Ingersoll, 2012) were used to classify the shorelines into six broad tectonic basin categories: foreland; fore-arc; passive margin; intracratonic; extensional or strike-slip (Fig 20). The aim here is not provide the same level of detail as the process classification but a generalized global overview of tectonic regimes of shorelines. While an erosional coastline may not be associated with the tectonics of a terrestrial sedimentary basin, its link to a continental shelf provide a reasonable definition.

Globally, intracratonic and passive margins represent over half of all shorelines, fore-arc are at 18% and foreland basins represent 14% whereas extensional and strike-slip basins are less than 4% combined. Similarly passive margins and intracratonic settings are potentially the most significant of depositional settings although foreland basins are twice as prevalent at 20% in comparison to 10% of fore-arc basins. In addition, extensional and strike-slip regimes appear to be more common within depositional settings than erosional shorelines.

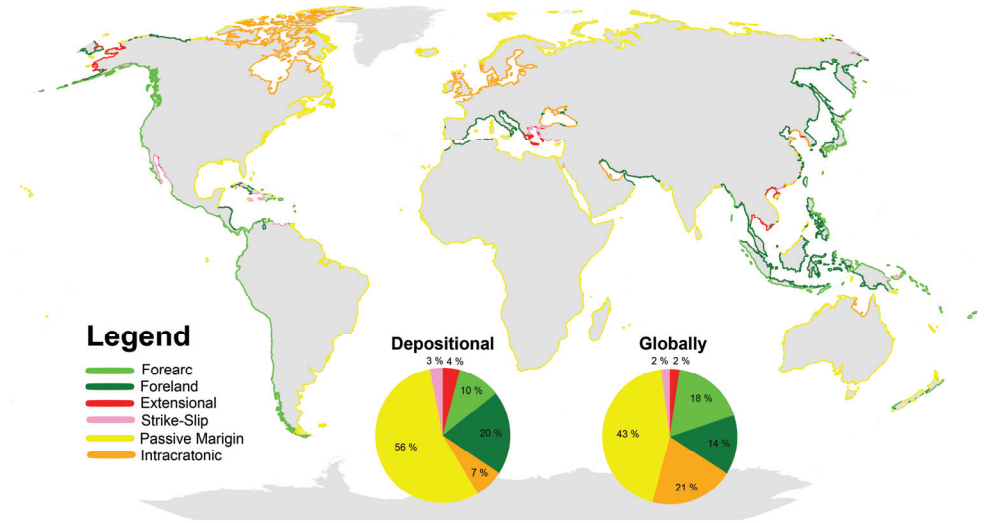

Figure 20. Global distribution of shorelines by tectonic classification. Two pie charts are shown to relate the tectonics within depositional settings and globally (see Figure 4).

6.4.1. Ternary Process and Tectonics

Figure 21 shows the distribution of ternary process by tectonics within areas of net shoreline deposition. Fore-arc basins are the most wave-dominated environments while foreland, extensional and strike-slip basins are the most tidally-influenced settings. Passive margins are typically wave dominated but show a significant tidal influence. Intracratonic settings are even more wave dominated although this partially because much of the Black Sea is included in this definition. Examining the proportion of those processes related with each basin type, Figure 21B, highlights this relationship further. Tidal systems associated with a fluvial input (**Ft**,**Tf**) are typically found within foreland basins. **F**, **Fw**, **T**, **Tw**, **W**, **Wf** and **Wt** systems are otherwise more common on passive margins and the wave-modified elements of **W**, **Wt** and **Wf** are increasingly significant on fore-arc basins. Extensional and strike-slip settings that are otherwise of a low sample representation have a significant mixed-influenced process including **Ft**, **Tw** and **Wt**.

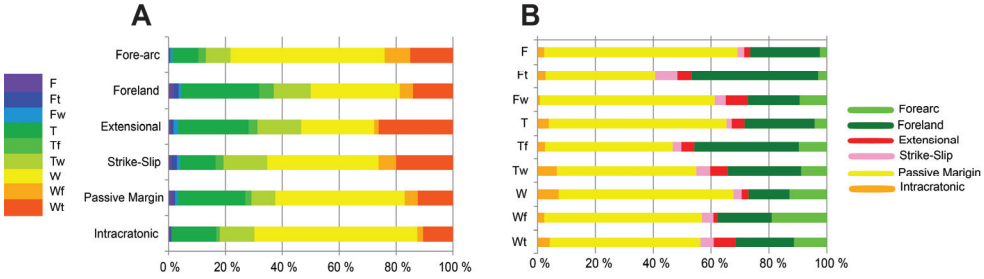

Figure 21. Plots comparing tectonics versus ternary process distribution within depositional settings. **A** plots the ternary process distribution by tectonic setting while **B** shows the tectonic distribution by ternary process.

6.4.2. Climate and Tectonics

An examination of climate (Kottek, 2006) by tectonic regime, Table 3, has shown in particular that most tectonic settings are within equatorial, warm temperate and arid conditions. Snow and polar conditions are mainly constrained to passive margins, foreland or fore-arc basins. Passive margins are the most dominant within equatorial and warm-temperate climates followed by foreland basins in equatorial settings. Extensional basins are a mere 4% and are constrained primarily to extensional basins of Alaska and Southeast Asia whereas strike-slip basins are even fewer although some may be associated with the Mediterranean. Most fore-arc basins are within equatorial conditions.

Table 3 - Tectonic Setting and Climate of Depositional Shorelines

	Foreland	Fore-arc	Strike-Slip	Extensional	Intracratonic	Passive Margin	Total
Arid	2	2	1	0	1	9	15
Equatorial	11	5	1	1	1	23	43
Temperate	3	2	1	1	4	16	27
Snow	2	1	0	2	1	6	10
Polar	1	1	0	0	0	2	5
Total	20	10	3	4	7	56	100

6.4.3. Shelf Width and Tectonics

Mapping shelf width versus tectonics show that extensional, strike-slip, intracratonic and passive margins are generally associated within epicontinental seaways or wide shelves, Table 4. Most significantly, over half of passive margins and extensional settings are on wide continental shelves. In contrast most fore-arc basins are of narrow or mid width shelves. Foreland basins also have a relatively high proportion of basins within epicontinental seaways (5%) or wide shelves (7%) whereas strike-slip settings are evenly distributed among narrow, mid and wide at 1%.

Table 4 - Tectonic Setting and Shelf Width of Depositional Shorelines

	Foreland	Fore-arc	Strike-Slip	Extensional	Intracratonic	Passive Margin	Total
Narrow	3	4	1	0	0	10	18
Mid	5	4	1	0	0	14	24
Misc.	5	0	0	2	5	3	16
Wide	7	2	1	2	1	29	42
Total	20	10	3	4	7	56	100

7. Discussion

This study illustrates that shoreline typology by ternary process can be classified on a global scale using publically available data on mean significant wave height, tidal range, calculated fluvial discharge and coastline geomorphology. The results indicate that process dominance is primarily a product of tidal range and mean significant wave height. Though, those parameters alone do not accurately predict the observed distribution of ternary process and shoreline geomorphology is a significant component.

Mapping modern shoreline geometry is important for three principal reasons. Firstly,

mapping and understanding modern systems have implications for identifying the fundamental controls on shoreline type which in turn maybe useful to predict shoreline type in ancient systems. Given that shallow marine shoreline type has a fundamental impact on reservoir behavior, predicting it is highly desirable from a hydrocarbon exploration perspective.

Secondly, modern systems are commonly used as analogs for ancient systems (Tye, 2004; Weissmann et al., 2010; Ainsworth et al., 2011; Howell et al., 2014). To identify suitable analogues remains a key challenge, which can be easily addressed once global mapping has been undertaken. This is especially important from a hydrocarbon production scenario when analogues will be used to derive geometries and dimensions for reservoir models (Tye, 2004; Nanson et al., 2012). Finally, a global mapping of shoreline typology has application beyond the hydrocarbon industry in numerous areas of coastal management. These applications are beyond the scope of this discussion but it is considered that the data and methods presented here, could be widely applied.

The analysis of the global distribution of modern shorelines described above suggests that basin morphology, shelf width, latitude, tectonics and climate are key factors that control shoreline typology. These and other controlling factors are interlinked in a complex web of interdependency (Figure 22). Plate tectonics is the first order controls which in turn control the other parameters. The following discussion attempts to address the role and interplay between some of these factors in a way that is potential predictive for hydrocarbon exploration.

Plate tectonics is the continental drift of the Earth's tectonic plates, generating orogenic belts, sedimentary basins and new oceanic floor (Dickinson, 1974). The horizontal and vertical movement of the plates controls the tectonic setting at the coastline, which in turn, influences the shelf width. It also controls the size of fluvial drainage basins and the volumes of sediment supplied to a portion of coastline which is typically much greater on passive margins, draining major continental land masses, than in tectonically active settings. Plate tectonics controls the distribution of sedimentary basins and the creation and destruction of accommodation. It also controls the latitude of the palaeogeographic setting which in turn controls the climate at the shoreline. Finally plate tectonics controls the configuration of the continents and oceans which is a fundamental control on wave energy.

Likewise, base-level controls shelf width. Low stand will create narrower shelves increasing wave-dominated shorelines and high stands will vice versa increase tidal-dominated shorelines by amplifying tides on wider shelves (Figure 18; Cram, 1979; Clarke and Battisti, 1981; Ainsworth et al. 2011; Longhitano et al., 2012).

Climate is mainly controlled by latitude and the distribution of the continental land masses by plate tectonics which in turn control the distribution of major ocean and air currents, heat transfer, orogenic effects and geochemical cycles (Hay, 1996). Climate, both at the coastline and in the hinter land influences sediment delivery to the shoreline and also the degree of wave activity. Longer term climatic change at high latitudes leads to glaciation cutting fjords and glacial retreat causing isostatic rebound, which removes significant amounts of high latitude accommodation. Climate also controls weathering and erosion with higher volumes of clay being derived from tropical source areas.

Tectonic setting, which is a function of plate tectonics, is the key control on the nature and rates of accommodation creation (Dickinson, 1974; Van Wagoner et al., 1990) and are also a major control on sediment supply to the shoreline (Milliman and Syvitski, 1992).

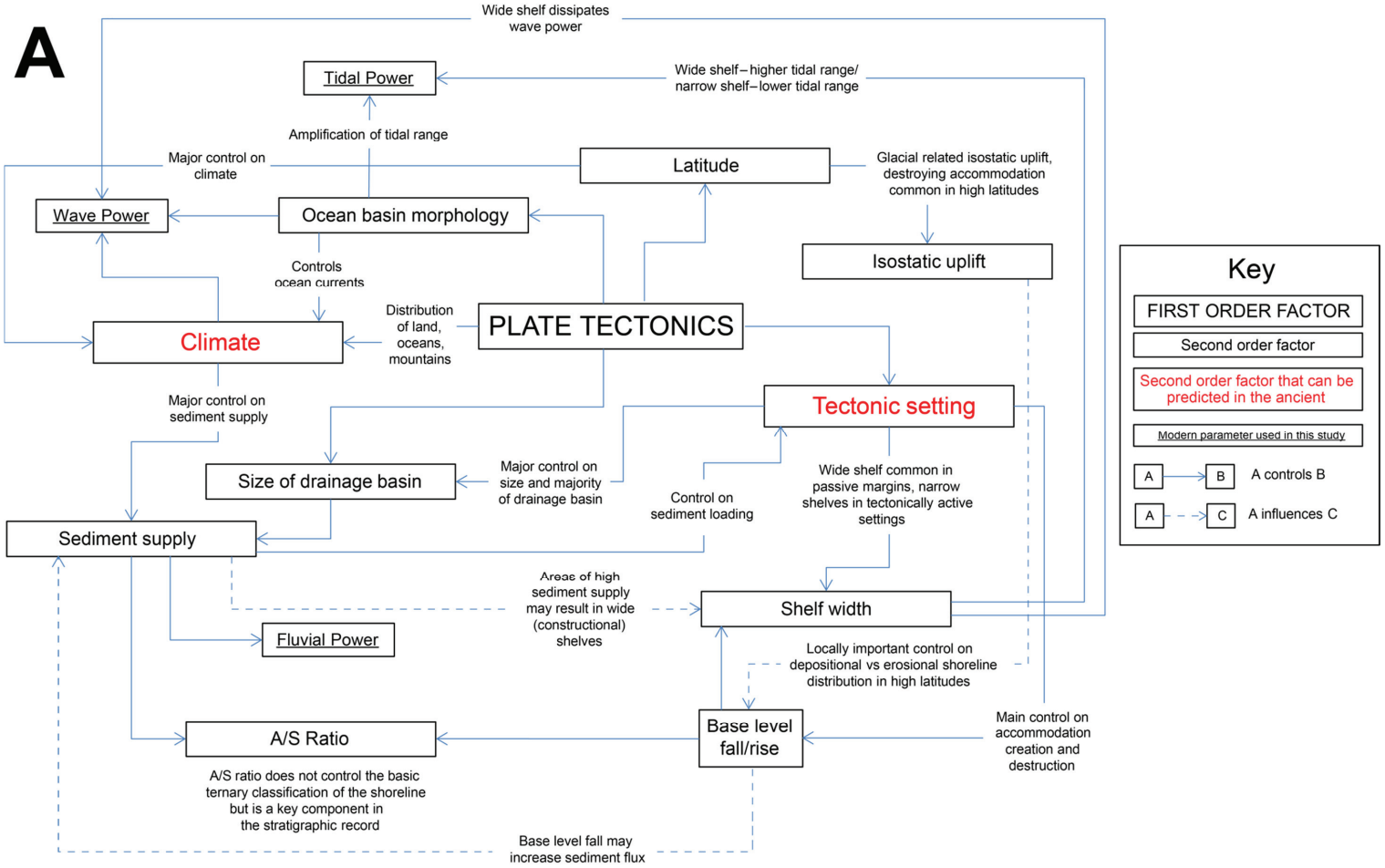
A
Wide shelf dissipates wave power
Tidal Power
Wide shelf – higher tidal range/ narrow shelf – lower tidal range
Amplification of tidal range
Major control on climate
Latitude
Glacial related isostatic uplift, destroying accommodation common in high latitudes
Wave Power
Ocean basin morphology
Isostatic uplift
Controls ocean currents
Distribution of land, oceans, mountains
PLATE TECTONICS
Climate
Major control on sediment supply
Tectonic setting
Size of drainage basin
Major control on size and majority of drainage basin
Control on sediment loading
Wide shelf common in passive margins, narrow shelves in tectonically active settings
Sediment supply
Areas of high sediment supply may result in wide (constructional) shelves
Shelf width
Fluvial Power
Locally important control on depositional vs erosional shoreline distribution in high latitudes
Base level fall/rise
Main control on accommodation creation and destruction
A/S Ratio
A/S ratio does not control the basic ternary classification of the shoreline but is a key component in the stratigraphic record
Base level fall may increase sediment flux
Key
FIRST ORDER FACTOR
Second order factor
Second order factor that can be predicted in the ancient
Modern parameter used in this study
A
B
A controls B
A
C
A influences C

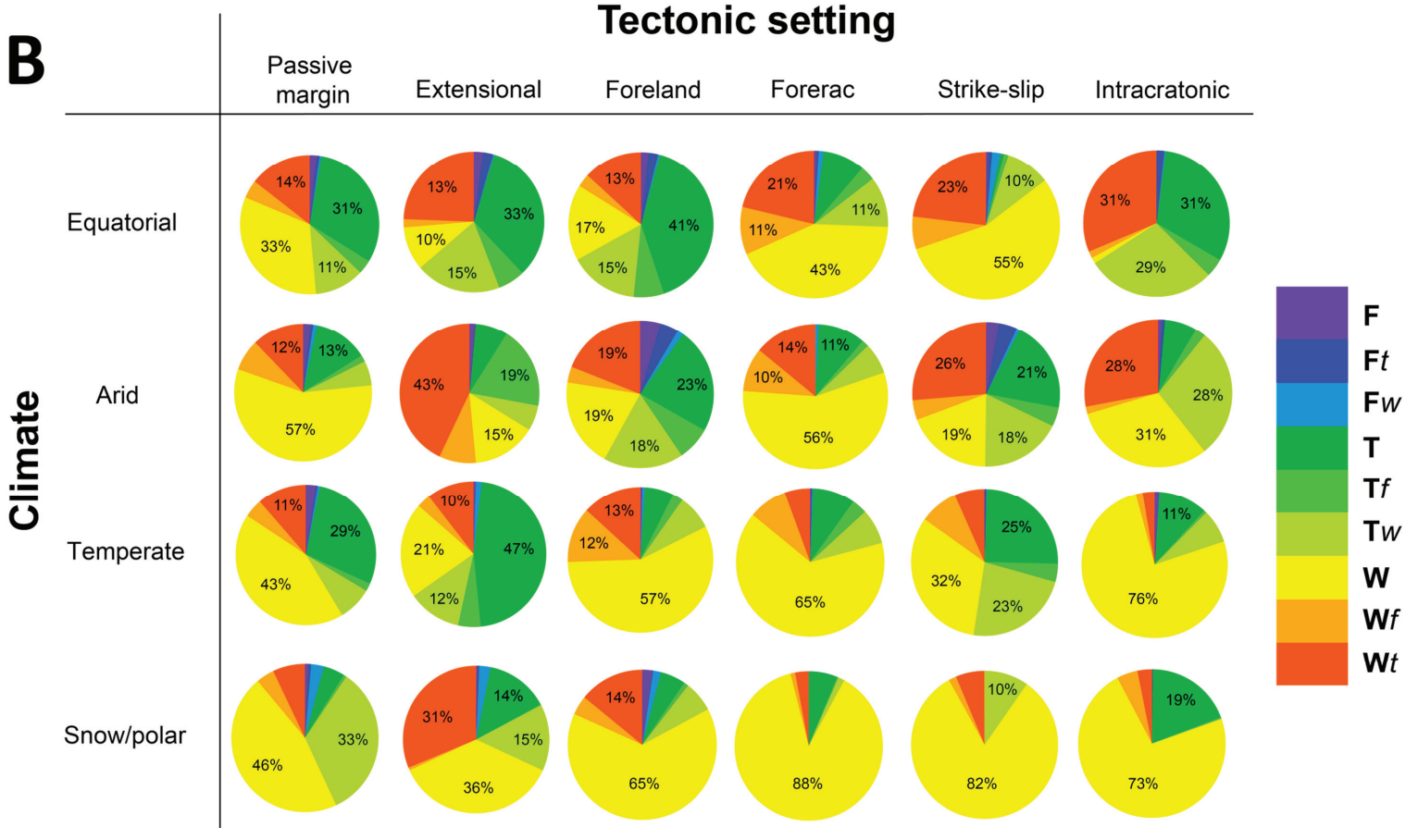
B
Tectonic setting
Passive margin
Extensional
Foreland
Forerac
Strike-slip
Intracratonic
Climate
Equatorial
Arid
Temperate
Snow/polar
14%
31%
33%
11%
13%
33%
10%
15%
13%
41%
17%
15%
21%
11%
11%
43%
23%
10%
55%
31%
31%
29%
12%
13%
57%
43%
19%
15%
19%
23%
19%
18%
14%
11%
10%
56%
26%
21%
19%
18%
28%
28%
31%
11%
29%
43%
10%
47%
21%
12%
13%
12%
57%
65%
25%
32%
23%
11%
76%
46%
33%
31%
14%
15%
36%
14%
65%
88%
10%
82%
19%
73%
F
Ft
Fw
T
Tf
Tw
W
Wf
Wt

Figure 22. (previous page) **A** shows the interplay between factors that influence shoreline typology. This is separated into first and second order controls including those parameters that can be predicted in the modern and ancient, namely climate and tectonics. **B** displays the relationship of climate and tectonics by ternary process from the modern. Percentages displayed where proportion is greater than 10%. This could be used to predict the probability of a particular shoreline type in a given climatic and tectonic setting.

Passive continental margins will tend to have broad shelves with relatively slow subsidence, increasing in a basinward direction. Passive margins commonly lay on the edge of large, stable continental landmasses with well established, drainage basins that deliver major volumes of sediment to the shoreline. The wide shelves will typical promote tidal conditions (Ainsworth et al., 2011). Active margins in fore arc settings will conversely be associated with narrow shelves and while newly uplifted mountains along the coastline will be an excellent source of sediment an absence of large drainage systems will result in multiple, small delivery points (Milliman and Syvitski, 1992). Shorelines in rift, strike-slip and foreland basins will generally have lower basinal energy, although tidal amplification may occur in funnel shaped basins. Rates of accommodation creation are typically high and sediment supply is partitioned by complex topography at the shoreline. Consequently such systems are commonly aggradational to transgressive (e.g., Howell et al. 1996).

Large progradational systems where sediment supply exceeds accommodation create low-gradient typologies. The channels of those vast low gradient settings are subsequently susceptible to tidal amplification and modification. The majority of the world's largest deltas that occur on passive margins, foreland and intracratonic settings (Figure 15) are thereby tide-modified except in restricted low basinal energy environments (e.g., Gulf of Mexico, Mediterranean and Black Sea).

In summary, plate tectonics is the fundamental control on shoreline morphology, controlling latitude distribution of continental landmass, shelf width, ocean basin morphology and the A/S ratio (accommodation to supply) at the coastline. Secondary controls, which can be used predictively, include climate and tectonic setting, which is a product of latitude, basin morphology and plate tectonics. The results described above suggest that majority of modern depositional shorelines are wave dominated. Tidal systems are more likely in low to mid latitudes in basins with wide shelves or more complex morphologies. Fluvial dominated shorelines are rare and major systems only occur on passive margins and foreland basins (Figure 8; 21).

The secondary goal of this study is to provide a systematic methodology for locating modern analogues for ancient reservoir systems. Outcrop analogues have long been used to provide important information on sediment body geometry and the lateral relationships between facies in cross section (see Howell et al. 2014 for a review). More recently the advent of freely available remote sensing data (e.g., Google Earth; Tooth, 2013) has seen a major increase in the use of modern analogues (e.g., Weissmann et al. 2010; Ainsworth et. 2011) to provide key information on the plan view geometries and relationships within systems. A key challenge remains the identification of suitable analogues. The maps presented in this paper (Fig 8) allow suitable process classified shoreline segments to be identified. This can be combined with additional information on climate (Table 3; Figure 21); tectonic setting (Figure 20; 21); latitude (Figure 12) or shelf width (Figure 17) to identify suitable modern systems that can then be studied in greater detail to extract reservoir body dimensions.

8. Conclusions

This study has demonstrated a unique mapping of 927,577 km of shorelines from across the globe. Of this 28% are depositional, while the remaining 72% are rocky coastlines in net erosion. The shorelines have been further classified using a two tier, ternary classification based upon (Galloway, 1975; Ainsworth et al., 2011) which considers the relative importance of fluvial discharge, mean significant wave height and mean tidal range. The study has shown that the majority of the coastlines are wave dominated with an increase in tidal systems towards the equator. Fluvial dominated systems make up a very small proportion of coastlines. More specifically:

1) Shorelines in net deposition are more mixed-influenced than their erosional shoreline counterparts and this observed difference has been accounted for by the algorithm. Depositional settings are more pronounced in the equatorial and mid-latitudes and thereby mix-influenced shorelines are more pronounced in those regions.

2) The highest frequency of fluvial outputs are likewise distributed along the equatorial and mid-latitudes. The major rivers of the world that are depositing into open-body of waters are typically tide-modified. In contrast wave-modified shorelines are of higher frequency though smaller discharge.

3) Wider shelves amplify tidal processes by threefold in comparison to narrow shelves, they also dampen wave energy.

4) Passive margins and foreland basins are globally the most representative distributions of tectonic regimes of shorelines. A significant portion of shorelines related to those tectonic regimes are of wide continental shelves. Fore-arc basins represent one tenth of shorelines and are almost exclusively of narrow or mid shelves that are predominately of wave-dominated processes.

5) The energy environment of the marginal marine at present is related to the distribution of continents. This has created a restricted low energy arctic environment that is of a predominately wave-dominated erosional environment. Although tidal environments do develop in this low energy environment due to funneling and restricted shoreline geometry associated with unconsolidated sediments.

6) Controls on shallow marine systems include a complex interplay between climate, latitude, tectonic setting, shoreline morphology and A/S ratio.

The digitized and global distribution of process shown here has demonstrated a valuable tool that may find appropriate modern analogues of the marginal marine. This may provide an initial basis for continued improvements to map globally marginal marine environments by a systems paleo-evolution by showing the distribution of potential depositional units to study. The initial classification of process, shelf width, latitude, tectonic, climate, fluvial discharge and basinal energy may aid in selecting a representative sample size to study as well as to quantify the controls on that future research into a global perspective.

Acknowledgements

Support for this work came from the SAFARI consortium which was funded by Bayern Gas, ConocoPhillips, Dana Petroleum, Dong Energy, Eni Norge, GDF Suez, Idemitsu, Lundin, Noreco, OMV, Repsol, Rocksource, RWE, Statoil, Suncor, Total, PDO, VNG and

the Norwegian Petroleum Directorate (NPD). This manuscript has benefited from discussion with Bruce Ainsworth, Boyan Vakarelov, Rachel Nanson and Christian Haug Eide.

References

Ainsworth, R., Flint, S.S., Howell, J.A., 2008. Predicting Coastal Depositional Style: Influence of Basin Morphology and Accommodation To Sediment Supply Ratio Within A Sequence Stratigraphic Framework SPEM Spec. Publ. Recent Advances in Models of Siliciclastic Shallow-Marine Stratigraphy 90.

Ainsworth, R., Vakarelov, B., Nanson, R., 2011. Dynamic Spatial and temporal prediction of changes in depositional processes on clastic shorelines: Towards improved subsurface uncertainty reduction and management. AAPG Bulletin 95, 267-297.

Aviso, 2012. FES2012 was produced by Legos and CLS Space Oceanography Division and distributed by Aviso, with support from Cnes

Bhattacharya, J.P., Giosan, L., 2003. Wave-influenced deltas: geomorphological implications for facies reconstruction. Sedimentology 50, 187-210.

Bird, C.E., Franklin, E.C., Smith, C.M., Toonen, R.J., 2013. Between tide and wave marks: a unifying model of physical zonation on littoral shores. PeerJ 1, e154.

Bird, P., 2003. An updated digital model of plate boundaries. Geochemistry, Geophysics, Geosystems 4, 1027.

Boyd, R., Dalrymple, R., Zaitlin, B.A., 1992. Classification of clastic coastal depositional environments. Sedimentary Geology 80, 139-150.

Buddemeier, R.W., Smith, S.V., Swaney, D.P., Crossland, C.J., Maxwell, B.A., 2008. Coastal typology: An integrative "neutral" technique for coastal zone characterization and analysis. Estuarine, Coastal and Shelf Science 77, 197-205.

Carrère, L., Lyard, F., Cancet, M., Guillot, A., Roblou, L., 2012. FES2012: A new global tidal model taking taking advantage of nearly 20 years of altimetry, Proceedings of meeting "20 Years of Altimetry", Venice.

Clarke, A.J., Battisti, D.S., 1981. The effect of continental shelves on tides. Deep Sea Research Part A. Oceanographic Research Papers 28, 665-682.

Costanza, R., d'Arge, R., Groot, R.d., Farber, S., Grasso, M., Hannon, B., Limburg, K., Naeem, S., O'Neill, R.V., Paruelo, J., Raskin, R.G., Sutton, P., Belt, M.v.d., 1998. The value of the world's ecosystem services and natural capital. Nature 387, 253-260.

Cram, J.M., 1979. The Influence of Continental Shelf Width on Tidal Range: Paleoceanographic Implications. The Journal of Geology 87, 441-447.

Crossland, C.J., Kremer, H.H., Lindeboom, H.J., Crossland, J.I.M., LeTissier, M.D.A., 2003. Coastal fluxes in the Anthropocene. Global change the IGBP Series. Springer, Berlin.

Danielson, J.J., Gesch, D.B., 2011. Global multi-resolution terrain elevation data 2010 (GMTED2010): U.S. Geological Survey Open-File Report 2011–107. 26.

Davies, J.L., 1964. A morphogenic approach to world shorelines. Z. Geomorphol. 8, 27-42.

Davis Jr, R.A., Hayes, M.O., 1984. What is a wave-dominated coast? Marine Geology 60, 313-329.

Deveugle, P.E.K., Jackson, M.D., Hampson, G.J., Stewart, J., Clough, M.D., Ehighebolo, T., Farrell, M.E., Calvert, C.S., Miller, J.K., 2014. A comparative study of reservoir modeling techniques and their impact on predicted performance of fluvial-dominated deltaic reservoirs. AAPG Bulletin 98, 729-763.

Dickinson, W.R., 1974. Plate tectonics and sedimentation. Society of Economic Paleontologists and Mineralogists Special Publication 22, 1-27.

Dürr, H., Laruelle, G., van Kempen, C., Slomp, C., Meybeck, M., Middelkoop, H., 2011. Worldwide Typology of Nearshore Coastal Systems: Defining the Estuarine Filter of River Inputs to the Oceans. Estuaries and Coasts 34, 441-458.

Dürr, H.H., Meybeck, M., Dürr, S.H., 2005. Lithologic composition of the Earth's continental surfaces derived from a new digital map emphasizing riverine material transfer. Global Biogeochemical Cycles 19, GB4S10.

Eide, C.H., Howell, J., Buckley, S., 2014. Distribution of discontinuous mudstone beds within wave-dominated shallow-marine deposits: Star Point Sandstone and Blackhawk Formation, Eastern Utah The American Association of Petroleum Geologists Bulletin 98, 1401-1429.
Enge, H.D., Howell, J.A., 2010. Impact of deltaic clinothems on reservoir performance: dynamic studies of reservoir analogs from the Ferron Sandstone Member and Panther Tongue, Utah. AAPG Bulletin 94, 139-161.
ESRI, 2014. ESRI (Environmental Systems Resource Institute). 2014. ArcMap 10.1. ESRI, Redlands, California.
Fekete, B.M., Vörösmarty, C.J., Grabs, W., 2002. High-resolution fields of global runoff combining observed river discharge and simulated water balances. Global Biogeochemical Cycles 16, 15-11-15-10.
Galloway, W.E., 1975. Process Framework for Describing the Morphologic and Stratigraphic Evolution of Deltaic Depositional Systems, Deltas: Models for Exploration, 1975. Houston Geological Society, Houston, Texas, pp. 87-98.
Global Runoff Data Centre, 2007. Major River Basins of the World / Global Runoff Data Centre. Koblenz, Federal Institute of Hydrology (BfG).
Goodbred, S., Jr., Saito, Y., 2012. Tide-Dominated Deltas, in: Davis Jr, R.A., Dalrymple, R.W. (Eds.), Principles of Tidal Sedimentology. Springer Netherlands, pp. 129-149.
Hampson, G.J., Storms, J.E.A., 2003. Geomorphological and sequence stratigraphic variability in wave-dominated, shoreface-shelf parasequences. Sedimentology 50, 667-701.
Harris, P.T., Heap, A.D., Bryce, S.M., Porter-Smith, R., Ryan, D.A., Heggie, D.T., 2002. Classification of Australian Clastic Coastal Depositional Environments Based Upon a Quantitative Analysis of Wave, Tidal, and River Power Journal of Sedimentary Research 6, 858-870.
Hartmann, J., Moosdorf, N., 2012. The new global lithological map database GLiM: A representation of rock properties at the Earth surface. Geochemistry, Geophysics, Geosystems 13, Q12004.
Hay, W.W., 1996. Tectonics and climate. Geol Rundsch 85, 409-437.
Howell, J., Skorstad, A., MacDonald, A., Fordham, A., Flint, S., Fjellvoll, B., Manzocchi, T., 2008. Sedimentological parameterization of shallow-marine reservoirs. Petroleum Geoscience 14.
Howell, J.A., Flint, S.S., Hunt, C., 1996. Sedimentological aspects of the Humber Group (Upper Jurassic) of the South Central Graben, UK North Sea. Sedimentology 43, 89-114.
Howell, J.A., Martinius, A.W., Good, T.R., 2014. The application of outcrop analogues in geological modelling: a review, present status and future outlook. Sediment-Body Geometry and Heterogeneity: Analogue Studies for Modelling the Subsurface. Geological Society, London, Special Publications 387.
Ingersoll, R.V., 2012. Tectonics of sedimentary basins with revised nomenclature, in: Bursby, C., Azor, A. (Eds.), Tectonics of Sedimentary Basins Recent Advances, First Edition ed. Blackwell Publishing Ltd, Chichester, West Sussex, pp. 3-43.
Inman, D.L., Nordstrom, C.E., 1971. On the Tectonic and Morphologic Classification of Coasts. The Journal of Geology 79, 1-21.
Jorgenson, M.T., Brown, J., 2005. Classification of the Alaskan Beaufort Sea Coast and estimation of carbon and sediment inputs from coastal erosion. Geo-Mar Lett 25, 69-80.
Kottek, M., 2006. World map of the Köppen-Giger climate classification updated. Meterologische Zeitschrift 15, 259-263.
Lehner, B., Verdin, K., Jarvis, A., 2008. New Global Hydrography Derived From Spaceborne Elevation Data. Eos, Transactions American Geophysical Union 89, 93-94.
Longhitano, S.G., Mellere, D., Steel, R.J., Ainsworth, R.B., 2012. Tidal depositional systems in the rock record: A review and new insights. Sedimentary Geology 279, 2-22.
Martinius, A. W., Ravnås, R., Howell, J. A., Steel, R. J., and Wonham, J. P., 2014, From Depositional Systems to Sedimentary Successions on the Norwegian Continental Margin, John Wiley & Sons, Special Publication Number 46 of the International Association of Sedimentologists.
McIlroy, D., Flint, S., Howell, J.A., Timms, N., 2005. Sedimentology of the tide-dominated Jurassic

Lajas Formation, Neuquén Basin, Argentina. Geological Society, London, Special Publications 252, 83-107.
Menot, L., Sibuet, M., Carney, R.S., Levin, L.A., Rowe, G.T., Billett, D.S.M., Poore, G., Kitazato, H., Vanreusel, A., Galéron, J., Lavrado, H.P., Sellanes, J., Ingole, B., Krylova, E., 2010. New Perceptions of Continental Margin Biodiversity, Life in the World's Oceans. Wiley-Blackwell, pp. 79-102.
Milliman, J.D., Syvitski, J.P.M., 1992. Geomorphic/Tectonic Control of Sediment Discharge to the Ocean: The Importance of Small Mountainous Rivers. The Journal of Geology 100, 525-544.
Milliman, J.D., Syvitski, J.P.M., 2007. Geology, Geography, and Humans Battle for Dominance over the Delivery of Fluvial Sediment to the Coastal Ocean. The Journal of Geology 115, 1-19.
Mørk, G., Barstow, S., Kabuth, A., Pontes, T., 2010. Assessing the global wave energy potential, Proc. of OMAE2010, 29th International Conference on Ocean, Offshore Mechanics and Arctic Engineering, Shanghai, China.
Nanson, R., Ainsworth, R., Vakarelov, B., Fernie, J., Massey, A., 2012. Geometric attributes of reservoir elements in a modern, low accommodation, tide-dominated delta. APPEA Journal, 483-492.
Nanson, R.A., Vakarelov, B.K., Ainsworth, R.B., Williams, F.M., Price, D.M., 2013. Evolution of a Holocene, mixed-process, forced regressive shoreline: The Mitchell River delta, Queensland, Australia. Marine Geology 339, 22-43.
NASA LP DAAC, 2001. NASA Land Processes Distributed Active Archive Center (LP DAAC) USGS/Earth Resources Observation and Science (EROS) Center. MOD 11 - Land Surface Temperature and Emissivity
Orton, G.J., Reading, H.G., 1993. Variability of deltaic processes in terms of sediment supply, with particular emphasis on grain size. Sedimentology 40, 475-512.
Overeem, I., Anderson, R.S., Wobus, C.W., Clow, G.D., Urban, F.E., Matell, N., 2011. Sea ice loss enhances wave action at the Arctic coast. Geophysical Research Letters 38, L17503.
Reuter, H.I., Nelson, A., Jarvis, A., 2007. An evaluation of void ‐ filling interpolation methods for SRTM data. International Journal of Geographical Information Science 21, 983-1008.
Short, A.D., 2006. Australian Beach Systems—Nature and Distribution. Journal of Coastal Research 22, 11-27.
Sperner, B., Müller, B., Heidbach, O., Delvaux, D., Reinecker, J., Fuchs, K., 2003. Tectonic stress in the Earth's crust: advances in the World Stress Map project. - In: Nieuwland D. (ed.): New insights into structural interpretation and modelling. Geological Society of London Special Publications 212, 101-116.
Talaue-McManus, L., Smith, S.V., Buddemeier, R.W., 2003. Biophysical and socio-economic assessments of the coastal zone: the LOICZ approach. Ocean & Coastal Management 46, 323-333.
Tolman, H.L., 2002. Validation of WAVEWATCH III Version 1.15 for a Global Domain. NOAA/NWS/NCEP/OMB Technical Note Nr. 213, p. 33.
Tooth, S., 2013. 14.5 Google Earth™ in Geomorphology: Re-Enchanting, Revolutionizing, or Just another Resource?, in: Shroder, J.F. (Ed.), Treatise on Geomorphology. Academic Press, San Diego, pp. 53-64.
Tye, R.S., 2004. Geomorphology: An approach to determining subsurface reservoir dimensions. AAPG Bulletin 88, 1123 -1147.
Vafeidis, A.T., Nicholls, R.J., McFadden, L., Tol, R.S.J., Hinkel, J., Spencer, T., Grashoff, P.S., Boot, G., Klein, R.J.T., 2008. A New Global Coastal Database for Impact and Vulnerability Analysis to Sea-Level Rise. Journal of Coastal Research, 917-924.
Vakarelov, B., Ainsworth, R., 2013. A hierarchical approach to architectural classification in marginal-marine systems: Bridging the gap between sedimentology and sequence stratigraphy. AAPG Bulletin 97, 1121-1161.
Vakarelov, B.K., Ainsworth, R.B., MacEachern, J.A., 2012. Recognition of wave-dominated, tide-influenced shoreline systems in the rock record: Variations from a microtidal shoreline model. Sedimentary Geology 279, 23-41.

Van Wagoner, J.C., Mitchum, R.M., Campion, K.M., Rahmanian, V.D., 1990. Siliciclastic Sequence Stratigraphy in Well Logs, Cores, and Outcrops: Concepts for High-Resolution Correlation of Time and Facies: AAPG Methods in Exploration 7., Tulsa, USA.

Vörösmarty, C.J., Fekete, B.M., Meybeck, M., Lammers, R.B., 2000a. Geomorphometric attributes of the global system of rivers at 30-minute spatial resolution. Journal of Hydrology 237, 17-39.

Vörösmarty, C.J., Fekete, B.M., Meybeck, M., Lammers, R.B., 2000b. Global system of rivers: Its role in organizing continental land mass and defining land-to-ocean linkages. Global Biogeochemical Cycles 14, 599-621.

Weissmann, G.S., Hartley, A.J., Nichols, G.J., Scuderi, L.A., Olson, M., Buehler, H., Banteah, R., 2010. Fluvial form in modern continental sedimentary basins: Distributive fluvial systems. Geology 38, 39-42.

Wellner, R., Beaubouef, R., Wagoner, J.V., Roberts, H., Sun, T., 2005. Jet-Plume Depositional Bodies—The Primary Building Blocks of Wax Lake Delta. Gulf Coast Association of Geological Societies Transactions 55, 867-909.

Wessel, P., Smith, W., 1996. A global, self-consistent, hierarchical, high-resolution shoreline database. Journal of Geophysical Research 101, 8741-8743.

Wright, L.D., Coleman, J.M., 1973. Variations in morphology of major river deltas as functions of ocean wave and river discharge regimes. AAPG Bulletin 57, 370 - 398.

Zoback, M.L., 1992. First- and second-order patterns of stress in the lithosphere: The World Stress Map Project. Journal of Geophysical Research: Solid Earth 97, 11703-11728.

PAPER III

Geometric Attribute and Shape Characterization of Modern Depositional Elements: A Quantitative GIS Method for Empirical Analysis

IV

Geometric Attribute and Shape Characterization of Modern Depositional Elements: A Quantitative GIS Method for Empirical Analysis

Björn Nyberg[1,2*], Simon J. Buckley[1], John A. Howell[3], Rachel A. Nanson[4]

Uni Research CIPR, P.O. Box 7810, 5020 Bergen Norway.[1]
Department of Earth Sciences, University of Bergen, P.O. Box 7803, 5020 Bergen, Norway.[2]
Department of Geology and Petroleum Geology, University of Aberdeen, Meston Building, Old Aberdeen, AB24 3UE UK[3]
Australian School of Petroleum, Centre for Tectonics, Resources and Exploration (TRaX), Santos Petroleum Engineering Building, University of Adelaide, Adelaide SA 5005, Australia[4]
*corresponding author – bjorn.nyberg@uni.no

Abstract

The recent rise in the quality and availability of remote sensing data has benefitted the petroleum industry by allowing high resolution studies of the geometry of modern depositional elements, which are analogous to the elements that control flow in subsurface reservoirs. Established methods used to describe the geometry of these features have been predominantly subjective. We present a new objective technique to automate the characterization of *absolute* geometric attributes (AB) of mapped depositional elements. This technique measures key parameters at a defined sampling interval along a calculated centerline for each input shape, which are then automatically analyzed to define geometric shape, length, width, sinuosity, connectivity and centerline deviation. To demonstrate the applicability of the method to a range of depositional environments, mapped sandbodies from two contrasting modern systems were analyzed: (1) the 520 km^2 mixed-process Mitchell River Delta, Gulf of Carpentaria, Australia; (2) a 1 200 km reach of the anabranching Congo River, Democratic Republic of the Congo.

1 759 wave- and fluvial-derived elements from the Mitchell Delta were analyzed using our new AB method and the conventional minimum bounding box (MBB) approach. The MBB results defined the regression slopes as 1.25-4.47 times wider and 0.31-0.97 times shorter than their AB values. Results applied to 2 221 mid-channel bar elements in the Congo River showed similar AB and MBB relationships, with linear regression slopes of a MBB as 1.06 times wider and 0.97 times shorter. The inconsistency in the comparative MBB and AB results for these two datasets is attributed to the very different geometries of the sandbodies in these contrasting depositional environments. This suggests that caution should be exercised when applying current methods. A major benefit of the proposed AB method is that it allows quantitative study at scales and levels of detail typically not practical using manual solutions.

1. Introduction

In recent years, research and debate on quantitative global distributions of depositional environments and their importance to the preserved sedimentary record has increased within the scientific community (Stutz and Pilkey, 2002; Hartley et al., 2010; Weissmann et al., 2010; Holzweber et al., 2014), and has been largely driven by the availability and accessibility of global, remotely sensed datasets. Google Earth (Lisle, 2006) embodies this move from isolated analogue maps and photographs to complete global coverage on a geoscientist's computer. As the trend for investigating the relational, geometric and distribution statistics of depositional environments at the global scale continues, with focus on increasingly smaller-scale geological features, deriving quantitative geometric data using traditional subjective and manual methods becomes impractical and inefficient. However, such quantitative measurements are important for deriving empirical and statistically-valid relationships on the spatial variability of elements within modern systems.

Quantitative measures for describing the geometric attributes of depositional elements are currently limited to standard geographical information system (GIS) operations, which cannot adequately represent the length, width, sinuosity, connectivity or orientation of these units beyond basic individual maximum or minimum values. The problem of automatically and more objectively determining the shape of, and interactions between, such features has been approached by authors in numerous fields (Gardoll et al., 2000; van der Werff and van der Meer, 2008; Tafesse et al., 2012; Kröner and Doménech Carbó, 2013). Object Based Image Analysis (OBIA) exemplifies the movement of combining measures of shape and geometry to improve automated image classification for the purpose of categorizing remotely sensed data with similar spectral responses (Benz et al., 2004; Blaschke, 2010). These descriptive shapes and geometric attributes, however, typically rely on numerical/mathematical relationships between a feature's geometric parameters, such as the minimum bounding box (MBB) axis lengths, area, perimeter, compactness and convexity, to define them into classes such as circular, rounded, elongated or rectangular, rather than an absolute set of measurements to objectively define their shapes.

Pavelsky and Smith (2008) and Fisher et al. (2013) have recently shown the potential for obtaining quantitative width measurements for river channel geomorphology research. Although the methodology to classify the broad spectrum of depositional environments, characterization of shape, heterogeneity and connectivity of elements is not considered that otherwise have important implications for relating modern analog studies for subsurface reservoir modeling (Howell et al., 2008; Nanson et al., 2012; Massey et al., 2013). The MBB remains the most accessible methodology for quantitative data analysis within standard GIS suites. A final consideration is that an accurate set of measurements (Holzweber et al., 2014) and shapes (Nanson et al., 2012) of modern elements can be achieved using manual interpretation and mapping. This is both time-consuming and subjective, however, and limits the comprehensive quantification of the large amounts of global data available today.

In this paper we present a new method for the quantification of the geometric attributes of shapes that can aid geomorphologists and sedimentologists in interpreting the heterogeneity and spatial variability of elements within modern depositional systems. This new method is applied to both fluvial and coastal systems. By describing the centerline of a mapped feature and measuring multiple equally spaced width and centerline deviation

(sinuosity) measurements along that centerline, variability can be quantified in terms of these absolute geometric attributes. Furthermore these geometric attributes can aid in classifying features into one of nine geomorphological classes by describing symmetry and centerline deviation with distance. The spatial occurrence of each feature's geometric attributes in the context of a depositional system allows for further analysis to examine the interaction of elements, important for understanding potential reservoir connectivity. The aims of the paper are therefore twofold: i) to describe the individual measurements and calculations using the proposed method; ii) to demonstrate the applicability of the method to two case studies, with results and considered implications.

2. Method

The proposed methodologies are implemented as individual scripts running in the Quantum GIS (QGIS) environment (QGIS Development Team, 2014) and based on the integrated GRASS GIS suite (GRASS Development Team, 2014). Depending on the desired application, these scripts can be combined into automated workflows based on a number of predefined parameters, as described below. The algorithms require a vector dataset as input, provided in a projected coordinate system that preserves distance measurements (e.g. UTM), representing individual polygon features of interest. It is not within the scope of this paper to describe mapping methods in great detail, instead it is assumed that features of interest have already been mapped. Each of these algorithms is described below.

2.1. Centerline

The centerline of an object is used to define the length of an individual shape within its spatial context. Numerous solutions have been proposed to define that centerline, particularly within the fields of computer science, mathematics and the medical sciences (McAllister and Snoeyink, 2000; Bouix et al., 2005; Cornea et al., 2007; Haunert and Sester, 2008; van der Werff and van der Meer, 2008; Lakshmi and Punithavalli, 2009; Wang et al., 2011). The most common solution is to define a skeletal line representation of each individual feature using Voronoi tessellation lines that calculate line segments as the furthest from all input vertices defining a particular polygon (Fig 1A). The Voronoi (Thiessen) algorithm was selected here, as it is a standardized procedure available in most GIS suites, though any skeletal line generation would be appropriate as input for the following method.

Typically the centerline of an individual polygon is generated by "pruning" the skeletal lines (Svensson and Sanniti di Baja, 2003; Bouix et al., 2005; Palágyi et al., 2006), by continuously removing peripheral lines at the polygon boundary until only the line segments in the center remain. However the complexity of modern depositional elements make it difficult to apply this in reality without losing information, as the amount required to be pruned varies according to geometry, shape and size (Fig 1B). Rather, the centerline recovered here defines the longest cumulative or multiple line segment distance between one to one (Fig 1B) or one to many end vertices (Fig 1C) within a skeletal line graph (Hagberg et al., 2008).

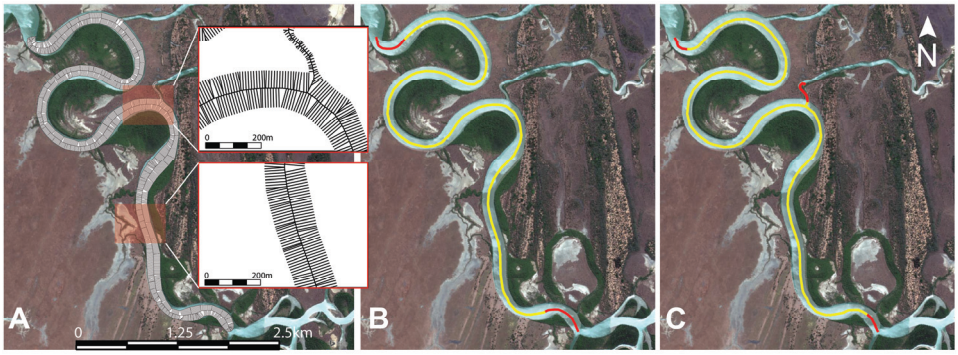

Fig. 1. A) Overview of a small portion of a meandering channel traversing the Mitchell River delta with its skeletal lines identified by Voronoi tessellation. Inset: close ups of the high resolution line (minimum 10m [vertex] spacing) segment mesh, with the uppermost box identifying a potential branch. **B)** Typical result of the pruned skeletal line (yellow) made by removing excess line segments, including the branch, overlain by the proposed double single source-Dijkstra method result (red). **C)** Multiple (three) endpoints identified by first pruning the skeletal line (yellow) and then extending that data to the polygon edge (red). Background imagery © Bing™.

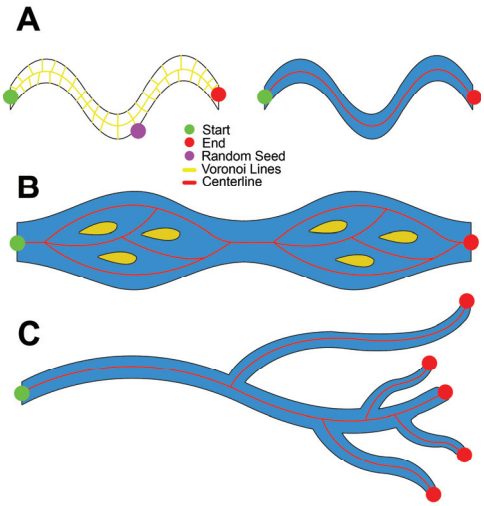

Fig 2A illustrates a simple centerline between two end vertices (start and end), which describes the centerline as the shortest distance between these two endpoints. To achieve full automation, the two endpoints must also be selected automatically. To this end, a double single-source Dijkstra algorithm (Dijkstra, 1956) is used to select a random seed within the skeletal line graph to determine the start coordinates as those which are furthest away from the initial seed.

Fig. 2. (left) Scenarios that define a centerline of any given feature. **A)** Example of a random seed selection within the skeletal line that is subsequently used to define the start and end points by the double single-source Dijkstra method. **B)** Centerline created with internal closed loops; **C)** expansion of A and B using multiple endpoint (branch) members.

A second cumulative distance from this start point selects the end point and defines the centerline of the feature as well as the set of vertices that comprise the shortest path between the two selected vertices. Dijkstra's algorithm obtains the shortest path between two vertices by calculating the distances between all potential paths, and these additional paths can also be included in the centerline definition (Fig 2B). Furthermore, the approach can be expanded to centerlines with multiple endpoints by treating each branch as its own individual shape.

One assumption for a centerline with multiple endpoints is that it will have a clearly defined branch that deviates from the main centerline, depending on a subjective interpretation of the threshold used to constitute a branch (Fig 1C and Fig 2C). This can be calculated by pruning the skeletal line until the minimum desired number of segments (a function of length) of a branch is reached. The Dijkstra algorithm calculated from each endpoint of the individual branches determines the furthest cumulative distance, ensuring that it does not double back on itself. This allows for identification of each branch while retaining the full length, rather than a pruned subsample. In essence, each branch along the centerline is treated as a single centerline feature. In a sedimentological context this is particularly useful in defining the trend of channel width downstream in a distributive fluvial system (DFS, e.g., Weissmann et al. 2010).

2.2. Centerline Orientation

The automatically-generated centerlines are obtained without consideration of depositional dip direction, i.e. the start and endpoints are randomly defined according to the seed used to initiate the centerline calculation. This would result in undesirable consequences when e.g. orientation and width along the centerline is to be measured in relation to distance along a channel or other architectural element. In order to properly model the direction of the centerline requires the relationship between the depositional system orientation and the centerlines of the modeled polygons to also be established. This can be achieved by using a semi-automated method that takes a manual interpretation of the land-/basinward direction of the depositional system and assigns the start vertex of all centerlines as the coordinate that is closest to the manually interpreted referenced line (Fig 3).

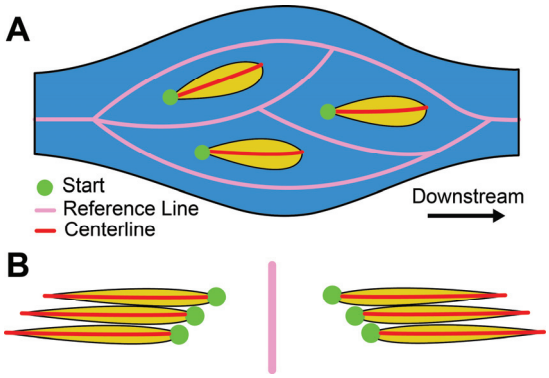

Fig. 3. (left) If the start vertex of an individual centerline is to be correlated to the depositional system direction, the cumulative shortest distance along the reference line to each polygon is used (**A**). Otherwise each centerline is oriented to its closest proximity to a single reference line, as shown in **B**.

By measuring the distance along a depositional system (Fig 3A), the start coordinate of each individual feature is defined as the shortest cumulative distance along the reference line. This function corrects the orientation of the centerline of a feature and also measures the distance along the depositional system to each individual feature (see also Congo River case study). The start of beach and chenier ridge centerlines can be defined to start in relation to the closest distance to a channel (Fig 3B). Once an appropriate centerline has been obtained for the desired polygon, the orientation is determined using the endpoint coordinates of the shortest path by atan ($\frac{\Delta y}{\Delta x}$), relative to grid north. The shortest path is defined here as the distance between the start and end coordinates of the centerline. The

orientation serves as an important component in determining change in geometric attributes within a depositional environment of interest.

2.3. Centerline Deviation

The ratio of the centerline length over the shortest path length yields a feature's sinuosity; however, sinuosity is of limited value as it is only a single measurement taken over the entire length of the element, and therefore does not consider its variation over distance. For example, multiple sinuosity measurements may be more appropriate to describe larger features, such as rivers, though the granularity must be carefully chosen to be representative of the actual sinuosity in the subdivided section. This is an issue when in quantitative analysis of elements that vary significantly in centerline profile and length.

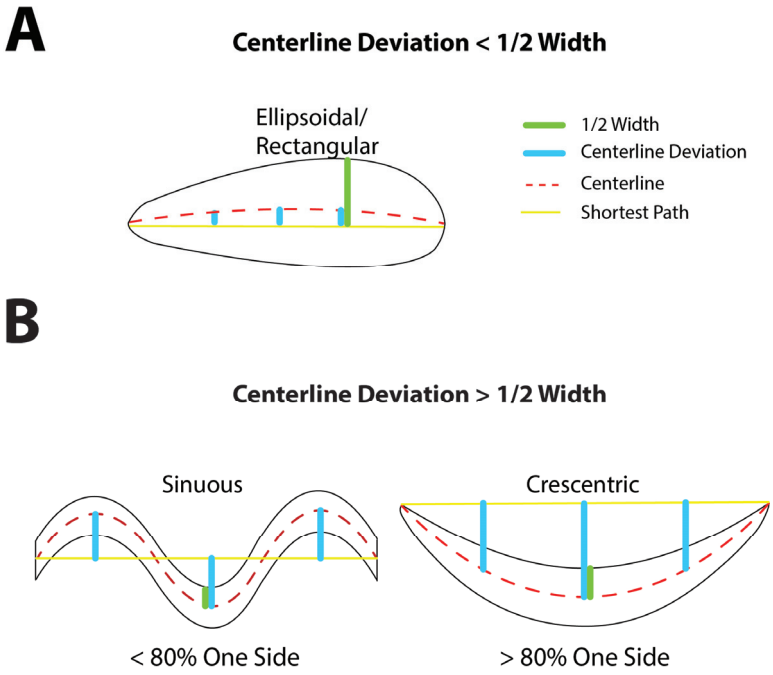

Fig. 4. A) A sinuosity threshold determines the degree of sinuosity that may classify an ellipsoidal or rectangular shape; **B)** Proportion of the centerline deviation occurring on each side of the shortest path line defines elements as crescentic or sinuous.

We propose to calculate centerline deviation using the perpendicular distance from the shortest path to the centerline (Fig 4), calculated at a user-defined sample spacing. This deviation, calculated along the centerline, can be used to establish parameters such as amplitude and variability as a function of distance. The advantage over a conventional sinuosity measurement is that features with similar sinuosities but different geomorphological characteristics can be differentiated.

2.4. Width

For each centerline deviation, a corresponding width measurement is taken perpendicular to the centerline and bounded by the polygon's spatial extent. This measurement is taken perpendicular to the angle between the endpoints of twice the user specified distance with the measurement being placed at the end of the first line (Fig 5). Considering that the midpoint of the perpendicular line is created at the endpoint of the first line segment, a measurement of distance versus width can be determined. The width is calculated from the points where the perpendicular line intersects the boundary of the original feature on either side of the centerline, resulting in a line that contains three vertices: the midpoint and the two intersection points on the boundary.

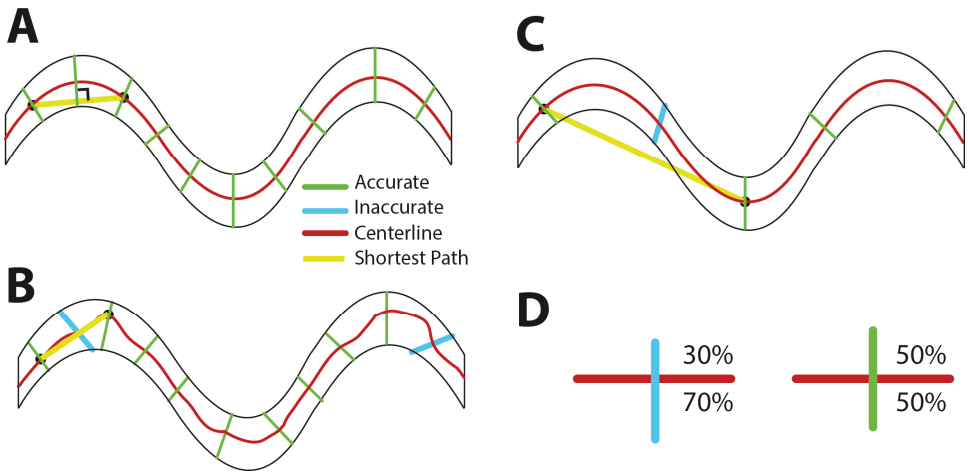

Fig. 5. Width measurements are calculated based on the line perpendicular to the shortest path, as defined between two endpoints along the centerline, and the intersection with the element boundary. High quality width measurements result from a good centerline representation and appropriate sample spacing, **A**. When the centerline is poorly defined (**B**), or sample spacing does not reflect the centerline variation (**C**), low quality width measurements will result. An unreliable width measurement can be identified using the proportion of the line that occurs on either side of the centerline (**D**).

The reliability of automated width measurements depends on two main criteria: the closeness of the centerline representation to the true element centerline, and the sampling distance chosen for each calculated measurement. As the perpendicular line is taken in relation to the centerline, a poor centerline representation may yield an unreliable width measurement (Fig 5B). The fidelity of the centerline depends principally on the vertex sampling of the enclosing polygon, which is defined in the centerline creation process, and is itself based on the input vector mapping data. Low sampling frequency may result in an unrepresentative width measurement, as the perpendicular line is taken at a spacing lower than the variability present in the dataset (Fig 5C). Taking a higher density of measurements at a shorter interval may solve the issue; however, the sampling must be chosen to be adaptive to elements from modern deposition systems of variable size. Therefore, to reduce the computational complexity whilst retaining equal sample spacing, an optional

implementation is suggested to only take the n^{th} sample per shape. Although an adaptive sampling would be beneficial to ensure appropriate point spacing in both straight and curved sections, in this case equal spacing is preferred to define geometric shape in later geomorphological classification (Section 2.5).

After automated width extraction there will undoubtedly be misrepresentative measurements, owing to the inherent complexity found in nature, and which need to be removed or corrected. The true width of any given feature is defined by the perpendicular lines on each side of the centerline being exactly equal (Fig 5D). By providing a threshold factor that determines the maximum allowed percentage difference between each side, lower quality width calculations can be removed. Alternatively, those width measurements flagged as low quality can be interpolated from the surrounding width measurements using, for example, a polynomial function.

2.5. Geometric Shape

Once length, centerline deviation and width have been defined along the centerline at the specified sample spacing, these geometric attributes can be used to make an objective classification of geomorphological shape. An object is described as belonging to one of nine classes through a combination of crescentic, sinuous or ellipsoidal/rectangular shapes (Fig 6A), with linear, symmetrical or asymmetrical characteristics (Fig 6B) which combine to indicate geomorphological shapes (Fig 6C). To describe these geometric shapes, four parameters (sinuosity, crescentiformity, symmetry and linearity) are combined to segregate the classes mentioned.

The sinuosity threshold determines whether an object is crescentic/sinuous or ellipsoidal/rectangular, as defined by the ratio of the maximum deviated centerline divided by half the maximum width. A value below one indicates that the shortest path of the centerline is contained completely within the modeled object, while a value approaching zero (i.e. no sinuosity) suggests either an ellipsoidal or rectangular feature (Fig 4A). In contrast, a value greater than one would indicate a feature whose amplitude is greater than width, indicating extreme sinuosity or potentially a crescent-like shape. By examining the proportion that the centerline deviates to one side or the other from its shortest path, a cresentic threshold, defined as greater than 80% on one side, determines that the object is crescentic rather than sinuous (Fig 4B).

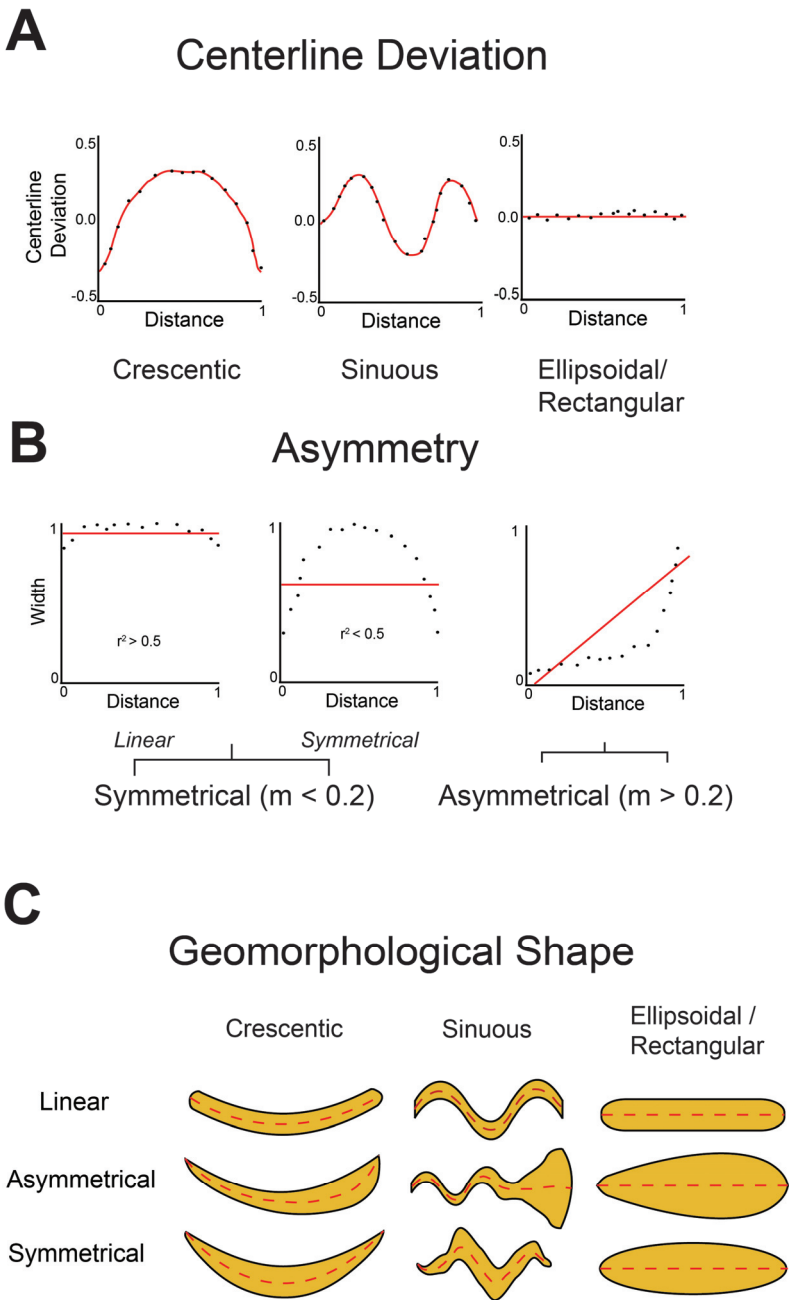

Fig. 6. A) Centerline deviation with a normalized profile along distance, whereby a value close to zero indicates no deviation; **B)** asymmetry, whereby a combination of slope and linear regression coefficients determine whether an object is linear, symmetrical or asymmetrical. **C)** The geomorphological shape of a feature can be determined by combining centerline deviation (**A**) and Asymmetry (**B**).

Each classification of sinuous, crescentic or ellipsoidal/rectangular shape on the X-axis (Fig 4A, Fig 6A) is combined with its linear, symmetrical or asymmetrical geometric profile on the Y-axis (Fig 6B). This profile is based on a symmetry threshold which defines whether a feature is symmetrical or asymmetrical in terms of an equal distribution of width to distance. For any given feature on a linear regression slope, if the width versus distance is greater than an empirically-defined symmetry threshold of 0.2, then that characteristic feature is classified as asymmetrical. Finally, if the feature is not asymmetrical, the linearity threshold examines the coefficient of determination (r^2) of a linear regression line for each individual object, classifying an object as linear when r^2 is greater than 0.5. Otherwise a feature is assigned as symmetrical (Fig 6B).

2.6. Spatial Connectivity

The heterogeneity of architectural elements, and subsequent connectivity seen in a depositional system, play an important factor in determining the relationship between elements, providing an understanding of the potential fluid flow dynamics in the subsurface (Howell et al., 2008). The connectivity of architectural elements can be measured in several ways, and two possibilities are considered here: i) the instances of features sharing a single edge, representing the number of connected sandbodies and the number and distribution of elements; ii) the surface area (perimeter) that spatially connects these elements in the depositional system.

To examine the instances where a polygon shares at least a single edge with another feature can be achieved by calculating any overlap or intersection between their vertices and registering that by a unique identifier. This groups all connected shapes while retaining their original shape and attributes, without the need to merge the complex shapes that would otherwise remove any additional attributes of each component polygon.

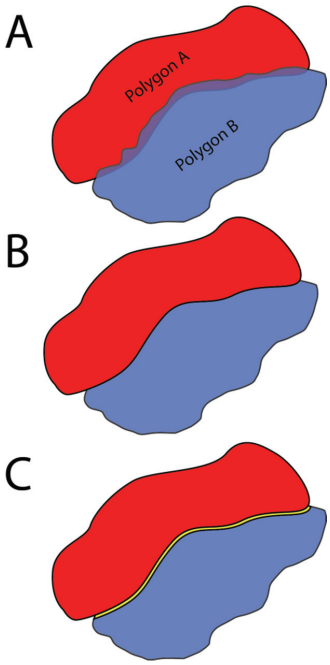

Fig. 7. Schematic showing workflow for calculation of the shared perimeter between two objects, Polygon A and Polygon B. **A)** Overlap of two mapped features; **B)** border corrected so that the perimeter is shared; **C**) buffers each object by a given amount creating a new sliver polygon with the shared border length taken as half the perimeter of this.

To examine the shared perimeter between two or more polygons is more complex, and is dependent on the given input vector data, as connectivity will be disturbed when shared edges do not have equal vertices To ensure that the shared part of a polygon's border is identical in all surrounding polygons, any given overlap is removed to create a new set of features, the geometry of which is revised (Fig 7A and 7B). If small gaps are present between the revised polygons, a buffer can be assigned to the operation above to ensure that overlap will be present. Despite a cleaned input vector dataset, the vertices that comprise the shared border may still differ, rendering a perimeter calculation between all polygons invalid. One solution to this

challenge is achieved by buffering each polygon by a proportion of its relative scale, and the perimeter of the resulting sliver polygon is halved to give the shared border length (Fig 7C).

3. Case Studies

To show the applicability of the described geometric attribute descriptions two different depositional environments are described, which represent a variety of scenarios that may improve geometric analytical capability. These include a comparison of geometric attributes and spatial connectivity from the Mitchell Delta, Gulf of Carpentaria, Australia – a tropical, tide-dominated, fluvial-influenced, and wave-affected marginal marine system (Nanson et al., 2013). Secondly, the method was a applied to the tropical intracratonic fluvial system of the Congo River, Democratic Republic of the Congo (Kadima et al., 2011), to assess attribute change analysis over 1,200 km of the river's extent.

As the minimum bounding box's shortest axis (width) and longest axis (length), hereby referred to as a MBB width and MBB length, has previously been used in a sedimentological and geomorphological context in a wide range of fields (Gardoll et al., 2000; Côté and Burn, 2002; Shugar and Clague, 2011; Nanson et al., 2012) for automated quantitative geometric attribute and shape characterization, this is used as a basis for comparison.

3.1. Mitchell Delta

The 520 km^2 northern Mitchell River Delta dataset consists of 1 759 reservoir elements (mouthbars, channel bars, channels, abandoned channels, cheniers and beach ridges), mapped using a combination of high resolution satellite imagery mapping, ground truthing, augering, digital elevation model (DEM) analysis, trenching and surface sampling (Nanson et al., 2012). Elements were analyzed using our new method, with centerline deviation and width measurements taken every 50 meters along the centerline at a maximum sampling number of 100.

Using our new objective (AB) methodology, the geomorphological shapes of reservoir elements in the Mitchell Delta show a wide distribution, similar to the findings of Nanson *et al* (2012) who used a more subjective approach. The elements are predominantly ellipsoidal and crescentic in form, excluding the meandering channels. Beach and chenier ridges are mostly ellipsoidal asymmetrical (30% and 23%) and crescentic asymmetrical (29% and 30%), mouthbars and pointbars are crescentic symmetrical (75%, 24%) and crescentic asymmetrical (25% and 47%), whilst midbars are mainly ellipsoidal asymmetrical (61%).

The results from our new AB method suggest no discernable trends of width with length (Fig 9A) for wave generated processes (beach ridges and cheniers). This shows a relatively constant mean around 65m with a degree of variability present within the dataset. In contrast, the results of MBB width versus MBB length show a definite trend that can be represented by a linear regression line (Fig 9B). Indeed, a comparison of the two methods show that MBB overestimates by a linear regression at 1.85x for width (Fig 9C) and underestimates length at 0.97x (Fig 9D).

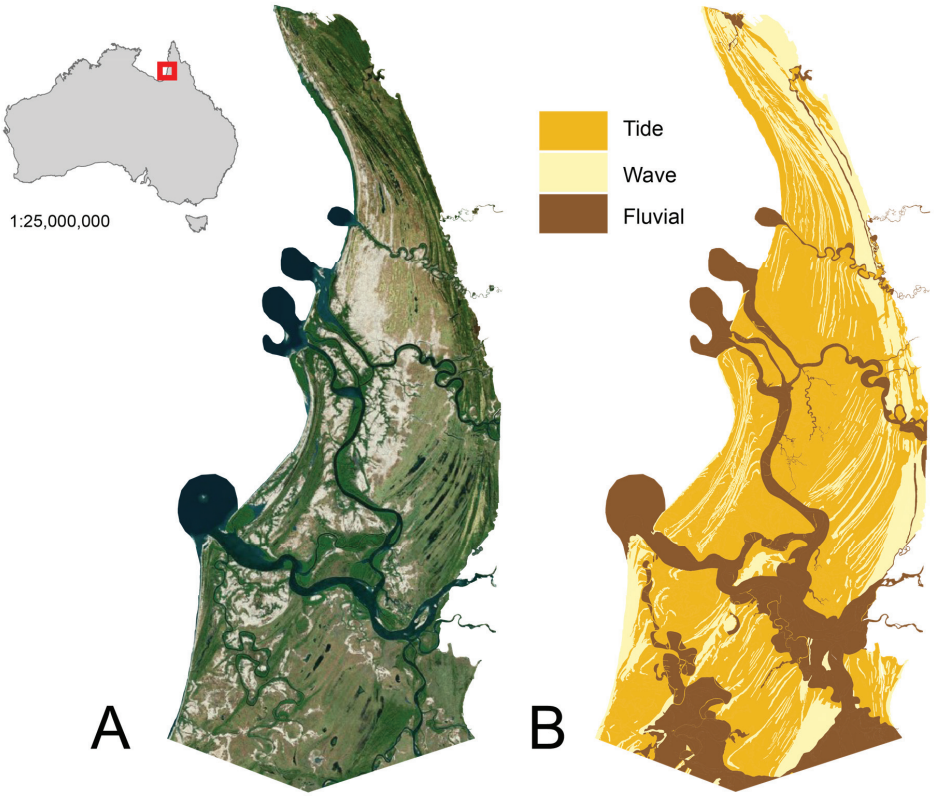

Fig. 8. A) The Mitchell River Delta; **B)** dominant processes of each depositional element (from Nanson et al., 2012). Background imagery © Bing™. Tide elements dominate the spatial extent of the delta, though potential reservoir elements are comprised of the less extensive fluvial and wave elements.

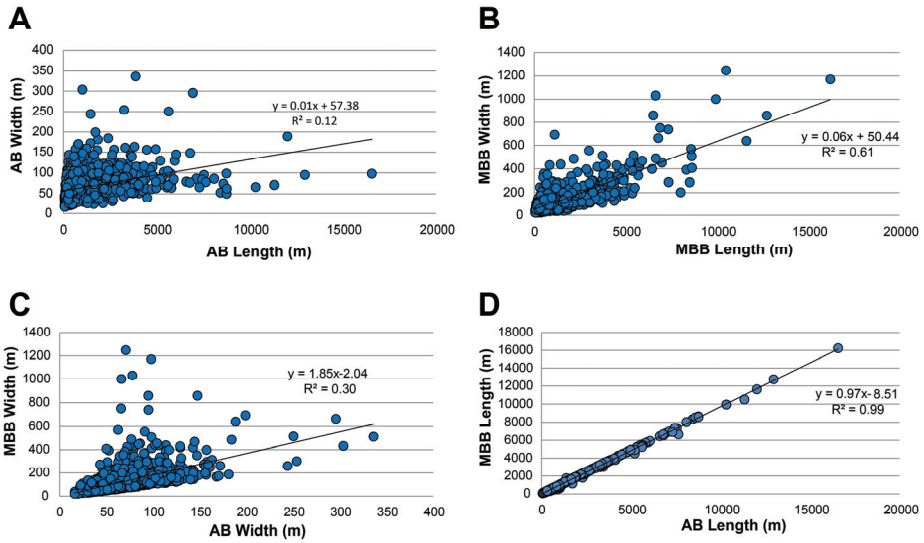

Fig. 9. **A)** wave-generated elements (beach and chenier ridges) AB width to length shows a bad correlation to suggest that the width of wave-generated elements do not increase with length. **B)** MBB width and MBB length reproduced after the method of Nanson et al. (2012) shows a strong relationship between length and width suggesting a misleading correlation. **C)** Comparison of MBB width to AB width shows that a MBB overestimated width while **D)** MBB length to AB length shows that the length is only slightly underestimated. The greatest source of error then is associated with the width measurement from a MBB method.

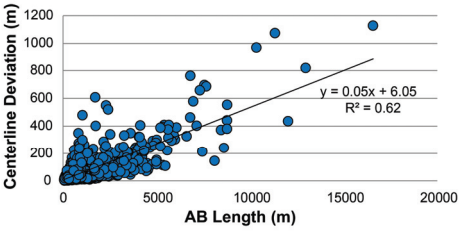

Fig. 10. AB length versus centerline deviation for wave-generated elements shows a strong correlation, with a similar linear regression line to that of the MBB length vs MBB width plot in Fig 9B. This shows that a MBB measurement of the crescentic wave-generated elements of the Mitchell Delta captures the cresencisity of elements rather than its width.

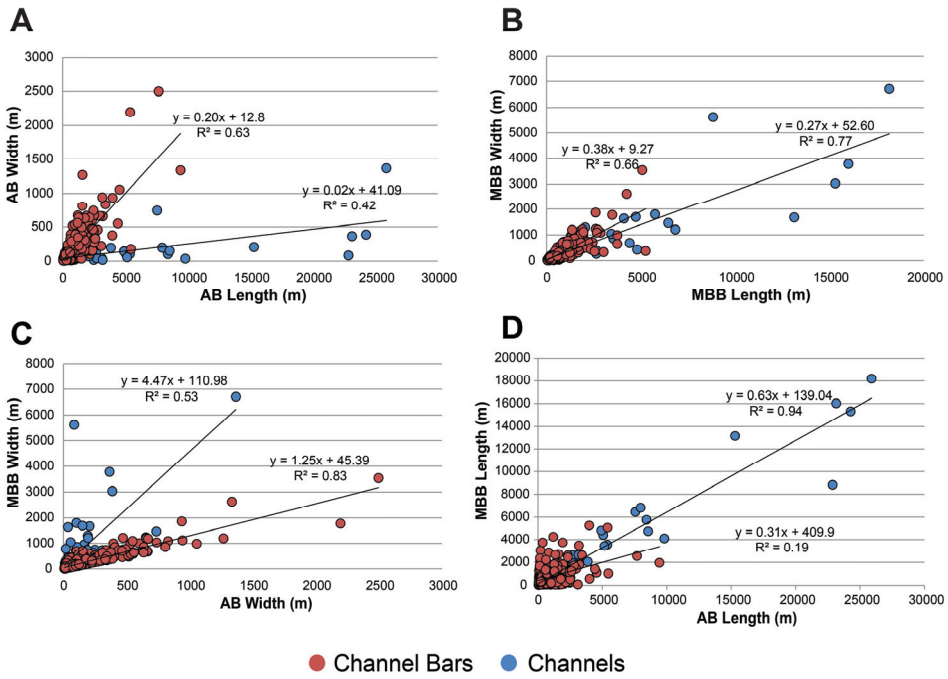

Fig 11- A compares fluvial generated elements (channels and channel bars) AB width to length and MBB width and MBB length in **B**. A comparison of MBB width to absolute width is shown in **C** and a MBB length to absolute length in **D**. These results suggest that MBB drastically overestimates the width of features while underestimating length implying any MBB relationship of length versus width will potentially be unreliable.

One explanation for this difference is demonstrated by a measurement of maximum centerline deviation versus length indicating a strikingly similar trend to MBB width and MBB length comparison (Fig 9B; Fig 10) and the linear regressions equations. Datasets with predominantly crescentic shapes greatly exaggerate the MBB width given the long features that are present, a fact emphasized by the maximum width values present in a MBB compared to an AB width measurement.

The geometric attributes from fluvial reservoir elements, split into channels and bars, indicate a similar disparity. While the new method (Fig 11A) and the MBB method (Fig 11B) both show a trend of width versus length, the range of values is significantly different where MBB overestimates widths (Fig 11C) and underestimates lengths (Fig 11D). For example, channel bars show a regression slope of the MBB measurements at nearly twice that of an absolute measurement (0.38 vs 0.20). The mean MBB width to length ratio is 0.42, falling outside the typical range between 0.15 to 0.35 by previous manual measurements of mid channel bar forms (Holzweber et al., 2014), compared to 0.24 in this study.

Fig 12A shows an illustration of all the shared borders between reservoir elements in the Mitchell Delta (see Fig 8). These connections are achieved mostly through a shared border with fluvial elements (i.e. channels), with up to 82 neighboring connections. The majority of

single sand body compartments are isolated chenier ridges and a small proportion of beach ridges. The 2D connectivity of the Mitchell Delta (Fig 12B) is then represented by 498 individual connected sandbodies, where the two largest connected sandbodies comprise 592 and 320 individual features (>50% of total) and an area of 125km^2 (>70% of total). The largest connected sand body by area consists of predominantly fluvial features (82%), whereas the second largest set of connected sandbodies is mainly wave-generated (79%).

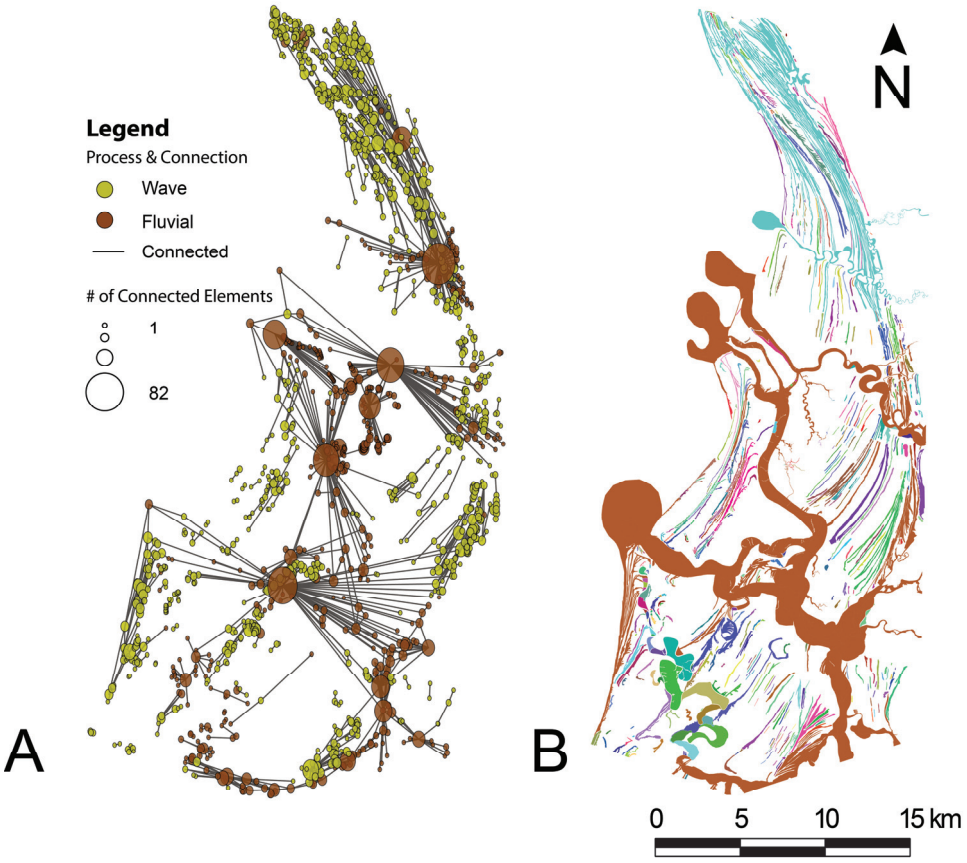

Fig. 12. **A** represents wave and fluvial element locations by their centroid coordinates, with node sizes relative to the number of reservoir elements it connects. **B** shows a random color coded scheme based on the 498 connected individual sandbody groups whereby the brown and cyan color represent the largest and second largest sandbody groups, respectively. The original geometry and attributes of individual elements within each group is retained by grouping the reservoir elements by their connection in **A** rather than merging and dissolving their adjacent boundary (see Fig 5, Nanson et al. 2012).

While these results suggest that fluvial elements provide a significant degree of connectivity (Fig 12A and B), the shared border between fluvial and wave-generated potential reservoir elements is minimal (Table 1). For channels, the highest connected

element type are to channel bars (52.2%) and non-reservoir element of tidal flats and floodplains (32.1%). Conversely, channel bars are predominantly connected to those channels where midbars are enclosed by the channel and channel sidebars having at least a 50% non-reservoir connection. Channel to beach and channel to chenier ridge connections show only low levels of connectivity (2.6% and 0.7% respectively). Beach and chenier ridges show a high degree of interconnectivity, with beach to beach ridge connections reaching 32.6% and chenier to chenier connections at 12.8%, suggesting clustering. The main heterogeneity of beach ridges are swales (46.1%) and tidal floodplains (17.0%), compared to tidal floodplains (57.4%) and swales (26.7%) for chenier ridges.

Category	Beach Ridges	Chenier Ridges	Channels	Channel Bars	Swales	Tidal Flats & Floodplains	Other	Total
Beach Ridges	32.6	0.4	0.6	0.5	46.1	17.0	2.9	100
Chenier Ridges	0.5	12.8	0.2	0.3	26.7	57.4	2.0	100
Channels	2.6	0.7	1.9	52.2	1.9	32.1	8.6	100
Channel Bars	1.6	0.7	37.1	11.6	0.0	18.1	30.9	100

Table 1. The % of the total perimeter within each category of beach ridges, chenier ridges, channels or channel bars that are connected to one of the six major reservoir or non-reservoir elements in the Mitchell Delta dataset. Reservoir elements comprise beach ridges, chenier ridges, channels and channel bars (including mouthbars). The two main non-reservoir elements of swales, and tidal flats and floodplains demonstrates the dominate heterogeneity associated with each reservoir element.

3.2. Congo River

The Congo River basin data is derived from Landsat 7 Enhanced Thematic Mapper Plus (ETM+) imagery available from the Landsat Global Land Survey 2000 dataset (USGS, 2009) and accessed through the seamless global coverage available within the Landsat-ESRI collaboration (ESRI, 2014). This imagery has a spatial resolution of 30 m in 6 spectral bands, as well as one 15 m panchromatic band and one 60 m thermal infrared band. The multispectral data were processed in ArcGIS, using a supervised classification to highlight the spectra of water in the dataset to identify the main river channel (Fig 13). The internal structures within the anabranching river were assumed to be the mid-channel bars (Fig 14).

The Congo River dataset extends 1 200 km, with an average width of 8.2 km and consists of 2 221 mid-channel bars. The centerline orientations of the mid-channel bars were corrected according to the distance along the anabranching river centerline, with start vertices assigned upstream along the Congo River (Section 2.2; Fig 14A and B). Width measurements of the anabranching river were calculated every kilometer, with an accuracy of 1%. The width and centerline deviation of the mid-channel bars (Fig 14C and D) were taken every 25m at a maximum sampling interval of 100 and to an accuracy of 10%.

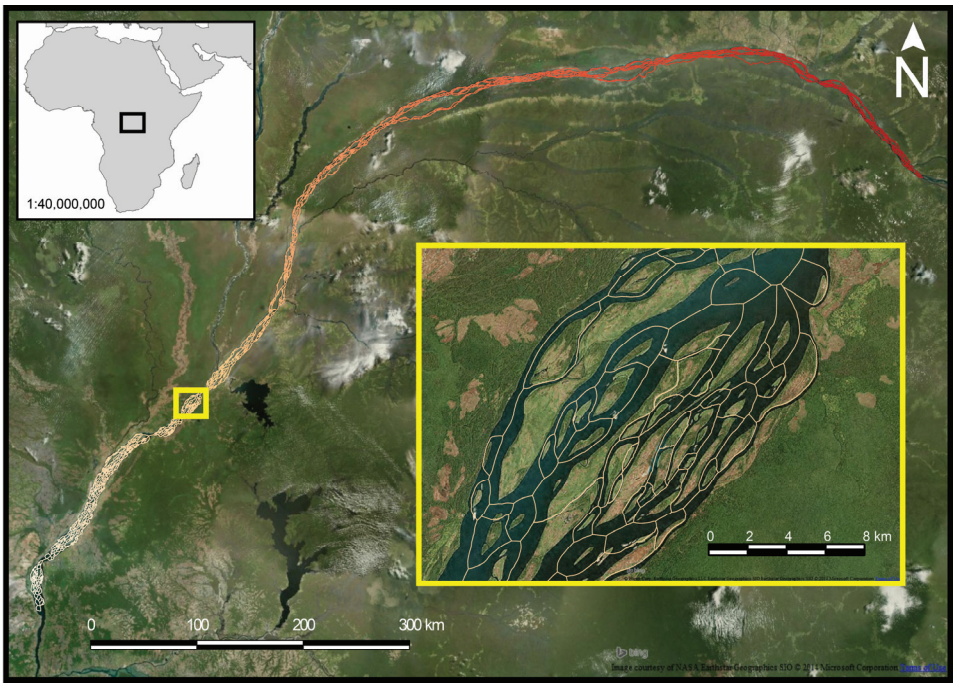

Fig 13 – The Congo River dataset showing the centerlines of the anabranching river with a colored increase indicating the cumulative distance upstream from 0 to ~1,200km. A zoomed subsection is shown that also represents the subsection used to illustrate the centerline correction, width and centerline deviation analyses performed on the mid channel bars in Fig 14. Background imagery © Bing™.

The results show that the geometric shape of the mid-channel bars in the Congo River basin are split into ellipsoidal (92%), crescentic (7%) and sinuous (1%) shapes, with the majority being asymmetrical (71%) as opposed to symmetrical (28%) and linear (1%) profiles. 90% of the asymmetry within the Congo river basin is oriented towards the upstream of the Congo river. The width to length ratio of all mid-channel bars demonstrates a strong relationship, with an arithmetic mean of approximately 0.16 to yield a regression line of $y = 0.14x + 160$ with an r^2 of 0.84, Fig 15A. The results for the MBB width and MBB length method for mid-channel bars in the Congo River (Fig 15B) are very similar to those proposed in this paper. Specifically, a comparison of width measurements (Fig 15C) shows a slight overestimation of MBB geometry with a regression line at 1.06x and a slight underestimation of MBB length geometry at 0.97x (Fig 15D). The mean width to length ratio found by the current method is 0.23, compared to 0.25 from the MBB approach.

Analysis of width to length and channel width binned by distance upstream of the Congo River (Fig 16) shows a decrease in both variables. The mean width to length ratio of mid-channel bars downstream is 0.26, compared to 0.21 upstream. Channel width changes from a mean of 925 m to 530 m. The change in geomorphological shape between asymmetrical and symmetrical ellipsoidal mid-channel bars (the two highest represented proportions of the mid-bars in the Congo) shows an increase in asymmetry of mid-channel

bars upstream (Fig 17).

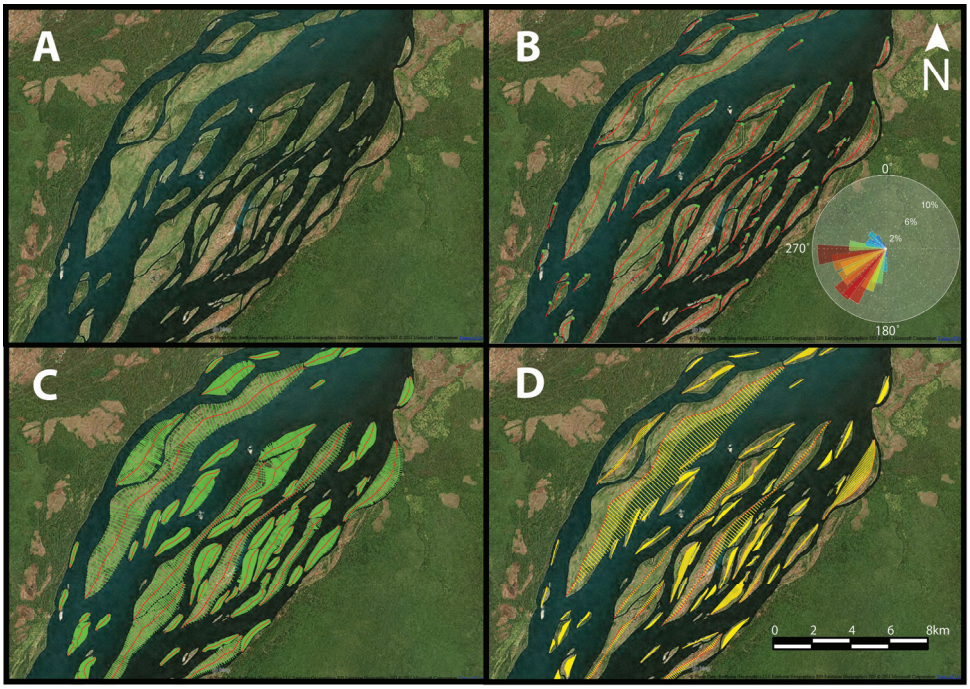

Fig. 14. A subsection of the Congo, see box in Fig 13, used to show the original image in **A**, and centerline generation in **B** with its start vertex corrected upstream along the river. A rose diagram is used to show the direction of all mid channel bars in Congo River. This centerline can subsequently be utilized to generated equally spaced width measurements in **C** and centerline deviation in **D**. Background imagery © Bing™.

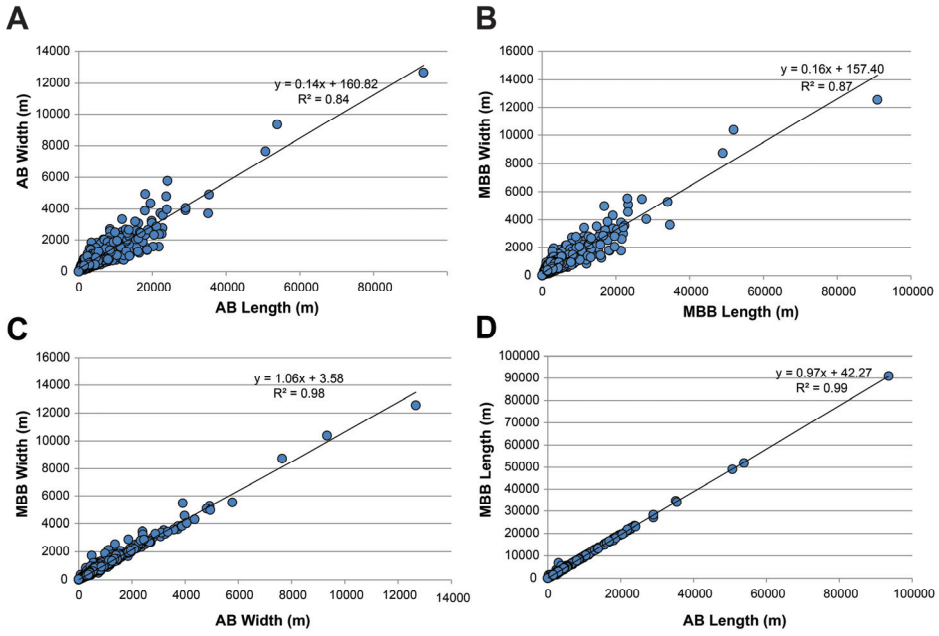

Fig. 15. **A** compares AB width to length features of mid-channel bars in the Congo River. **B** shows MBB width and MBB length of those same bar forms. A MBB width to AB width comparison is shown in **C** while **D** shows a MBB length to AB length comparison. The strong correlation between the AB and MBB suggests that both methods produce reasonable measurements for the predominately ellipsoidal shapes of the mid-channel bars of the Congo River.

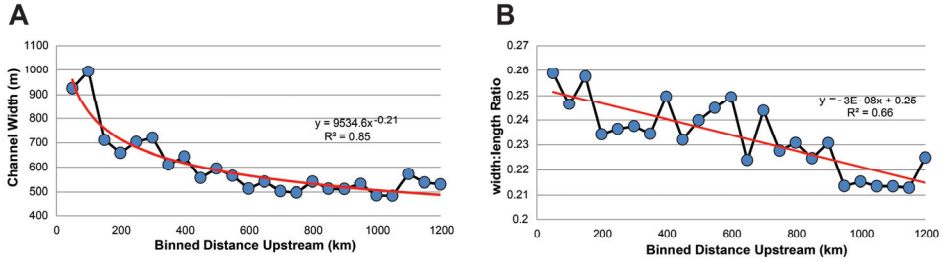

Fig 16 – Average channel width and width:length ratio binned into 50km sections along the Congo River showing that both channel width and width:length ratio decrease with distance upstream.

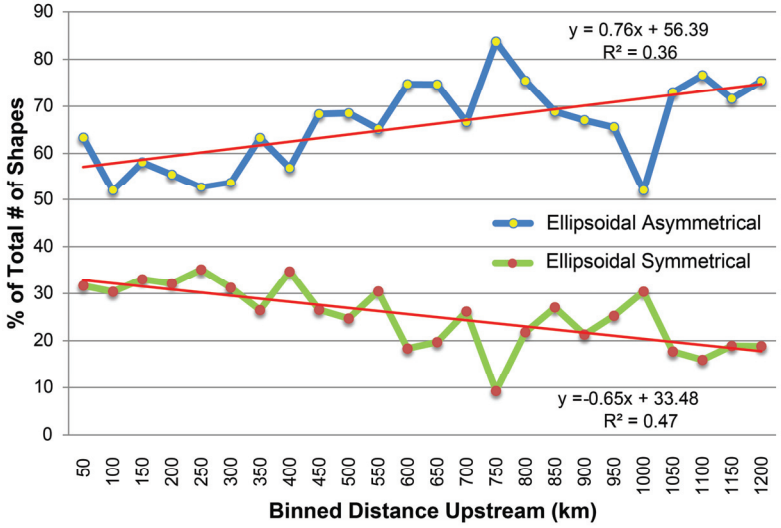

Fig. 17. – Change in proportion of ellipsoidal symmetrical and ellipsoidal asymmetrical features as a % of total with distance upstream along the Congo River binned into 50km sections.

4. Discussion

The application of MBB to describe shape and geometry of geo-spatial data has been applied in the past due to its ease of use and accessibility within standard GIS suites. The width, length and area from a MBB provide the ability to measure maximum and minimum geometric values and the basis to describe shape, such as elongation and circularity (Gardoll et al., 2000; van der Werff and van der Meer, 2008; Tafesse et al., 2012; Kröner and Doménech Carbó, 2013). However the measurements derived from a MBB analysis are limited and our proposed method shows potential in describing the complexity of geometric shapes and element connectivity of modern depositional systems. The complexity of shapes and their geometries in reservoir models are important to quantify heterogeneities and compartmentalization (Larue and Legarre, 2004), and studies of modern systems can aid in differentiating planform geometries that vary by depositional environments (Tye, 2004; Nanson et al., 2012; Massey et al., 2013; Vakarelov and Ainsworth, 2013). The tools presented in this paper have demonstrated an initial progress towards achieving that goal in a quantitative and objective scheme.

The case studies have shown that in comparison to the conventional MBB approach, the present study has significant advantages for measuring the absolute internal dimensions of target elements. The MBB method inherently exaggerates the width and underestimates the length of the polygon it is used to describe. As such, the use of these measures in describing the internal geometries of target elements provides potentially misleading results, as indicated by the Mitchell River Delta dataset. Conversely, the mid-channel bars of the Congo River were found to be well-represented by MBB geometry. This discrepancy is attributed to the greater complexity of elements found in the tide-influenced Mitchell Delta (Nanson et al., 2013), with more crescentic and sinuous shapes compared to the

predominately ellipsoidal shapes found in the Congo.

Connectivity between potential reservoir elements in the Mitchell Delta has been shown, with channels indicated as the most connected elements (Figure 12A). While fluvial channels supply shorelines with the sediment needed to construct beach and chenier ridges (Rhodes, 1982), intervening non-reservoir elements can form barriers between fluvial and wave elements to reduce connectivity (Howell et al., 2008). This is significant, as of the channels and ridge forms that are connected, the connection pathways are often along narrow conduits of beach and chenier ridges (Table1; Figure 12B; Nanson et al. (2013)) to considerably reduce the connectivity of the entire reservoir sandbody. A quantification of the connected sandbodies and the perimeter connecting sandbodies as proposed in the new methodology allows for another technique to compare the relative heterogeneity and compartmentalization between different modern systems.

In addition to the geometric attribute characterization, the proposed AB method has shown its applicability to study the variability in geometric attributes and shape with distance along a depositional system. As demonstrated by the Congo River study, this provides a unique insight into the change in shape classification and attributes for example, as channel width and symmetrical ellipsoidal shapes decrease with distance upstream. This may reflect a transition from an open portion of the anabranching river to narrower channels and lower width:length mid channel-bars upstream. Defining trends within depositional environments is an essential component in the framework of any depositional model (e.g., Boyd et al. (1992); Nichols and Fisher (2007)) and geometric attribute and shape characterization proposed in the methods here can help to quantify that variability of the modern.

The case studies demonstrate the method using modern depositional systems. However, there is broader potential application to any two-dimensional object. One example within the geosciences is application to two-dimensional along strike or dip sections of outcrop analogs (Rittersbacher et al., 2014), where current methods to retrieve geometric attributes and describe element shape are largely performed manually and subjectively (Howell et al., 2014). Our method may address these limitations by adding automation and systematic measurement to reduce error.

5. Conclusion

This paper presents a method to calculate the geometric attributes in relation to shape and connectivity of mapped depositional features for improved empirical analysis in sedimentology and geomorphology. The method is implemented as a set of scripts for use in a GIS environment, where in-built capabilities have traditionally been lacking. By sampling multiple equally-spaced measurements of two-dimensional objects along their centerlines, a better representation of width and centerline deviation variability has been achieved compared to conventional GIS approaches. This systematic and objective measurement can be used to analyze the geomorphological shape of features and their distribution within modern depositional systems.

Acknowledgements

This work has been funded by the FORCE Sedimentology and Stratigraphy Group and the Norwegian Petroleum Directorate as part of Phase 2 of the SAFARI program.

References

Benz, U.C., Hofmann, P., Willhauck, G., Lingenfelder, I., Heynen, M., 2004. Multi-resolution, object-oriented fuzzy analysis of remote sensing data for GIS-ready information. ISPRS Journal of Photogrammetry and Remote Sensing 58, 239-258.

Blaschke, T., 2010. Object based image analysis for remote sensing. ISPRS Journal of Photogrammetry and Remote Sensing 65, 2-16.

Bouix, S., Siddiqi, K., Tannenbaum, A., 2005. Flux driven automatic centerline extraction. Medical Image Analysis 9, 209-221.

Boyd, R., Dalrymple, R., Zaitlin, B.A., 1992. Classification of clastic coastal depositional environments. Sedimentary Geology 80, 139-150.

Cornea, N.D., Silver, D., Min, P., 2007. Curve-Skeleton Properties, Applications, and Algorithms. Visualization and Computer Graphics, IEEE Transactions on 13, 530-548.

Côté, M.M., Burn, C.R., 2002. The oriented lakes of Tuktoyaktuk Peninsula, Western Arctic Coast, Canada: a GIS-based analysis. Permafrost and Periglacial Processes 13, 61-70.

Dijkstra, E.W., 1956. A note on two problems in connexion with graphs. Numerische Mathematik 1, 269-271.

ESRI, 2014. ESRI (Environmental Systems Resource Institute). 2014. ArcMap 10.1. ESRI, Redlands, California.

Fisher, G.B., Bookhagen, B., Amos, C.B., 2013. Channel planform geometry and slopes from freely available high-spatial resolution imagery and DEM fusion: Implications for channel width scalings, erosion proxies, and fluvial signatures in tectonically active landscapes. Geomorphology 194, 46-56.

Gardoll, S.J., Groves, D.I., Knox-Robinson, C.M., Yun, G.Y., Elliott, N., 2000. Developing the tools for geological shape analysis, with regional- to local-scale examples from the Kalgoorlie Terrane of Western Australia. Australian Journal of Earth Sciences 47, 943-953.

GRASS Development Team, 2014. Geographic Resources Analysis Support System (GRASS) Software. Open Source Geospatial Foundation Project.

Hagberg, A., Schult, D., Swart, P., 2008. Exploring Network Structure, Dynamics and Function using NetworkX, in: Varoquaux, G., Vaught, T., Millman, J. (Eds.), Proceedings of the 7th Python in Science Conference (SciPy2008), Pasadena, CA USA, pp. 11–15.

Hartley, A., Weissmann, G., Nichols, G., Warwick, G., 2010. Large Distributive Fluvial Systems: Characteristics, Distribution, and Controls on Development. Journal of Sedimentary Research 80, 167-183.

Haunert, J.-H., Sester, M., 2008. Area Collapse and Road Centerlines based on Straight Skeletons. Geoinformatica 12, 169-191.

Holzweber, B., Hartley, A., Weissmann, G., 2014. Scale invariance in fluvial barforms: implications for interpretation of fluvial systems in the rock record. Petroleum Geoscience 20, 221-224.

Howell, J., Skorstad, A., MacDonald, A., Fordham, A., Flint, S., Fjellvoll, B., Manzocchi, T., 2008. Sedimentological parameterization of shallow-marine reservoirs. Petroleum Geoscience 14.

Howell, J.A., Martinius, A.W., Good, T.R., 2014. The application of outcrop analogues in geological modelling: a review, present status and future outlook. Sediment-Body Geometry and Heterogeneity: Analogue Studies for Modelling the Subsurface. Geological Society, London, Special Publications 387.

Kadima, E., Delvaux, D., Sebagenzi, S.N., Tack, L., Kabeya, S.M., 2011. Structure and geological history of the Congo Basin: an integrated interpretation of gravity, magnetic and reflection seismic data. Basin Research 23, 499-527.

Kröner, S., Doménech Carbó, M.T., 2013. Determination of minimum pixel resolution for shape analysis: Proposal of a new data validation method for computerized images. Powder Technology 245, 297-313.
Lakshmi, J.K., Punithavalli, M., 2009. A Survey on Skeletons in Digital Image Processing, Digital Image Processing, 2009 International Conference on, pp. 260-269.
Larue, D.K., Legarre, H., 2004. Flow units, connectivity, and reservoir characterization in a wave-dominated deltaic reservoir: Meren reservoir, Nigeria. AAPG Bulletin 88, 303-324.
Lisle, R.J., 2006. Google Earth: a new geological resource. Geology Today 22, 29-32.
Massey, T.A., Fernie, A.J., Ainsworth, R., Nanson, R.A., Vakarelov, B.K., 2013. Detailed mapping, three-dimensional modelling and upscaling of a mixed-influence delta system, Mitchell River delta, Gulf of Carpentaria, Australia. In: Sediment Body Geometry and Heterogeneity: Analogue Studies for Modelling the Subsurface. Geological Society of London Special Publications 387.
McAllister, M., Snoeyink, J., 2000. Medial Axis Generalization of River Networks. Cartography and Geographic Information Science 27, 129-138.
Nanson, R., Ainsworth, R., Vakarelov, B., Fernie, J., Massey, A., 2012. Geometric attributes of reservoir elements in a modern, low accommodation, tide-dominated delta. APPEA Journal, 483-492.
Nanson, R.A., Vakarelov, B.K., Ainsworth, R.B., Williams, F.M., Price, D.M., 2013. Evolution of a Holocene, mixed-process, forced regressive shoreline: The Mitchell River delta, Queensland, Australia. Marine Geology 339, 22-43.
Nichols, G.J., Fisher, J.A., 2007. Processes, facies and architecture of fluvial distributary system deposits. Sedimentary Geology 195, 75-90.
Palágyi, K., Tschirren, J., Hoffman, E.A., Sonka, M., 2006. Quantitative analysis of pulmonary airway tree structures. Computers in Biology and Medicine 36, 974-996.
Pavelsky, T.M., Smith, L.C., 2008. RivWidth: A Software Tool for the Calculation of River Widths From Remotely Sensed Imagery. Geoscience and Remote Sensing Letters, IEEE 5, 70-73.
QGIS Development Team, 2014. QGIS Geographic Information System. Open Source Geospatial Foundation Project.
Rhodes, E.G., 1982. Depositional model for a chenier plain, Gulf of Carpentaria, Australia. Sedimentology 29, 201-221.
Rittersbacher, A., Buckley, S., Howell, J., Hampson, G., Vallet, J., 2014. Helicopter-based laser scanning: a method for quantitative analysis of large-scale sedimentary architecture. in Sediment-body geometry and heterogeneity; analogue studies for modelling the subsurface Special Publication - Geological Society of London 387.
Shugar, D.H., Clague, J.J., 2011. The sedimentology and geomorphology of rock avalanche deposits on glaciers. Sedimentology 58, 1762-1783.
Stutz, M., Pilkey, O., 2002. Global Distribution and Morphology of Deltaic Barrier Island Systems. Journal of Coastal Research, 694-707.
Svensson, S., Sanniti di Baja, G., 2003. Simplifying curve skeletons in volume images. Computer Vision and Image Understanding 90, 242-257.
Tafesse, S., Fernlund, J.M.R., Bergholm, F., 2012. Digital sieving-Matlab based 3-D image analysis. Engineering Geology 137–138, 74-84.
Tye, R.S., 2004. Geomorphology: An approach to determining subsurface reservoir dimensions. AAPG Bulletin 88, 1123 -1147.
USGS, 2009. Global Land Survey, 2000, Landsat ETM+. Sioux Falls, South Dakota, USGS.
Vakarelov, B., Ainsworth, R., 2013. A hierarchical approach to architectural classification in marginal-marine systems: Bridging the gap between sedimentology and sequence stratigraphy. AAPG Bulletin 97, 1121-1161.
van der Werff, H.M.A., van der Meer, F.D., 2008. Shape-based classification of spectrally identical objects. ISPRS Journal of Photogrammetry and Remote Sensing 63, 251-258.
Wang, C., Ren, C., Lei, X., Dai, S., 2011. Automatic skeleton generation and character skinning, VR Innovation (ISVRI), 2011 IEEE International Symposium on, pp. 299-304.

Weissmann, G.S., Hartley, A.J., Nichols, G.J., Scuderi, L.A., Olson, M., Buehler, H., Banteah, R., 2010. Fluvial form in modern continental sedimentary basins: Distributive fluvial systems. Geology 38, 39-42.

DISCUSSION, OUTLOOK AND CONCLUSIONS

VI

6. Discussion and Synthesis

The contribution of this work to the broader sedimentological and geomorphological fields facilitates further global scale characterization of modern depositional environments. This demonstrates an improved workflow that can be used to characterize modern depositional environments globally and that may lead to increased studies in the future to define important factors controlling sedimentary architecture. For instance, the global shoreline classification by ternary process in **Paper II**, has provided an initial definition that has been used to quantify the significance of tectonics and climate on modern shoreline geomorphology. Furthermore, the thesis highlights the methodology needed to describe the increased quantitative information that may arise from the definition of modern sedimentary basins, thereby renewing an interest for global based geomorphological studies. Finally, methodologies have been introduced to describe geometric attributes and shapes from outcrop that combined with characteristics of the modern, improve object-based reservoir modelling. This has been accomplished through three main stages.

1) Describing modern sedimentary basins that define the bounds of terrestrial sedimentary analogues for the rock record.

2) Using automated GIS methods to bridge the gap between the classification of modern depositional environments from remotely sensed imagery and the description of geometric attributes and shapes that interpret those environments.

3) Providing methodology to define user-defined objects for improved object-based modelling captures complex and realistic shapes of modern and ancient geometries of architectural elements.

The results, workflow and methodologies gathered in this thesis can serve as tools that future research can exploit to quantify the distribution of modern depositional environments in a global context. The geometric data gathered from that research can populate sedimentological databases to be applied for improved reservoir models. There is also a broader scope to improve or quantify the fundamental principles that controls the distribution and architecture geomorphological features in a global perspective. This work builds the foundation for exciting new opportunities and directions for global scale research of modern depositional environments as analogues for reservoir modelling.

6.1. Main Results

Analogous Modern Sedimentary Environments

Paper I describes the spatial distribution of modern sedimentary basins (Figure 9). Globally terrestrial sedimentary basins account for a mere 4.5% of earth's land surface (or approximately 16% of the terrestrial land surface; Figure 8). An additional 63 million km^2 or 13% of earth's land surface (41% of continental lithosphere) may represent the sub-aqueous continental lithosphere that combined suggest that approximately 17% of the continental lithosphere may be in net deposition. The significance of this research is that it defines "a" boundary of modern sedimentary basins to provide a first step in quantifying the distribution

of modern depositional environments that has been of considerable difficultly in the past (Weissmann et al. 2010). This is of considerable value when quantifying the aerial distribution of modern depositional environments for analogues to the rock record. Furthermore it adds to previous discussions on the preservation potential of modern sedimentary systems, for example the heated debate on the prevalence of distributary fluvial systems (DFS) in the rock record (Hartley et al. 2010a; Hartley et al. 2010b; Sambrook Smith et al. 2010; Weissmann et al. 2010; Fielding et al. 2012) by potentially providing the means to which to quantify the aerial distribution of modern DFS. It is important to consider though, that with any modern analogue, a discrepancy in time between the observable present and the preserved sedimentary record exists (Hampson and Storms 2003; Hartley et al. 2010a; Fielding et al. 2012) and therefore a definition of modern sedimentary basins does not in of itself answer that question. Nonetheless, while the present is not the same as the past, it is a key window into understanding the past.

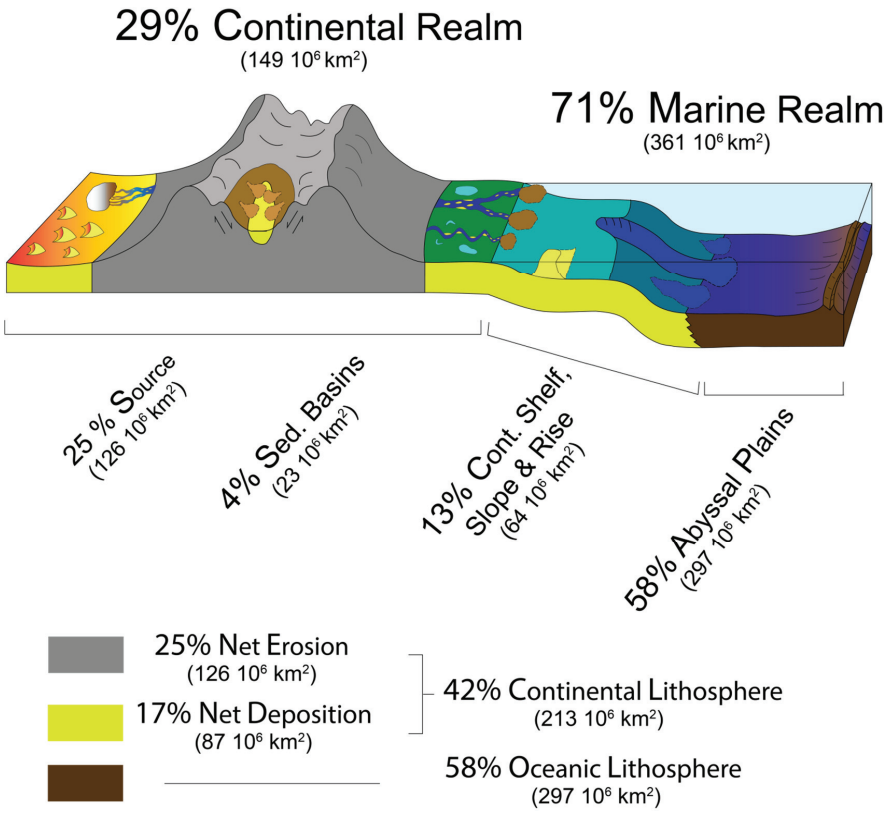

Figure 9 – A summary of the results gathered in **Paper I** showing the proportions of net depositional settings in relation to earth's, continental lithosphere's and oceanic lithosphere's surface area. Note that percentages have been rounded to the nearest whole number.

The results suggest a bias of modern sedimentary basins towards specific climates and basin types and that has important implications in how representative global studies of modern depositional environments are as analogous for the rock record. If the goal is to derive a

global, statistically representative sample across the spectrum of depositional environments and the range of climates and tectonics controls, this bias may be reflected in those studies. Indeed, research by Hartley et al. (2010a) based on global interpretation of DFS systems collected the lowest sample size from snow and polar climates in comparison to dry arid conditions causing a lower statistical reliance within those environments. Considering the distribution of climate and tectonics of modern sedimentary basins largely depends on the current plate tectonic distribution and that the past is of different tectonic and climatic distribution, the proportion of modern analogues is more appropriate to certain epochs than others.

Quantitative Characterization of Modern Depositional Environments

From a GIS and remote sensing perspective, removing 84% of the terrestrial land surface as irrelevant is of significant improvement if continued work is to be done on classifying modern depositional environments globally. This benefit has been demonstrated for the marginal marine of **Paper II** whereby approximately 28% of the global shoreline is in net deposition. The results here have shown that the global ternary process of Galloway (1975) and Ainsworth et al. (2011) are controlled and influence by elements of shelf width, climate, latitude, tectonics and distribution of sedimentary basins.

Depositional versus erosional settings is of primary importance controlling ternary process of the marginal marine. Globally, wave-dominated settings represent 84% of shorelines and tide-dominated regions represent a mere 16%. Within depositional settings however, tidal influence on process increase to 35%. The study has shown that shelf width influence on tidal prevalence of the marginal marine from narrow to wide shelves increase tidal presence by nearly threefold. Tectonically foreland basins and more restrictive extensional and strike-slip regimes appear to be more tidally influenced that fore-arc, passive margins and intracratonic settings. Ternary process by latitude and climate both appear related to the distribution of modern sedimentary basins (**Paper I**) that are concentrated around the equatorial and mid-latitudes and thereby are more mixed-influenced than their erosional polar shoreline counterparts. The parameter that controls shelf width, climate, tectonic regime, sedimentary basins and by extension, fluvial, wave and tide power, relate to the present day tectonic plate configuration.

The significance of the current research is that it defines and quantifies for the first time, the global distribution of ternary process. This has subsequently quantified the controls on those systems globally, that otherwise have only been based on conceptualized ideas and limited numerical data (e.g., Ainsworth et al. 2011). The challenge in defining the marginal marine typology globally by previous authors (Dürr et al. 2011) has been adressed in part by higher resolution data but more importantly by treating the shoreline as segments to characterize the shoreline geomorphology. The complexity of modern depositional environments is defined by more than the available resolution of global datasets and novel approaches such as that proposed in **Paper II** need to be considered for similar studies. On another note, the distribution of ternary process globally provides the ability to study in further detail, a representative sample of marginal marine depositional environments as analogues that display a range of tectonics, climates and ternary process. That in turn may yield further insightful results on the controls and geomorphology of modern marginal marine environments.

Beyond improvements to the worldwide classification of marginal marine shorelines, **Paper II** has shown the advantage of global based studies in fundamentally understanding the controls on modern depositional environments and how an automated and subjective approach may be used to achieve that goal. This provides further incentive to study other depositional environments on a global scale and to quantify controls (i.e., known, conceptualized or otherwise unknown), that can aid in predicting the geomorphology and prevalence of those systems in the rock record. For example, Hartley et al. (2010a) has shown the relationship of climate, tectonics and gradient on planform character of DFS systems and Peakall et al. (2011) has shown the influence of Coriolis effects on global submarine channel sinuosity, to name a few. A further contribution of the present thesis is the global definition of modern sedimentary basins (**Paper I**) that provides the bounds to quantify those terrestrial/marginal marine depositional environments and the main controls of climate and tectonics to analyze variation within those systems.

Geometric Information from Analogous Modern Systems

To quantify geometric variation that various controls pose on the geomorphology of depositional environments requires numerical information to define the disparity between different systems. **Paper III** has shown methodology to address the challenges faced by extracting geometric information from mapped modern depositional environments of increasingly large volumes of geospatial data. This methodology has shown that a quantitative characterization of mapped modern depositional elements can be achieved through a number of measured parameters related to a features centerline such as centerline deviation, width, connectivity, surface perimeter connectivity, orientation and shape (Figure 10). Not only is this done objectively but quantitatively in the sense that multiple samples are registered to get a representative statistic across the entire element.

The contribution from this portion of the thesis is that it can provide an improved methodology to analyze the geometry of modern depositional elements in a perspective that can aid in differentiating the geometric variations influencing geomorphology by various controls. For example, Hartley et al. (2010a) applied gradient attributes along DFS length to map relationships to controls of tectonics and climate. The methods proposed here could provide additional tools to quantify known or otherwise unexpected trends along depositional dip and strike of those systems in an automated and objective manner. In addition the methodology provides a reservoir modeling angle by relating the geometries of the modern to improve the parameterization used to define the extent of subsurface sandbodies. This has been the focus of **Paper III**.

To validate the methodology, two modern tropical intracratonic examples of the Mitchell Delta in the Gulf of Carpentaria, Australia and the anabranching mid channel bars of the Congo River in the Democratic Republic of the Congo River were analyzed. These results show that an objective and automated classification can significantly improve the characterization of geometric attributes in terms of accuracy over existing methodologies. The results have raised caution that previous quantitative geometric attribute characterization that rely on the properties of the feature shape like a minimum bounding box geometry (MBB) may lead to inaccurate interpretations without prior knowledge of its limitation.
For instance, the Mitchell Delta is a complex mixed influenced paralic environment (Nanson et al. 2013) that are represented by multiple sandbody geometries of varying size and shape. In particular the beach ridge sandbodies are long elongated cresentric features that in

previous studies were found to have a strong correlation between length and width (Nanson et al. 2012). In other words, beach ridges become wider with increasing length along a shoreline. However these measurements were based on a MBB whereby the longest axis (length) and shortest axis (width) of an object defines its parameters. While automated allowing for a quantitative analysis of the large dataset, the technique greatly exaggerates the width and underestimates the length of an object giving a false relationship. In comparison to the new methodology, the widths of beach ridges were found not to be related to its length. This would suggest that the energy regime creating beach and chenier ridges in the Gulf of Carpentaria (Jones 2010) was relatively uniform during deposition and does not vary significantly along strike. A quantitative geometric confirmation that otherwise would not be numerically observed without considerable manual effort.

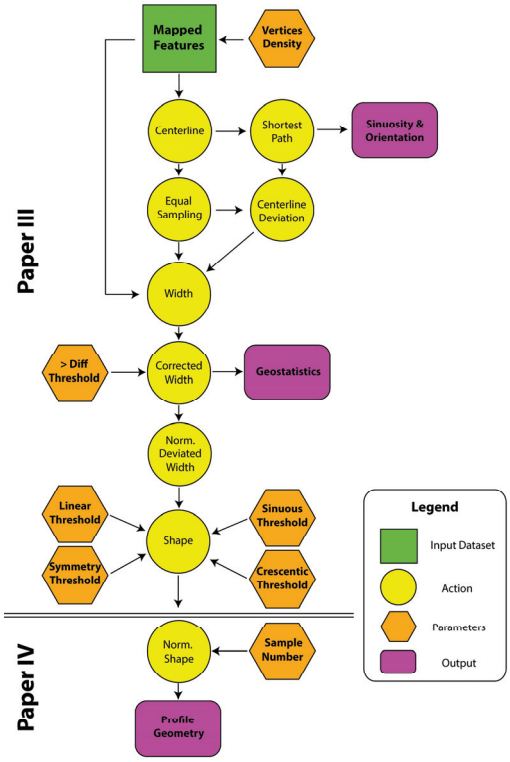

Figure 10 – A schematic workflow showing the process of geometric attribute description and characterization of modern depositional elements in **Paper III** to its application to outcrop and reservoir modeling in **Paper IV**. This starts at the input dataset that is used to describe a centerline, width and centerline deviation measurements are made in relation to that centerline to create a shape. That geometric profile may then be used directly into reservoir modeling applications as a user-defined object for object-based modeling.

In other circumstances, the methodology has shown potential for quantitative description of modern depositional environments like the mid-channel bars of the Congo. This dataset of 2221 bar forms were analyzed to measure the change in asymmetry of mid channel bars upstream of the river. This quantitative dataset is nearly 5 times larger than that presented by (Holzweber et al. 2014). The processing time that follows the automated procedure outlined in Figure 10 for the mid-channel bars of the Congo is also reasonable taking approximately 45minutes on an 8 core, 8 GB ram laptop. An automated approach allows time that otherwise would be spent manually measuring attributes to be allocated elsewhere, such as interpreting or mapping additional architectural elements.

This methodology has an advantage to describe the relationship of features geometric connectivity that in a reservoir modeling perspective would be beneficial to quantify (Tye 2004; Howell et al. 2008). The Mitchell Delta shows that within the system, channel deposits potentially connect the most number of reservoir elements but that the surface area that connect those elements is rather low which might promote heterogeneities

and compartmentalization in a similar subsurface reservoir field (Massey et al. 2013). In many aspects the methodology of **Paper III** incorporates advances in graph network theory from the computer sciences and applies that towards the challenges presented in describing connectivity of modern depositional environments.

The uniqueness of the methodology given here for the classification of depositional environments is that it is scale independent, suggesting that it will work on any scale of a hierarchical classification schema (e.g, SAFARI, WAVE Vakarelov and Ainsworth 2013). This could provide a wider applicability in the analysis of modern depositional environments by not only associating the geometries to a single element but also provide the geometry of those elements within its broader hierarchical classification, geometry and shape.

The same principles defined in **Paper III** can be applied to annotations made on virtual outcrops of the ancient (**Paper IV**) that often suffer from similar subjective manual interpretations that are more prone to human error and inefficiencies (Wang et al. 2005) . In addition to automatically extracting geometric attributes from mapped elements, the fact that the multiple measurements represent a single feature, its absolute geometric shape can be reproduced. That entails that complex geometric shapes can be described automatically as user-defined objects for object based modeling within standard reservoir suites. This could be a unique way to store a new form of geometric information within the range of sedimentological databases (Colombera et al. 2012; Vakarelov and Ainsworth 2013). It is a shame to place significant time and effort into mapping and interpreting architectural elements, only to lose that information by describing it in terms of a single maximum value.

6.2. Outlook

Global Classification of Modern Depositional Environments

Looking forward, the results, methodologies and tools defined in this thesis may serve as a platform for continued nomenclature classification and quantitative attribute characterization of modern depositional systems globally. This research would involve mapping depositional environments to the architectural element scale and to use the tools presented here to efficiently and objectively quantify their statistical significance, attributes and shapes within a framework of modern sedimentary basins (**Paper I**, Figure 11). That may help as shown in **Paper II** and by previous authors (Hartley et al. 2010a; Weissmann et al. 2010; Ainsworth et al. 2011) to demonstrate some of the global overriding controls influencing geomorphology of those systems.

While the present study has focused on the global study of the ternary process classification of the marginal marine (i.e., **Paper II**), there is broader scope within the SAFARI nomenclature standard to define the range of modern depositional environments. For instance, the continental realm may be defined at the depositional environment hierarchy in the SAFARI nomenclature as either Fluvial/Alluvial, Aeolian or Lacustrine. Considering that definitions of Aeolian and lacustrine have previously been defined by earlier work (Wessel and Smith 1996; Pidwirny 2006) and one assumes that those regions within sedimentary basins that do not occur in either of those environments to be alluvial, a global distribution of depositional environment for the continental realm may be achieved, classified by tectonics and climate (i.e. **Appendix III**). The next stage of this research would then continue the

hierarchical classification and to map the depositional and sub-environments in further geometric detail (Figure 11).

Mapping Modern Depositional Environments

To accomplish the goals for continued nomenclature characterization, one aspect that needs to be addressed is the methodology to map those architectural elements within depositional environments in a feasible, quantitative and global perspective. This is a complex and broad topic due to the varied nature of different geomorphologies found in the range of depositional environments. Each depositional environment will likely require a separate methodology and approach. Realistically this challenge may be resolved through one of three different options; 1) a manual interpretation (e.g., Hartley et al. 2010a; Vakarelov and Ainsworth 2013; Holzweber et al. 2014 and others), 2) an automated perspective (e.g., Congo River, **Paper III**) or 3) a combination of the two.

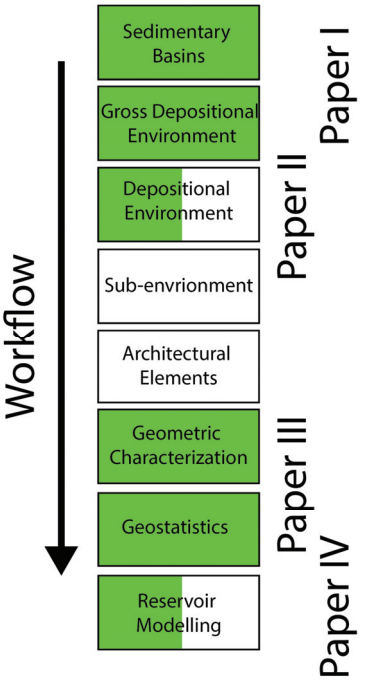

Figure 11 – An overview of the workflow process for characterizing modern depositional environments and its relation to the papers in this thesis. Green boxes indicate the completion of a task, a half green box indicate initial progress on a task, while white boxes indicate future work. Note a gap in the center that involves mapping depositional environments down to the architectural elements scale that was beyond the scope of this thesis.

While automated approaches have shown potential at the global scale characterization of the broad depositional environments (**Paper II** and **Appendix III**), the hierarchical classification of depositional elements at lower and more detailed resolutions become increasingly difficult. In part, due to the limited relevant data available at those resolutions and the complexity of sandbody geometries found within those depositional environments. For instance the classification of elements in the modern from satellite derived imagery is often made from their geomorphology rather than their spectral characteristics (refer to section 1.3). However, as has been demonstrated with the Congo River (**Paper III**), in certain environments, it may be conceivable that an automated method would work and be more efficient. It may be probable then, that a combination of both manual and automated classifications be used for different solutions. An interesting avenue for automated classification of remotely sensed imagery is the used of Object-Based Image Analysis (OBIA) that relies on the spectral character of an imagery and geometric characteristics to classify objects (Blaschke 2010).

If a manual approach is used, knowledge on the distribution of analogous depositional environments (i.e., **Paper I**, **Paper II** and **Appendix III**) would provide an ability to define

a representative sample of case studies to study across the spectrum of tectonics, climates and other controlling parameters on geomorphology.

Data Improvements & Programming

As with any study, the accuracy of the final product depends on the initial quality of the input data. As technology and methodologies to process and acquire data advance, the accuracy and volume of information will continuously improve. That data can subsequently be used to improve the level of detail captured in global based studies of the modern. However, caution should be taken here as while increased accuracy is always desired, an increase in volume of data could obscure the over-riding bigger picture making it difficult to recognize the relevant information. This trend is doubtful to change as the magnitude of data increases and only through novel approaches to address those challenges will that additional data remain valuable.

For example, the accuracy of high resolution digital elevation models (DEM) in **Paper I** provided a unique ability to map globally, the potential onlap of modern sedimentary basins. However the sheer volume of data (several hundred gigabytes) and exponential increase of that data with each analysis, makes it difficult to store, manage and process that information. It is only through programming that manages and processes that data through multiprocessing techniques where this feat can be achieved efficiently. Similarly in **Paper II**, the large dataset (>200 thousand polylines, each polyline represented by thousands of points) was difficult to manage, and in particular, to map the coastline geomorphology, though partitioning the large datasets resolved many issues related to processing time. **Paper III** and **Paper IV** have relied on the advantages of programming to provide customized algorithms (see **Appendix IV**) that are efficient and accurate enough to be of benefit in an appropriate context.

The geometric tools presented in this thesis represent an initial start in an attempt to bridge the gap between automating geometric extraction from quantitative interpretations acquired from both modern and ancient systems. As many of these tools have not been needed in the past due to limited large volumes of datasets, this research represents a new trend with the emergence of quantitative databases (e.g., Dreyer et al. 1993; Baas et al. 2005; Colombera et al. 2012; Vakarelov and Ainsworth 2013) and datasets (e.g., Nanson et al. 2012). The challenge is to recognize when programming may be appropriate for an application and where the time spent developing such code may impede the overall progress of research in comparison to an alternative approach (e.g. manual analysis).

Sedimentary Basins

The distribution of modern sedimentary basins represents an initial classification on a global scale. A continual improvement to this original classification is the ultimate desire. Namely, the tectonic classification is based on a simplified nomenclature of Ingersoll (1988) that could be expanded further to include the broad spectrum of basins including oceanic basins. In addition it may help to subdivide the basin classification based on tectonic mechanisms to be able to efficiently map the transition from one basin type to another. At present, the tectonic classification is primarily based on global data (e.g., Zoback 1992; Sperner et al. 2003; Ingersoll 2012) and a more detailed literature review would be beneficial. However, as with many broad global studies, literature is often incomplete and that is in part the aim of

this thesis to narrow. Gravitational maps can provide some insight into sediment thickness associated with these sedimentary basins, although at present and on a global scale, this remains of lower resolution and quality (e.g., Mooney et al. 1998). Another interesting avenue of research would be to map the evolution of those modern sedimentary basins as the current geomorphological character of a modern sedimentary basin will largely depend on the evolution its past (Kingston et al. 1983). By extension, this would influence the geomorphology of sedimentary systems within those basins.

6.3. Conclusions

The plethora of new geospatial information has opened a nuance within the geosciences to study large volumes of data. This avenue of research will undoubtedly continue as technology to gather, analyze and process that information improves. This signals perhaps a transition from isolated regional scale studies of modern depositional environments to a global perspective. This thesis has addressed the original hypothesis to define new methodologies and strategies that can improve global classification of modern depositional environments by showing the limited breath of the modern that may be analogous for the ancient, demonstrating the benefit of globally classifying depositional environments by automated and objective means and the methods to define geometric information for those environments quantitatively.

The first stage of this work has highlighted the global distribution of modern sedimentary basins. This work shows that approximately 16% of the terrestrial land surface represents active sedimentary systems that may be preserved in the rock record. Tectonic and climatic subdivisions have shown that those sedimentary systems are composed primarily of intracratonic and foreland basins of arid climates within an equatorial to mid latitude constraint. The boundary of modern sedimentary defines for the first time, the limits by which to quantify modern depositional environments on a global perspective.

One such environment, the marginal marine, is represented by one of the most complex zones of interaction between process dynamics of fluvial, wave and tide. High-resolution data combined with a novel approach to define coastline geomorphology, has shown that a global classification of shoreline's ternary process is feasible. These results have provided, to our knowledge, the first global classification of shoreline typology by process type offering a new and quantitative perspective on the controls of those environments, as well as the tools needed to find appropriate modern marginal marine analogues for the ancient.

Finally, the geometric description of those depositional environments, in an objective, quantitative and auditable method has been presented. This has provided an ability to extract quantitative and accurate information from modern depositional environments of interest allowing for an unprecedented ability to describe large volumes of modern data. The expansion of this to the ancient has been shown by using mapped elements from virtual outcrops to show its advantage in describing geometric attribute information in a similar automated and objective approach. In addition, a descriptive method to define customized user-defined objects for improved object based modeling has been explored that may better represent the variability of geometries exposed in the sedimentary record.

This thesis has suggested a workflow to classify modern depositional environments by 1) refining the results within sedimentary basins, 2) to use a sequential and hierarchical classification from the gross depositional environment to the architectural element scale and 3) to define geometric attributes from those elements. That hierarchical classification of depositional environments and geometric characterization on a global scale may lead to improved understanding on the controls of depositional environments, yet this work is in its infancy and a significant body of work lies ahead to attain that goal. The results presented here have given a complete picture in achieving global scale characterization of modern depositional environments as analogues for reservoir modeling.

References cited in Introduction and Synthesis

Ainsworth, R., Flint, S.S. & Howell, J.A. 2008. Predicting Coastal Depositional Style: Influence of Basin Morphology and Accommodation To Sediment Supply Ratio Within A Sequence Stratigraphic Framework *SPEM Spec. Publ. Recent Advances in Models of Siliciclastic Shallow-Marine Stratigraphy*, **90**.

Ainsworth, R., Vakarelov, B. & Nanson, R. 2011. Dynamic Spatial and temporal prediction of changes in depositional processes on clastic shorelines: Towards improved subsurface uncertainty reduction and management. *AAPG Bulletin*, **95**, 267-297.

Allen, P.A. & Allen, J.R. 2013. Basin Analysis: Principles and Application to Petroleum Play Assessment. 3rd Edition ed. John Wiley & Sons, Ltd., Chichester, West Sussex.

Ashworth, P.J. & Lewin, J. 2012. How do big rivers come to be different? *Earth-Science Reviews*, **114**, 84-107, doi: http://dx.doi.org/10.1016/j.earscirev.2012.05.003.

Baas, J., McCaffrey, W. & Knipe, R. 2005. The Deep-Water Architecture Knowledge Base: towards an objective comparison of deep-marine sedimentary systems. *Petroleum Geoscience*, **11**, 309-320.

Best, J.L., Ashworth, P.J., Bristow, C.S. & Roden, J. 2003. Three-Dimensional Sedimentary Architecture of a Large, Mid-Channel Sand Braid Bar, Jamuna River, Bangladesh. *Society for Sedimentary Geology*, **73**, 516-530, doi: doi: 10.1306/010603730516.

Blaschke, T. 2010. Object based image analysis for remote sensing. *ISPRS Journal of Photogrammetry and Remote Sensing*, **65**, 2-16, doi: http://dx.doi.org/10.1016/j.isprsjprs.2009.06.004.

Blum, M.D. & Törnqvist, T.E. 2000. Fluvial responses to climate and sea-level change: a review and look forward. *Sedimentology*, **47**, 2-48, doi: 10.1046/j.1365-3091.2000.00008.x.

Boyd, R., Dalrymple, R. & Zaitlin, B.A. 1992. Classification of clastic coastal depositional environments. *Sedimentary Geology*, **80**, 139-150, doi: http://dx.doi.org/10.1016/0037-0738(92)90037-R.

Buckley, S.J., Vallet, J., Braathen, A. & Wheeler, W. 2008. Oblique helicopter-based laser scanning for digital terrain modelling and visualisation of geological outcrops. *International Archives of the Photogrammetry, Remote Sensing and Spatial Information Sciences*, **37**, 493-498.

Caers, J. 2001. Geostatistical reservoir modelling using statistical pattern recognition. *Journal of Petroleum Science and Engineering*, **29**, 177-188, doi: http://dx.doi.org/10.1016/S0920-4105(01)00088-2.

Caers, J. & Zhang, T. 2004. Multiple-point Geostatistics: A Quantitative Vehicle for Integrating Geologic Analogs into Multiple Reservoir Models. *Integration of outcrop and modern analogs in reservoir modeling: AAPG Memoir*, **80**, 383-394.

Choi, K., Hong, C.M., Kim, M.H., Oh, C.R. & Jung, J.H. 2013. Morphologic evolution of macrotidal estuarine channels in Gomso Bay, west coast of Korea: Implications for the architectural development of inclined heterolithic stratification. *Marine Geology*, **346**, 343-354, doi: http://dx.doi.org/10.1016/j.margeo.2013.10.005.

Colombera, L., Felletti, F., Mountney, N. & McCaffrey, W. 2012. A Database Approach for Constraining Stochastic Simulations of the Sedimentary Heterogeneity of Fluvial Reservoirs. *AAPG Bulletin*, **96**, 2143-2166, doi: DOI:10.1306/04211211179.

Comunian, A., Renard, P. & Straubhaar, J. 2012. 3D multiple-point statistics simulation using 2D training images. *Computers & Geosciences*, **40**, 49-65, doi: http://dx.doi.org/10.1016/j.cageo.2011.07.009.

Dalrymple, R.W., Zaitlin, B.A. & Boyd, R. 1992. Estuarine facies models; conceptual basis and stratigraphic implications. *Journal of Sedimentary Petrology*, **62**, 1130-1146.

Decelles, P.G. & Giles, K.A. 1996. Foreland basin systems. *Basin Research*, **8**, 105-123.

Dickinson, W.R. 1974. Plate tectonics and sedimentation. *Society of Economic Paleontologists and Mineralogists Special Publication*, **22**, 1-27.

Dickinson, W.R. 1995. Forearc basins. Blackwell Science, Oxford, UK.

Dickinson, W.R. & Seely, D.R. 1979. Structure and stratigraphy of forearc regions. *AAPG Bulletin*, **63**, 2-31.

Dreyer, T., Fält, L.M., Høy, T., Knarud, R., Steel§, R. & Cuevas, J.L. 1993. Sedimentary Architecture of Field Analogues for Reservoir Information (SAFARI): A Case Study of the Fluvial Escanilla Formation, Spanish Pyrenees. *The Geological Modelling of Hydrocarbon Reservoirs and Outcrop Analogues*. Blackwell Publishing Ltd., 57-80.

Dürr, H., Laruelle, G., van Kempen, C., Slomp, C., Meybeck, M. & Middelkoop, H. 2011. Worldwide Typology of Nearshore Coastal Systems: Defining the Estuarine Filter of River Inputs to the Oceans. *Estuaries and Coasts*, **34**, 441-458, doi: 10.1007/s12237-011-9381-y.

Eide, C.H., Howell, J. & Buckley, S. 2014. Distribution of discontinuous mudstone beds within wave-dominated shallow-marine deposits: Star Point Sandstone and Blackhawk Formation, Eastern Utah *The American Association of Petroleum Geologists Bulletin*, **98**, 1401-1429.

Enge, H.D., Buckley, S., Rotevatn, A. & Howell, J.A. 2007. From outcrop to reservoir simulation model: Workflow and procedures. *Geosphere*, **3**, 469-490.

Fielding, C.R., Ashworth, P.J., Best, J.L., Prokocki, E.W. & Sambrook Smith, G.H. 2012. Tributary, distributary and other fluvial patterns: What really represents the norm in the continental rock record? *Sedimentary Geology*, **261–262**, 15-32, doi: http://dx.doi.org/10.1016/j.sedgeo.2012.03.004.

Fossen, H. 2012. Structural Geology. 3rd ed. Cambridge University Press, Cambridge, UK.

Fugro Robertson 2008. Robertson Tellus Sedimentary Basins of the World Map. World Wide Web Address: http://www.datapages.com/AssociatedWebsites/GISOpenFiles/RobertsTellusSedimentaryBasinsoftheWorldMap.aspx.

Galloway, W.E. 1975. Process Framework for Describing the Morphologic and Stratigraphic Evolution of Deltaic Depositional Systems. *Deltas: Models for Exploration, 1975*. Houston Geological Society, Houston, Texas, 87-98.

Gardoll, S.J., Groves, D.I., Knox-Robinson, C.M., Yun, G.Y. & Elliott, N. 2000. Developing the tools for geological shape analysis, with regional- to local-scale examples from the Kalgoorlie Terrane of Western Australia. *Australian Journal of Earth Sciences*, **47**, 943-953, doi: 10.1046/j.1440-0952.2000.00822.x.

Gawthorpe, R.L. & Leeder, M.R. 2000. Tectono-sedimentary evolution of active extensional basins. *Basin Research*, **12**, 195-218, doi: 10.1111/j.1365-2117.2000.00121.x.

Geehan, G. & Underwood, J. 1993. The Use of Length Distributions in Geological Modelling. *The Geological Modelling of Hydrocarbon Reservoirs and Outcrop Analogues*. Blackwell Publishing Ltd., 205-212.

Goodbred, S., Jr. & Saito, Y. 2012. Tide-Dominated Deltas. *In*: Davis Jr, R.A. & Dalrymple, R.W. (eds.) *Principles of Tidal Sedimentology*. Springer Netherlands, 129-149.

Grammer, G.M., Harris, P.M. & Eberli, G.P. 2004. Integration of outcrop and modern analogs in reservoir modeling: Overview with examples from the bahamas. In: Grammer, G.M., Harris, P.M. & Eberli, G.P. (eds) *Integration of outcrop and modern analogs in reservoir modeling. American Association of Petroleum Geologists, AAPG Memoir*, **80**, 1 - 22.

Hampson, G.J. & Storms, J.E.A. 2003. Geomorphological and sequence stratigraphic variability in wave-dominated, shoreface-shelf parasequences. *Sedimentology*, **50**, 667-701, doi: 10.1046/j.1365-3091.2003.00570.x.

Hartley, A., Weissmann, G., Nichols, G. & Warwick, G. 2010a. Large Distributive Fluvial Systems: Characteristics, Distribution, and Controls on Development. *Journal of Sedimentary Research*, **80**, 167-183, doi: doi: 10.2110/jsr.2010.016

Hartley, A.J., Weissmann, G.S., Nichols, G.J. & Scuderi, L.A. 2010b. Fluvial form in modern continental sedimentary basins: Distributive fluvial systems: REPLY. *Geology*, **38**, e231, doi: doi: 10.1130/G31588Y.1.

Hashemi, S., Javaherian, A., Ataee-pour, M., Tahmasebi, P. & Khoshdel, H. 2014. Channel characterization using multiple-point geostatistics, neural network, and modern analogy: A case study from a carbonate reservoir, southwest Iran. *Journal of Applied Geophysics*, **111**, 47-58, doi: http://dx.doi.org/10.1016/j.jappgeo.2014.09.015.

Heap, A.D., Bryce, S. & Ryan, D.A. 2004. Facies evolution of Holocene estuaries and deltas: a large-sample statistical study from Australia. *Sedimentary Geology*, **168**, 1-17, doi: http://dx.doi.org/10.1016/j.sedgeo.2004.01.016.

Holzweber, B., Hartley, A. & Weissmann, G. 2014. Scale invariance in fluvial barforms: implications for interpretation of fluvial systems in the rock record. *Petroleum Geoscience*, **20**, 221-224, doi: http://dx.doi.org/10.1144/petgeo2011-056.

Howell, J., Skorstad, A., MacDonald, A., Fordham, A., Flint, S., Fjellvoll, B. & Manzocchi, T. 2008. Sedimentological parameterization of shallow-marine reservoirs. *Petroleum Geoscience*, **14**.

Howell, J.A., Martinius, A.W. & Good, T.R. 2014. The application of outcrop analogues in geological modelling: a review, present status and future outlook. *Sediment-Body Geometry and Heterogeneity: Analogue Studies for Modelling the Subsurface. Geological Society, London, Special Publications*, **387**.

Hu, L.Y. & Chugunova, T. 2008. Multiple-point geostatistics for modeling subsurface heterogeneity: A comprehensive review. *Water Resources Research*, **44**, W11413, doi: 10.1029/2008WR006993.

Hudock, J.W., Flaig, P.P. & Wood, L.J. 2014. Washover Fans: A Modern Geomorphologic Analysis and Proposed Classification Scheme To Improve Reservoir Models. *Journal of Sedimentary Research*, **84**, 854-865, doi: doi: 10.2110/jsr.2014.64.

Ingersoll, R.V. 1988. Tectonics of Sedimentary Basins. *Geological Society of America Bulletin*, **100**, 1704-1719.

Ingersoll, R.V. 2012. Tectonics of sedimentary basins with revised nomenclature. *In*: Bursby, C. & Azor, A. (eds.) *Tectonics of Sedimentary Basins Recent Advances*. Blackwell Publishing Ltd, Chichester, West Sussex, 3-43.

Jensen, J.R. 2007. Remote Sensing of the Environment: An Earth Resource Perspective. 2nd ed. Pearson Prentice Hall, Upper Sadle River, NJ.

Jervey, M.T. 1988. Quantitative Geological Modeling of Siliciclastic Rock Sequences and Their Seismic Expression. *Sea-Level Changes*, **42**, 47-69.

Jones. 2010. Deltas in the Gulf of Carpentaria, Australia: Forms, Processes, and Products. *Society of Petroleum*, doi: doi: 10.2110/pec.03.76.0021.

Kingston, D.R., Dishroon, C.P. & Williams, P.A. 1983. Global Basin Classification System. *The American Association of Petroleum Geologists Bulletin*, **67**, 2175-2193.

Kocurek, G. & Ewing, R.C. 2005. Aeolian dune field self-organization – implications for the formation of simple versus complex dune-field patterns. *Geomorphology*, **72**, 94-105, doi: http://dx.doi.org/10.1016/j.geomorph.2005.05.005.

Larue, D.K. & Hovadik, J. 2008. Why is a reservoir architecture an insignificant uncertainty in many appraisal and development studies of clastic channelized reservoirs? . *Journal of Petroleum Geology*, **31**, 337-366, doi: 10.1111/j.1747-5457.2008.00426.x.

Larue, D.K. & Legarre, H. 2004. Flow units, connectivity, and reservoir characterization in a wave-dominated deltaic reservoir: Meren reservoir, Nigeria. *AAPG Bulletin*, **88**, 303-324, doi: doi: 10.1306/10100303043.

Lastras, G., Arzola, R.G., Masson, D.G., Wynn, R.B., Huvenne, V.A.I., Hühnerbach, V. & Canals, M. 2009. Geomorphology and sedimentary features in the Central Portuguese submarine canyons, Western Iberian margin. *Geomorphology*, **103**, 310-329, doi: http://dx.doi.org/10.1016/j.geomorph.2008.06.013.

Lisle, R.J. 2006. Google Earth: a new geological resource. *Geology Today*, **22**, 29-32, doi: 10.1111/j.1365-2451.2006.00546.x.

Marsaglia, K.M. 1995. Interarc and backarc basins. Blackwell Science, Oxford.

Massey, T.A., Fernie, A.J., Ainsworth, R., Nanson, R.A. & Vakarelov, B.K. 2013. Detailed mapping, three-dimensional modelling and upscaling of a mixed-influence delta system, Mitchell River delta, Gulf of Carpentaria, Australia. In: Sediment Body Geometry and Heterogeneity: Analogue Studies for Modelling the Subsurface. *Geological Society of London Special Publications*, **387**, doi: doi: 10.1144/SP387.4.

Mather, P. & Koch, M. 2011. Computer Processing of Remotely-Sensed Images. Fourth Edition ed. John Wiley & Sons Ltd., Chichester, West Sussex.

Miall, A. 2014. The Emptiness of the Stratigraphic Record: A Preliminary Evaluation of Missing Time In the Mesaverde Group, Book Cliffs, Utah, U.S.A *Journal of Sedimentary Research*, **84**, 457-469.

Miall, A.D. 1984. Principles of Sedimentary Basin Analysis. Springer-Verlag, New York. N.Y.

Mooney, W.D., Laske, G. & Masters, T.G. 1998. CRUST 5.1: A global crust model at 5 x 5. *Journal of Geophysical Research*, **103**, 727-747.

Nanson, R., Ainsworth, R., Vakarelov, B., Fernie, J. & Massey, A. 2012. Geometric attributes of reservoir elements in a modern, low accommodation, tide-dominated delta. *APPEA Journal*, 483-492.

Nanson, R.A., Vakarelov, B.K., Ainsworth, R.B., Williams, F.M. & Price, D.M. 2013. Evolution of a Holocene, mixed-process, forced regressive shoreline: The Mitchell River delta, Queensland, Australia. *Marine Geology*, **339**, 22-43, doi: http://dx.doi.org/10.1016/j.margeo.2013.04.004.

Nichols, G.J. & Fisher, J.A. 2007. Processes, facies and architecture of fluvial distributary system deposits. *Sedimentary Geology*, **195**, 75-90, doi: http://dx.doi.org/10.1016/j.sedgeo.2006.07.004.

Peakall, J., Kane, I.A., Masson, D.G., Keevil, G., McCaffrey, W. & Corney, R. 2011. Global (latitudinal) variation in submarine channel sinuosity. *Geology*, **40**, 11-14, doi: doi: 10.1130/G32295.1.

Pickup, G. & Hern, C. 2002. The Development of Appropriate Upscaling Procedures. *Transport in Porous Media*, **46**, 119-138, doi: 10.1023/A:1015055515059.

Pidwirny, M. 2006. "Eolian Processes and Landforms". World Wide Web Address: http://www.physicalgeography.net/fundamentals/10ah.html.

Popescu, I., Lericolais, G., Panin, N., Normand, A., Dinu, C. & Le Drezen, E. 2004. The Danube submarine canyon (Black Sea): morphology and sedimentary processes. *Marine Geology*, **206**, 249-265, doi: http://dx.doi.org/10.1016/j.margeo.2004.03.003.

Reading, H.G. & Levell, B.K. 1996. Controls on the sedimentary rock record. *In*: Reading, H.G. (ed.) *Sedimentary Environments: Processes, Facies and Stratigraphy*. Blackwell Publishing, Oxford.

Rittersbacher, A., Buckley, S., Howell, J., Hampson, G. & Vallet, J. 2014. Helicopter-based laser scanning: a method for quantitative analysis of large-scale sedimentary architecture. *in Sediment-body geometry and heterogeneity; analogue studies for modelling the subsurface Special Publication - Geological Society of London*, **387**.

Sambrook Smith, G.H., Best, J.L., Ashworth, P.J., Fielding, C.R., Goodbred, S.L. & Prokocki, E.W. 2010. Fluvial form in modern continental sedimentary basins: Distributive fluvial systems: COMMENT. *Geology*, **38**, e230, doi: doi:10.1130/G31507C.1.

Short, A.D. 2006. Australian Beach Systems—Nature and Distribution. *Journal of Coastal Research*, **22**, 11-27, doi: 10.2112/05A-0002.1.

Sperner, B., Müller, B., Heidbach, O., Delvaux, D., Reinecker, J. & Fuchs, K. 2003. Tectonic stress in the Earth's crust: advances in the World Stress Map project. - In: Nieuwland D. (ed.): New insights into structural interpretation and modelling. *Geological Society of London Special Publications*, **212**, 101-116, doi: 0305-8719/03/$15.

Steiniger, S. & Hunter, A.J.S. 2013. The 2012 free and open source GIS software map – A guide to facilitate research, development, and adoption. *Computers, Environment and Urban Systems*, **39**, 136-150, doi: http://dx.doi.org/10.1016/j.compenvurbsys.2012.10.003.

Sylvester, A.G. 1988. Strike-slip faults. *Geological Society of America*, **100**, 1666-1703.

Tye, R.S. 2004. Geomorphology: An approach to determining subsurface reservoir dimensions. *AAPG Bulletin*, **88**, 1123 -1147.

Vakarelov, B. & Ainsworth, R. 2013. A hierarchical approach to architectural classification in marginal-marine systems: Bridging the gap between sedimentology and sequence stratigraphy. *AAPG Bulletin*, **97**, 1121-1161, doi: DOI:10.1306/11011212024.

Van Wagoner, J.C., Mitchum, R.M., Campion, K.M. & Rahmanian, V.D. 1990. Siliciclastic Sequence Stratigraphy in Well Logs, Cores, and Outcrops: Concepts for High-Resolution Correlation of Time and Facies: AAPG Methods in Exploration 7., Tulsa, USA.

Wang, S., Shi, W., Yuan, H. & Chen, G. 2005. Attribute Uncertainty in GIS Data. *In*: Wang, L. & Jin, Y. (eds.) *Fuzzy Systems and Knowledge Discovery*. Springer Berlin Heidelberg, Lecture Notes in Computer Science, 614-623.

Weissmann, G.S., Hartley, A.J., Nichols, G.J., Scuderi, L.A., Olson, M., Buehler, H. & Banteah, R. 2010. Fluvial form in modern continental sedimentary basins: Distributive fluvial systems. *Geology*, **38**, 39-42, doi: doi: 10.1130/G30242.1.

Wessel, P. & Smith, W. 1996. A global, self-consistent, hierarchical, high-resolution shoreline database. *Journal of Geophysical Research*, **101**, 8741-8743.

Wilson, I.G. 1972. Aeolian bedforms - their development and origins. *Sedimentology*, **19**, 173-210, doi: 10.1111/j.1365-3091.1972.tb00020.x.

Xie, X. & Heller, P. 2009. Plate tectonics and basin subsidence history. *Geological Society of America Bulletin*, **121**, 55-64.

Zoback, M.L. 1992. First- and second-order patterns of stress in the lithosphere: The World Stress Map Project. *Journal of Geophysical Research: Solid Earth*, **97**, 11703-11728, doi: 10.1029/92JB00132.

APPENDICES

VII

Preface to the Appendices

The content in the appendices is used to provide additional information that supports the articles in the thesis. This section includes;

Appendix 1 – Supplementary Information for Paper I
This section was submitted with **Paper I** as supplementary information and contains additional detail on the GIS processing techniques used to gather the results. The tectonic classification and digital database design are explained in further detail.

Appendix 2 – Extended Conference Abstract
Appendix 2 is an extended abstract for the AAPG Hedberg Conference in Banff, Canada and highlights some of the earlier results from **Paper II**.

Appendix 3 – SAFARI Modern Analogue Finder
The SAFARI Modern Analogue Finder is a tool created directly from the results of **Paper I** and **Paper II**. This part details the challenges and solutions in developing a web-based tool for finding appropriate modern analogues for non-GIS specialists that need a better grasp of a clastic subsurface reservoir. The appendix further highlights initial work on classifying the gross depositional environment of the continental realm.

Appendix 4 – Geometric Shape & Attribute Tools
A brief description of the geometric tools, licensing and access to the open source scripts are outlined that establish the methodology of **Paper III** and **Paper IV**.

Please note that reference formatting is specific to each individual appendix and may differ from the referencing style of the thesis.

For access to any supplementary digital data produced in conjunction with this thesis please contact the main author.

Contact Information

Björn Burr Nyberg
UniCIPR, P.O. Box 8710, 5020 Bergen, Norway
bjorn.nyberg@uni.no / bjorn.burr.nyberg@gmail.com

Appendix 1 – Supplementary Information for Paper I

METHODS

The supplementary information here aims to highlight in further detail the geographical information system (GIS) and remote sensing techniques used to gather, store, process and classify global modern sedimentary basins.

Datasets

A tile based, global digital elevation model (DEM) at a high quality and resolution was obtained by combining two DEM products; SRTM v4.1(Reuter et al., 2007) at a 3 arc second resolution (approx. 90m) of 5x5 degree tiles and a mean elevation GMTED2010 (Danielson and Gesch, 2011) at a 7.5 arc second resolution (approx. 250m). These datasets provided coverage from 60°S to 60°N at a less than 16 m vertical error, and 60-90°N with a vertical error of 26 to 30 m, respectively, excluding the glacially covered Greenland and Antarctica. These polar regions were added but assumed to be in net erosion. In addition, a global DEM and bathymetric dataset, ETOPO1(Amante and Eakins, 2009) at a 1 arc minute (approx. 1.5km) provided opportunity to define oceanic contribution to the sedimentary record.

A quantified dataset of global present day Quaternary age sediments (Holocene and Pleistocene) was extracted and amalgamated from numerous spatial sources (Garrity and Soller, 2009; Pawlewicz et al., 1997; Persits et al., 2002; Persits et al., 1997; Pollastro et al., 1997a; Pollastro et al., 1997b; Schenk et al., 1997; Steinshouer et al., 1997; Wandrey and Law, 1997) of the World Energy Project of the USGS with a typical resolution between 1:2,000,000 to 1:7,500,000 (1:12,500,000 African Plate). The Global Self-consistent, Hierarchical, High Resolution Geography Database (GSHHG) V.2.2.0 (Wessel and Smith, 1996), coastline dataset was used as a reference for the terrestrial land. The marine portion of the continental lithosphere (continental shelf, slope & rise) is defined as the symmetrical difference to the oceanic lithosphere (Müller et al., 2008) that does not overlay the terrestrial land surface (Wessel and Smith, 1996).

All datasets were projected into the World Cylindrical Equal Area projection and to facilitate the large amount of data processing required in these analyses, automated multiprocessing workflows were scripted in the python programming language.

Sedimentary Basin Processing

The mountainous intermontane regions were firstly defined as the encompassing polygonized area of the world within a 30 x 30 grid cell majority of a gradient greater than 0.5degrees and an elevation greater than or equal to 500m using the global seamless ETOPO1 digital elevation model (Amante and Eakins, 2009). Low lying regions represent the symmetrical difference of the intermonante regions to the terrestrial land surface (Wessel and Smith, 1996), reflecting a simplified mountain typology (Meybeck et al., 2001).

A 0.8degree gradient threshold of the global SRTM/GTMED2010 DEM was processed within a 9x9 or a 30x30 grid cell majority to define areas of net deposition for intermontane and low lying basins, respectively. The resulting grids were polygonised into over 700 tiles

of low gradient regions of the world. To process the large amount of data into a seamless global coverage of net deposition, insignificant contributing areas of the tiled based polygons were removed, defined here as a polygon with an area less than 2km^2. The tiled vector regions were subsequently merged and dissolved into a single global dataset of low gradient regions where an area threshold was applied to define the major regions of interest defined as greater than 10,000km^2 for low-lying basins and a 250km^2 for intermontane basins or marginal marine basins (paralic environment connected to the shoreline). For the low lying regions only those low gradient regions that spatially coincide with Quaternary depositions were retained to remove low gradient features that are not active in deposition (i.e. Canadian or Siberian Shield). Smaller intermontane and marginal marine basins were based on a regional analysis of Quaternary age distribution with recognition of a resolution discrepancy between these datasests.

Sedimentary basins were subsequently simplified by removing inner polygons (holes) defined by an area of <100km^2 for intermontane and coastal basins and <1000km^2 for low-lying basins. Thresholds specified were originally defined by successive DEM evaluations and visual inspection of classifications originally over the western and southern part of the United States (Mississippi and Great Basin and Range), before applied and verified to the global scale. As limited research exists on the gradient boundary that defines a sedimentary basin onlap of the modern and as it will likely change with varying resolution of global DEM data (horizontal and vertical), the empirical relationship above was deemed reasonable.

Alluvial fan sediments were described as the contributing flow area (basin drainage) based on a 6.5° degree threshold of the SRTM/GMTED2010 DEM that is spatially connected to the intramontane sedimentary basins of interest (i.e. Great Basin and Range, Atacama Desert, Central Asia)**.** These parameters are similar to findings of previous studies (Miliaresis and Argialas, 2000) for alluvial fan delineating using similar DEM resolutions. Manual editing at this stage was minimal although alluvial fans were in certain circumstances excluded by using the 6.5 degree threshold to trace the edge of a ridge.

To define large scale desert regions, the definitions of mapped Quaternary geology that spatially coincide with dry desert climate (Bw on the Køppen-Giger Climate standard Kottek, 2006) were used to include regions of Sahara, Southern Africa and Australia. These regions represent areas of predominately Aeolian sediments of intractronic basins with poor sediment on-lap constraints whose basins are better defined by Quaternary age geology. The major resulting sedimentary basins were examined in detail and manually edited if needed by including where the quaternary age definition was insufficient in delineating all aeolian basins. Unidentified aeolian extents were included by tracing the outlying geometries of the basin from the previously established seamless global net depositional model (>2km^2 threshold) that typically shows the edge of the deserts by identifying the low lying interdune regions but not capturing the high gradient dune features themselves. This technique thereby ensures that the outlying geometry of the basin is preserved while limiting the subjective bias of the classification.

CLASSIFICATION OF SEDIMENTARY BASINS

Once the boundaries of sedimentary basins were defined, the primary tectonic and climatic controls were analyzed. To define tectonic regimes of sedimentary basins on a global scale is a challenging prospect as to our knowledge; a global seamless spatial dataset on the extent of

tectonic regimes of the world does not exist within present literature. Furthermore, comprehensive literature reviews on each individual modern sedimentary basin were beyond the scope of this research. To address this challenge, sedimentary basins were classified on a region by region basin (e.g. Basin and Range, Himalayas and the Andes) reflecting the global scale resolution of this study. In particular, global resources were used as a primary source of data such as stress maps (Sperner et al., 2003; Zoback, 1992), examples (Ingersoll, 2012), previous classification of tectonics by depositional environments (Hartley et al., 2010) and plate tectonic boundary (Bird, 2003). Regional scale published neotectonic maps supplemented this data (Table 1), particularly when data was poor or missing on a global scale. Neotectonics reflect recent fault and folding activity, typically of the Neogene and Quaternary (Pavlides, 1989). It may not provide the tectonic evolution of a basin system but particularly for smaller lived intermontane strike-slip and extensional basins (Ingersoll, 1988), it provides a useful constraint to differentiate those systems. The compiled information reflects the general primary tectonic regime regionally although we recognize that significant variability may exhibit within any given region.

A simplified tectonic nomenclature of Ingersoll (1988) is used to separate the basins into passive margins, extensional, foreland, back-arc, fore-arc, strike-slip or intracratonic basins is used to define that generalization.

TABLE 1. RESOURCES FOR THE CLASSIFICATION OF TECTONIC REGIMES

Region	References
Global	Zoback (1992); Sperner et al. (2003); Hartley et al. (2010); Ingersoll (2012);Bird et al. (2013)
Central Asia	Dewey et al. (1986)
Southeast Asia, Pacific	Marsaglia (1995); Honthaas et al. (1998); Yi et al. (2003)
Caribbean	Mann and Burke (1984)
South America	Allmendinger et al. (1997); DeCelles et al. (2011)
China/Mongolia	Watson et al. (1987); Yueqiao et al. (2003), Wang et al. (2006); Cunningham (2010)

The Köppen-Geiger climate classification defined by Kottek (2006) was used to define the climate classification of sedimentary basins. Due to discrepancies in resolution between the spatial datasets of climate (Kottek, 2006) and terrestrial land surface (Wessel and Smith, 1996), any region that was not allocated a climate was assigned to the spatially closest classification, merged and dissolved back into the original global classification.

DATABASE

The dataset for the global distribution of modern sedimentary basins represents version 1.0 and we encourage readers to contact the authors to improve the valuable resource through collaboration. This is distributed as a shapefile in the World Cylindrical Equal Distance projection with a WGS84 Datum that can be utilized in any standard geographical information system (GIS). The dataset is split into six main attributes of ID, Type, Structure, SubClass, MainClass and Area (Table 2). Each sedimentary basins region is subdivided based on the highest order Köppen-Giger classification and the structural setting nomenclature.

TABLE 2. SEDIMENTARY BASINS DATABASE STRUCTURE

Attribute	Values	Description
ID	Number	ID refers to the Basin ID that identifies a region of connected sedimentary basins
Type	Sedimentary Basin; Cont. Shelf, Slope & Rise	Identifies the region of the sedimentary basin classification
Structure	Foreland; Fore-arc; Back-arc; Strike-slip; Extensional; Intracratonic; Passive Margin	Identifies the primary tectonic regime of a sedimentary basin based on a simplified nomenclature standard of Ingersoll (1988)
SubClass	Af; Am; As; Aw; BWk; BWh; BSk; BSh; Cfa; Cfb; Cfc; Csa; Csb; Csc; Cwa; Cwb; Cwc; Dfa; Dfb; Dfc; Dfd; Dsa; Dsb; Dsc; Dsd; Dwa; Dwb; Dwc; Dwd; EF; ET	A subdivided category of the Köppen-Giger climate classification (see Kottek, 2006) that explores at the first level the main climates (A: Equatorial; B: Arid; C: Warm-Temperatre; D: Snow; E: Polar). The second level explores perpcipitation (W: desert; S:steppe; f: fully humid; s: summer dry; w: winter dry; m: monsoonal). Third level explores temperature (h: hot arid; k: cold arid; a: hot summer; b: warm summer; c: cool summer; d: extremely continental; F: polar frost; T: polar tundra)
MainClass	Equatorial; Arid; Warm-Temperate; Snow; Polar	A simplified Köppen-Giger climate classification (Kottek; 2006).
Area	Number	Area in km^2

REFERENCES CITED

Amante, C., and Eakins, B. W., 2009, ETOPO1 1 Arc-Minute Global Relief Model: Procedures, Data Sources and Analysis: NOAA Technical Memorandum NESDIS NGDC-24, p. 19.

Bird, P., 2003, An updated digital model of plate boundaries: Geochemistry, Geophysics, Geosystems, v. 4, no. 3, p. 1027.

Danielson, J. J., and Gesch, D. B., 2011, Global multi-resolution terrain elevation data 2010 (GMTED2010): U.S. Geological Survey Open-File Report 2011-1073, p. 26.

Garrity, C. P., and Soller, D. R., 2009, Database of the geological map of North America - adapted from the map by J.C. Reed, JR. and others (2005): United States Geological Survey.

Hartley, A., Weissmann, G., Nichols, G., and Warwick, G., 2010, Large Distributive Fluvial Systems: Characteristics, Distribution, and Controls on Development: Journal of Sedimentary Research, v. 80, no. 2, p. 167-183.

Ingersoll, R. V., 1988, Tectonics of Sedimentary Basins: Geological Society of America Bulletin, v. 100, no. 11, p. 1704-1719.

-, 2012, Tectonics of sedimentary basins with revised nomenclature, *in* Bursby, C., and Azor, A., eds., Tectonics of Sedimentary Basins Recent Advances: Chichester, West Sussex, Blackwell Publishing Ltd, p. 3-43.

Kottek, M., 2006, World map of the Köppen-Giger climate classification updated: Meterologische Zeitschrift, v. 15, no. 3, p. 259-263.

Meybeck, M., Green, P., and Vörösmarty, C., 2001, A New Typology for Mountains and Other Relief Classes: Mountain Research and Development, v. 21, no. 1, p. 34-45.

Miliaresis, G., and Argialas, D., 2000, Extraction and delineation of alluvial fans from DEMs and Landsat TM Images: Photogrammetric Engineering and Remote Sensing, v. 66, p. 1093-1101.

Müller, R. D., Sdrolias, M., Gaina, C., and Roest, W. R., 2008, Age, spreading rates, and spreading asymmetry of the world's ocean crust: Geochemistry, Geophysics, Geosystems, v. 9, no. 4, p. Q04006.

Pavlides, S. B., 1989, Looking for a Definition of Neotectonics: Terra Nova, v. 1, no. 3, p. 233-235.

Pawlewicz, M. J., Steinshouer, D. W., and Gautier, D. L., 1997, Maps showing geology, oil and gas fields, and geological provinces of Europe including Turkey: USGS Open File Report 97-470I.

Persits, F., Ahlbrandt, T., Tuttle, M., Charpentier, R., Brownfield, M., and Takahashi, K., 2002, Maps showing geology, oil and gas fields and geological provinces of Africa Ver. 2.0: USGS Open-File Report 97-470A.

Persits, F., Ulmishek, G. F., and Steinshouer, D. W., 1997, Maps showing geology, oil and gas fields and geological provinces of the former Soviet Union: USGS Open-File Report 97-470E.

Pollastro, R. M., Karshbaum, A. S., and Viger, R. J., 1997a, Maps showing geology, oil and gas fields and geological provinces of the Arabian Peninsula: USGS Open-File Report 97-470B version 2.0.

Pollastro, R. M., Persits, F., and Steinshouer, D. W., 1997b, Maps showing geology, oil and gas fields and geological provinces of iran: USGS Open-File Report 97-470G.

Reuter, H. I., Nelson, A., and Jarvis, A., 2007, An evaluation of void-filling interpolation methods for SRTM data: International Journal of Geographical Information Science, v. 21, no. 9, p. 983-1008.

Schenk, C. J., Viger, R. J., and Anderson, C. P., 1997, Maps showing geology, oil and gas fields and geological provinces of the south american region: USGS Open-File Report 97-470D.

Sperner, B., Müller, B., Heidbach, O., Delvaux, D., Reinecker, J., and Fuchs, K., 2003, Tectonic stress in the Earth's crust: advances in the World Stress Map project. - In: Nieuwland D. (ed.): New insights into structural interpretation and modelling: Geological Society of London Special Publications, v. 212, p. 101-116.

Steinshouer, D. W., Qiang, J., McCabe, P. J., and Ryder, R. T., 1997, Maps showing geology, oil and gas fields, and geological provinces of the asia pacific region: USGS Open-File Report 97-470F.

Wandrey, C. J., and Law, B. E., 1997, Maps showing geology, oil and gas fields and geological provinces of south asia: USGS Open-File Report 97-470C.

Wessel, P., and Smith, W., 1996, A global, self-consistent, hierarchical, high-resolution shoreline database: Journal of Geophysical Research, v. 101, p. 8741-8743.

Zoback, M. L., 1992, First- and second-order patterns of stress in the lithosphere: The World Stress Map Project: Journal of Geophysical Research: Solid Earth, v. 97, no. B8, p. 11703-11728.

Appendix 2 - Extended Conference Abstract

AAPG/SEPM HEDBERG RESEARCH CONFERENCE
"Latitudinal Controls on Stratigraphic Models and Sedimentary Concepts"
28 SEPTEMBER – 1 OCTOBER 2014 • BANFF, ALBERTA, CANADA
Latitudinal controls on modern shoreline geometries

Björn Nyberg[1] and John Howell[2,3]
[1] UniCIPR, Allegaten 41, Bergen Norway
[2]Geology & Petroleum Geology, University of Aberdeen, AB24 3UE UK
[3] Corresponding author

Paralic and shallow marine deposits comprise important yet potentially complex and heterolithic reservoirs in numerous fields around the World. The key control on reservoir architecture and consequently performance is the relative role of wave, tide or fluvial processes at the shoreline (Galloway 1975; Ainsworth et al. 2011). Shorelines dominated by wave processes tend to comprise good quality, clean reservoirs in sand bodies that are laterally extensive in a shore parallel direction (Howell et al. 2008). Fluvial dominated deltaic systems produce more lobate, sand bodies with a higher degree of heterogeneity related to dipping clinoforms and the compensational stacking of delta mouthbars. Tidal shoreline constitute the most heterolithic reservoirs with tidal channels, flats and subtidal bars arranged in complex lateral assemblages. Ainsworth et al. (2011) highlighted that in addition to the three end-members, a series of intermediate cases also exist which reflect different degrees of process impact on the shoreline.

Modern systems are commonly used as analogs for understanding the plan-view distribution of reservoir elements within a variety of depositional systems. The advent of free, global remote sensing data has significantly increased the availability of modern analogs and the frequency of their study. This is especially significant in shallow marine systems because many of the shallow marine reservoirs occur in major Tertiary delta systems (e.g. Niger, Baram, Nile, etc) which are still active today. In such cases the analoguesue comes directly from the same (or similar) depositional system as the reservoir. Whilst there have been numerous studies of modern systems, to date there has been no effort to systematically map the coastline of the entire World.

The goal of the present study has been to use GIS data to classify the coastline of the entire World with a view to improving understanding of the distribution of the key processes (WTF) and what controls their distribution and relative importance. The results of this study can be used to explore the impact of latitude upon the relative importance of the processes.
The first stage of classification was to determine whether the coastline was in net erosion or net deposition on geological timescales. This was achieved by looking at the gradient on the landward side of the shoreline. A very low gradient over an area larger than 250 sq km and areas with previously mapped Quaternary sediments typically equates to a delta or coastal plain and suggests that the associated shoreline is in long term progradation. A high relief adjacent to the shoreline suggests that the coastline is in net erosion. Of the global coastline of 350,000 km, 74,000 (21%) is in net deposition and 276,000 (79%) in in net erosion.

The second stage of the classification was to use three separate GIS layers to classify the shoreline with respect to the relative importance of the different processes (WTF). The first was mean global wave height from the World wave global database (Mørk et al. 2010). The second was mean tidal range from the global finite element solution model (Lyard 2006). Input on fluvial processes at shorelines was more difficult to obtain. No fluvial discharge models for all of the rivers on the planet was available, so a classification based on automated mapping of the area of all of World's drainage basins was used to provide a proxy for discharge at the river mouths (Lehner et al 2008).

These three parameters were then normalised and combined using a series of algorithms that account for the relative energy of the different processes, coupled with factors to account for climate and coastal morphology. The results allowed classification of the dominant process in 5 km stretches along the entire global coastline. Classification was done to the second order level ("influenced") of Ainsworth et al (2011). The data were then presented on a global map using an RGB color scheme (Fig 1). In addition to quantifying the dominant and subordinate processes around the coast, the "total energy" of the basinal processes (wave and tide) was also calculated to give a non-dimensional number that serves to distinguish shorelines that might be dominated by the same process but have very different energy levels.

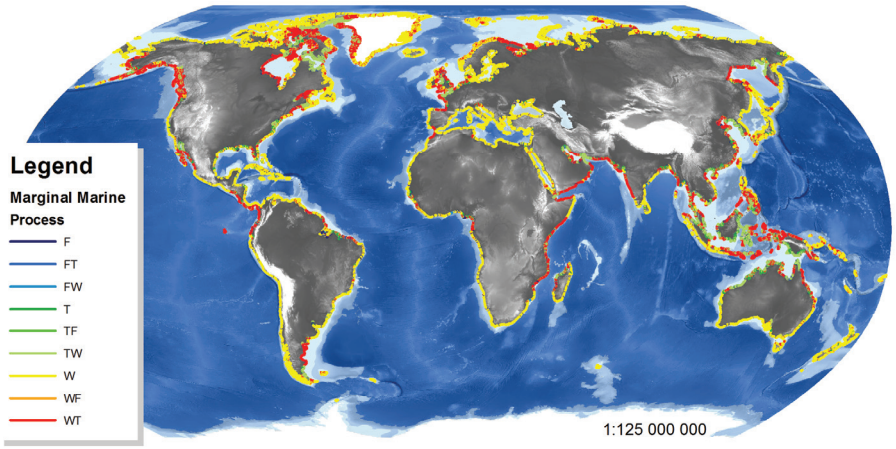

Figure 1. Global classification of shorelines in 5km increments. W- wave dominated; Wf - wave dominated, fluvial influenced; Wt - wave dominated, tidally influenced; T – tidal dominated, Tw – tidally dominated, wave influenced; Tf – tidally dominated, fluvial influenced; F – fluvial dominated; Fw – fluvial dominated, wave influenced; Ft – Fluvial dominated, tide influenced (classification after Ainsworth et al 2011).

Analysis of the data for the entire globe are presented in Figure 2. These demonstrate that globally wave processes are the most important, while tidal processes are of secondary importance and fluvial processes are only significant adjacent to river mouths. Analysis of the data by latitude (Fig 3) demonstrates that the highest energy shorelines exist in the southern ocean and there is a decrease northward to the equator and into the northern tropics (Fig 3). Energy then increases towards the northern high-latitude regions. This trend broadly corresponds with increase in the percentage area of land vs ocean at the different latitudes, with areas with a lower percentage of land receiving the greatest wave energy.

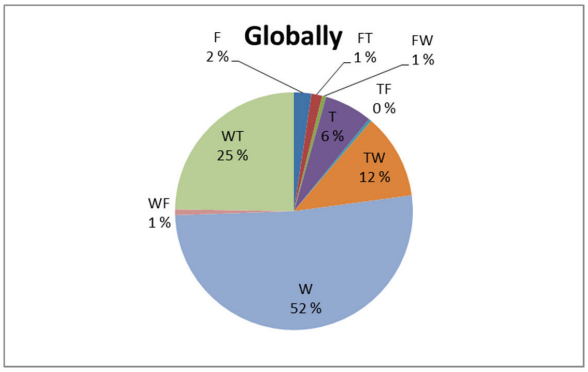

Figure 2. Global proportions of coastal processes.

The relative proportion of processes (Fig 3) by latitude shows an increase in both tidal and fluvial processes towards the equator, tropics and mid latitudes, which decrease towards the poles. There is also a decrease in tidally dominated or influenced shorelines towards the poles which is associated with a decrease in the size of the tidal bulge away from the equator.

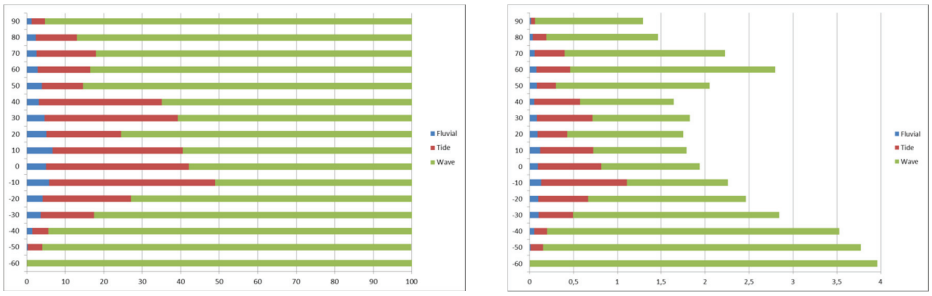

Figure 3. Left - Relative importance of Fluvial, Wave and Tidal Processes by latitude. Right – Key processes by latitude superimposed on total basinal energy.

The results of this study have a number of implications for exploration and production in shallow marine systems. Firstly, the global classification of shoreline type can be used to find suitable analogs for any shallow marine reservoir. These can be filtered by process, latitude, basin type, and climate, to ensure the optimal analoguesue is found.

From an exploration perspective in high latitudes, the increase in high energy wave dominated shoreline towards the poles is very positive. Such systems are commonly associated with high permeability, sand dominated shorelines which are laterally extensive along strike and lack significant internal heterogeneity. The mapping can be used to identify more detailed areas that warrant further investigation.

References

Ainsworth, R.B., B.V. Vakarelov, and R.A. Nanson, 2011, Dynamic Spatial and Temporal Prediction of Changes in Depositional Processes on Clastic Shorelines: Towards Improved Subsurface Uncertainty Reduction and Management. AAPG Bulletin, v. 95, p. 267-297.

Danielson, J.J., and Gesch, D.B., 2011, Global multi-resolution terrain elevation data 2010 (GMTED2010): U.S. Geological Survey Open-File Report 2011–1073, 26 p

Howell, J.A., A. Skorstad, A. MacDonald, A. Fordham, S. Flint, B. Fjellvoll, and T. Manzocchi, 2008, Sedimentological parameterization of shallow-marine reservoirs: Petroleum Geoscience, v. 14., p. 17-34.

Lehner, B., Verdin, K., Jarvis, A. (2008): New global hydrography derived from spaceborne elevation data. Eos, Transactions, AGU, 89(10): 93-94.

Lyard, F., F. Lefèvre, T. Letellier and O. Francis. Modelling the global ocean tides: a modern insight from FES2004, Ocean Dynamics, 56, 394-415, 200

Mørk G., Barstow, S., Kabuth, A. and Pontes, T. 2010. Assessing the global wave energy potential. Proc. of OMAE2010, 29th International Conference on Ocean, Offshore Mechanics and Arctic Engineering June 6-11, 2010, Shanghai, China; OMAE2010 – 20473

Appendix 3 – SAFARI Modern Analogue Finder

SAFARI Modern Analogue Finder

Björn Burr Nyberg[1,2], John Howell[3], Oliver Tynes[4]
[1] UniCIPR, P.O. Box 8710, 5020 Bergen, Norway
[2]Department of Earth Sciences, University of Bergen, P.O. Box 7803, 5020 Bergen, Norway
[3]Geology & Petroleum Geology, University of Aberdeen, AB24 3UE UK
[4]Mulelid-Tynes Development AS, P.O. Box 88, 6701 Måløy, Norway

1. Introduction

The following section describes a brief methodology used to create a modern analogue finder tool for the SAFARI database (http://safaridb.com/). The target audience for this tool is geared towards new geologist and reservoir engineers that have limited experience with marginal marine and continental systems and need modern analogues to better understand the heterogeneities within their own reservoir. The implementation of the tool is designed within a web viewer for the broadest potential audience within the industry.

This forms part of the SAFARI phase II deliverables that is sponsored by Bayern Gas, ConocoPhillips, Dana Petroleum, Dong Energy, Eni Norge, GDF Suez, Idemitsu, Lundin, Noreco, OMV, Repsol, Rocksource, RWE, Statoil, Suncor, Total, PDO, VNG and the Norwegian Petroleum Directorate (NPD).

2. Dataset

The dataset is based on four main parameters that include:

- The gross depositional environment split into the marginal marine (Figure 1) and the continental realm (Figure 2).

- The classification of the marginal marine is based on the relative influence of fluvial, wave and tide (Galloway, 1975, Ainsworth, 2011; Figure 3A and B). Whereas the classification of the continental realm is based on the relative proportion of fluvial/alluvial, aeolian and lacustrine deposits within sedimentary basins of equally spaced 0.5 degree grids globally (Figure 3C and D).

- Basin type are based on a simplified nomenclature standard of Ingersoll (2012) that include foreland, fore-arc, passive margins, intracratonic, strike-slip and extensional basins.

- Climate is based on five main climatic zones of equatorial, warm temperate, arid, snow and polar (Kottek, 2006).

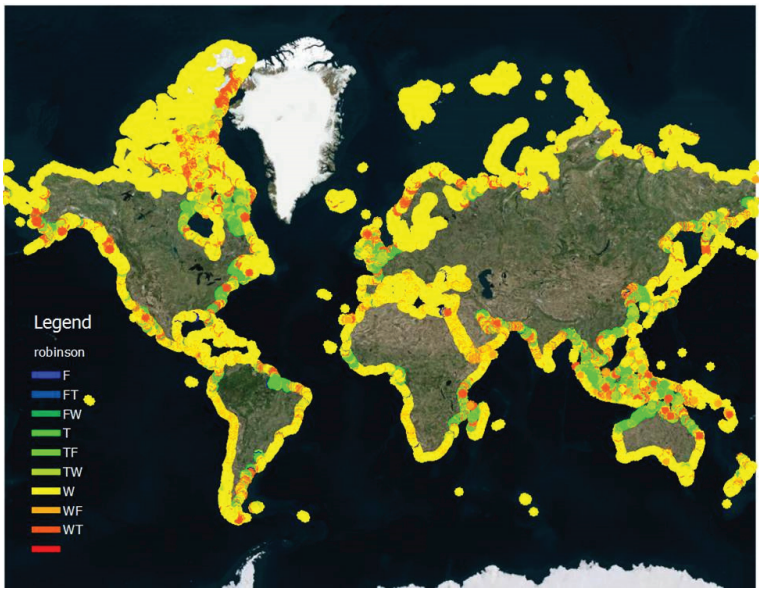

Figure 1 *– The global distribution of ternary process of Galloway (1975) and Ainsworth et al. (2011) to show the first two-tier classification (i.e. Dominant and Influenced).Bing Imagery ©, from http://safaridb.com/#/modern.*

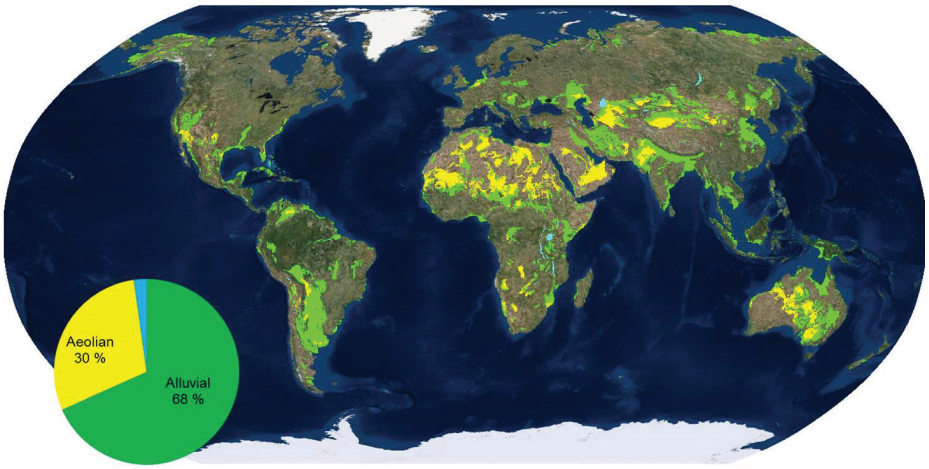

Figure 2 – Global distribution of Aeolian (Pidwirny, 2006), Lacustrine (Wessel and Smith 1996) and Fluvial/Alluvial deposits according to the SAFARI nomenclature standard. TerraColor Imagery©. From http://safaridb.com/#/modern.

2.1 Structure

The parameters mentioned above can be selected by the end-user to define the spatial bounds of modern analogues globally by a simple structured query language (SQL) within a GIS environment. The main challenge is that not all users have access to or familiarly with a GIS

environment and furthermore it eliminates any connection of the data to the broader SAFARI database and nomenclature standard that otherwise can be used to relate the modern to the ancient and wiki-knowledgebase available on www.safaridb.com. A fully web integrated solution to the SAFARI database would enhance its applicability to real world scenarios.

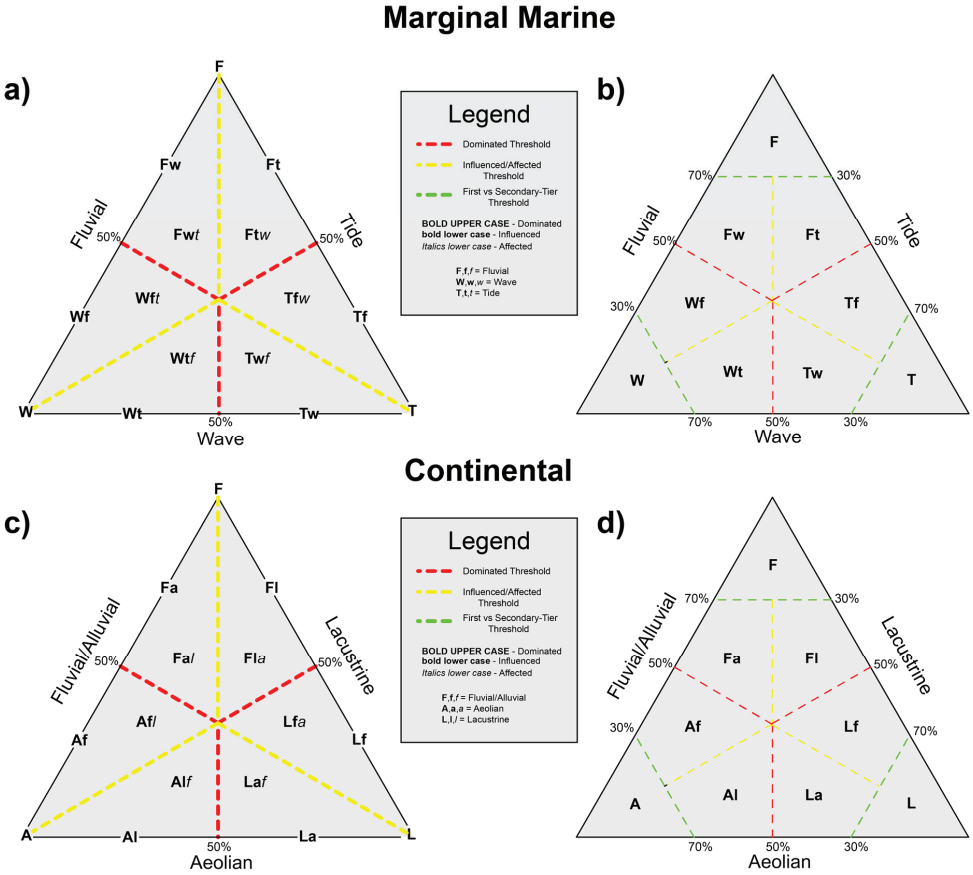

Figure 3 *– **a)** shows the full 15 category classification by Ainsworth et al. (2012) to describe the marginal marine into Dominated, Influenced and Affected. A simplified version of that diagram is used in **b)** to show a nine category classification up to the second-tier classification of "Influenced". **c)** shows a ternary plot classification of the continental realm based on the relative influences of fluvial, Aeolian and lacustrine according to the SAFARI standard. **d)** shows a simplified 9 category classification of that ternary plot model as used in the classification here.*

The integration of vast amounts of geospatial data into a web-based system poses its own unique challenges. The problem being that multiple user inquiries to the same structured network database cannot handle the volume required to retrieve and separate information from the over 200 thousand individual segments of the marginal marine and over 90 thousand individual grids of the continental realm. Furthermore the ability to visually display a query within Google Maps for instance, is difficult in itself as a single line segment can be represented by thousands of individual points. While a query of the three parameters may

significantly eliminate the number of datasets to be visualized, it ultimately cannot display the entirety of the dataset globally. A multiple level upscaling solution would need to be implemented to handle various zoom levels while representing the data at the highest possible resolution.

3. Upscaling

To accomplish upscaling, the coarsest zoom level would need to be no more than 1500 samples to handle the volume of potential end-user queries with a web based query.

3.1. Marginal Marine

For the marginal marine this is accomplished by segmenting the shoreline of the world (Wessel and Smith 1996) into a series of 17 zoom levels ranging from 750km to 5km in length. The customized algorithm would then create a bounding box around each upscaled line and determine its intersection with the original high resolution marginal marine dataset (5km segments). The majority of values for each parameter within that bounding box is then assigned to the upscaled line. The information for that upscaled shoreline segment is then defined as a single point coordinate locality (lat, long) to be displayed within Google Maps (e.g., Figure 4).

3.2. Continental Realm

As the boundary of sedimentary basins is often large irregular shaped features (Figure 2), assigning a single point to describe a large area of fluvial/alluvial, aeolian and lacustrine depositional environments within those basins was deemed inappropriate. Rather a series of four gridded subsamples of the sedimentary basins were defined ranging between 0.5 and 3 degree tiles. Each grid is then classified according to the relative proportions of fluvial/alluvial, aeolian and lacustrine (Figure 2) by the ternary plot in Figure 3D. The centroid coordinate of each grid (lat,long) can then be displayed within Google Maps (e.g., Figure 4).

4. Database Design

The web-based analogue finder displays a maximum of 1,500 points per end-user query. Each subsequent user criteria of the three available parameters (classification, basin type and climate), will further remove unwanted data points selecting the highest potential zoom resolution to display by examining each zoom level sequentially to determine if it can handle the query (i.e. <1,500). Sample size will also reduce based on the spatial view extent. Each location that honors the user criteria can then be examined and evaluated individually in Google Maps (Figure 4). Once a set of criteria has identified an appropriate modern analogue, its relation to the SAFARI nomenclature standard and database can relate that information to the wiki knowledgebase and ancient systems. Furthermore, the information gathered regarding a suitable modern analogue can be used to study those systems in further detail utilizing additional GIS software.

The principles outlined above can be expanded to provide additional parameters (and/or important controls on deposition) according to the SAFARI nomenclature standard, when such data becomes available, to further improve the detail of the finder tool for modern analogues.

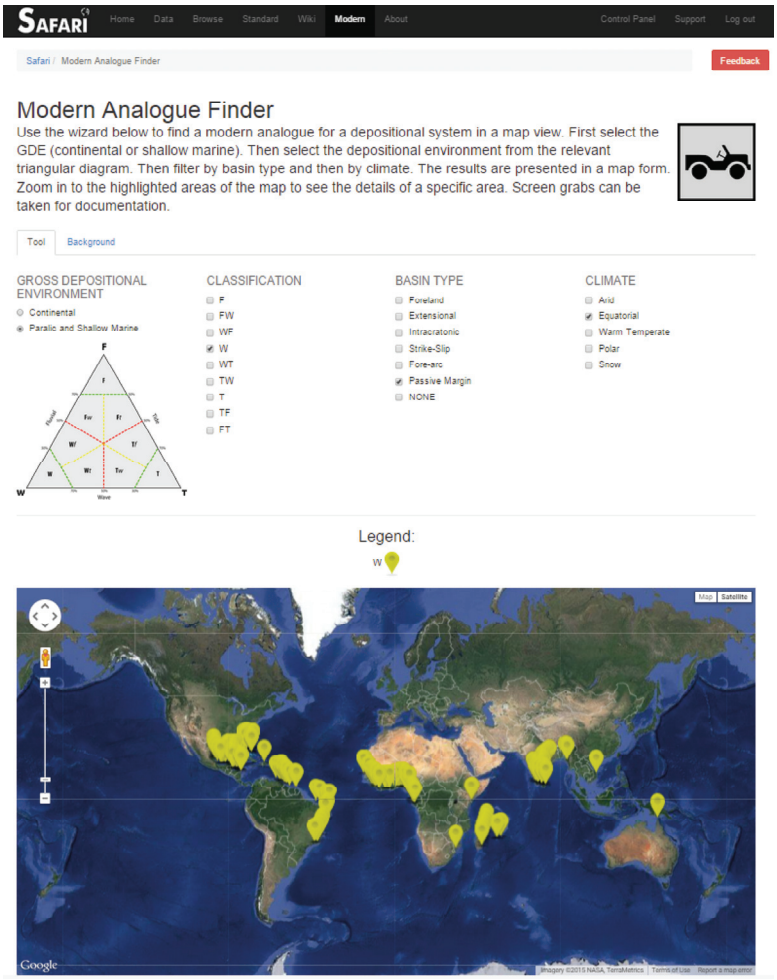

Figure 4 *– SAFARI Modern Analogue Finder Tool. Criteria can select from gross depositional environment of continental vs marginal marine, followed by a classification (see Figure 3), basin type and climate. The example used above displays wave-dominated shorelines on passive margins of equatorial climates within sedimentary basins (from safaridb.com). Google Earth Imagery©.*

5. References

Ainsworth, R., et al. (2008). "Predicting Coastal Depositional Style: Influence of Basin Morphology and Accommodation To Sediment Supply Ratio Within A Sequence Stratigraphic Framework " SPEM Spec. Publ. Recent Advances in Models of Siliciclastic Shallow-Marine Stratigraphy **90**.

Galloway, W. E. (1975). Process Framework for Describing the Morphologic and Stratigraphic Evolution of Deltaic Depositional Systems. Deltas: Models for Exploration, 1975. Houston, Texas, Houston Geological Society**:** 87-98.

Ingersoll, R. V. (2012). Tectonics of sedimentary basins with revised nomenclature. Tectonics of Sedimentary Basins Recent Advances. C. Bursby and A. Azor. Chichester, West Sussex, Blackwell Publishing Ltd**:** 3-43.

Kottek, M. (2006). "World map of the Köppen-Giger climate classification updated." Meterologische Zeitschrift **15**(3): 259-263.

Pidwirny, M. (2006). ""Eolian Processes and Landforms"." Fundamentals of Physical Geography 2nd Edition.Retrieved 01/10, 2014, from http://www.physicalgeography.net/fundamentals/10ah.html.

Wessel, P. and W. Smith (1996). "A global, self-consistent, hierarchical, high-resolution shoreline database." Journal of Geophysical Research **101**: 8741-8743.

Appendix 4 – Geometric Shape & Attribute Tools

Björn Burr Nyberg[1,2]

[1] UniCIPR, P.O. Box 8710, 5020 Bergen, Norway
[2]Department of Earth Sciences, University of Bergen, P.O. Box 7803, 5020 Bergen, Norway

Background

The automated scripts presented in **Paper III** and **Paper IV** are implemented in a graphical user-interface (GUI) within the framework of the QGIS software package (QGIS Development Team, 2014). The algorithms assume that a unique ID attribute labelled as "FID" identifies each individual polygon of interest. These algorithms are coded within the python programming language and are dependent on multiple data analysis libraries that need to be installed including pandas and pysal.

The code is provided open source in the hope that they will continue to develop for improve geometric characterization of modern depositional environments. For a complete list of open-source scripts produced in conjunction with this thesis visit the github website at https://github.com/BJEBN/Geometric-Analysis.

These scripts may be directly used in the processing tool of a QGIS desktop environment by the "Create new script" function (Figure 1). Refer to the QGIS manual at docs.qgis.org/2.2/en/docs/user_manual/processing for additional information.

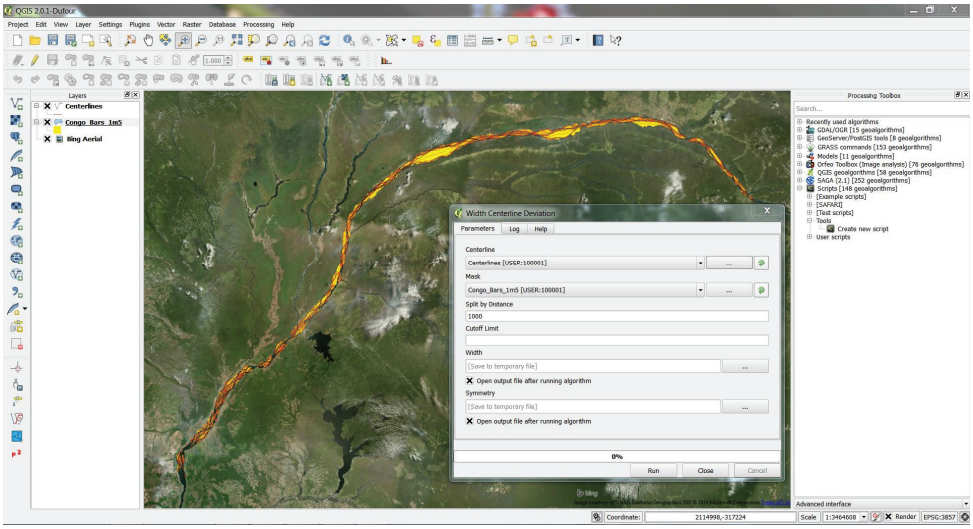

Figure 1 *– Example window from QGIS showing the GUI for the Width and Centerline Deviation tool with the Congo Dataset as an example. Bing Imagery © as background.*

All scripts are provided under the GNU General Public License V3 and contain the following restrictions.

'"This program is free software: you can redistribute it and/or modify it under the terms of the GNU General Public License as published by the Free Software Foundation, either version 3 of the License, or (at your option) any later version.
This program is distributed in the hope that it will be useful, but WITHOUT ANY WARRANTY; without even the implied warranty of MERCHANTABILITY or FITNESS FOR A PARTICULAR PURPOSE. See the GNU General Public License for more details.
You should have received a copy of the GNU General Public License along with this program. If not, see <http://www.gnu.org/licenses/>."'

References

QGIS Development Team (2014). "QGIS Geographic Information System. Open Source Geospatial Foundation Project." from http://qgis.osgeo.org.